2) Abundance and Occurrence

(1) Morphological distribution of manganese nodules

The morphological distribution of manganese nodules is shown in Fig. 3-5-4. The pebble and ellipsoidal types occur widely in both the western and eastern seas of the survey area. In the outer fringes of the area, spheroidal and massive types occur sporadically. The manganese nodules in the western part of the western sea, the eastern part of the eastern sea, and the southern fringe of the survey area consist mostly of ellipsoidal type. In some localities of the eastern sea, The spheroidal and pebble types are predominant and there, the coverage is very dense. Also in some localities of the northeastern part of the eastern sea, massive type is predominant and the coverage is very dense.

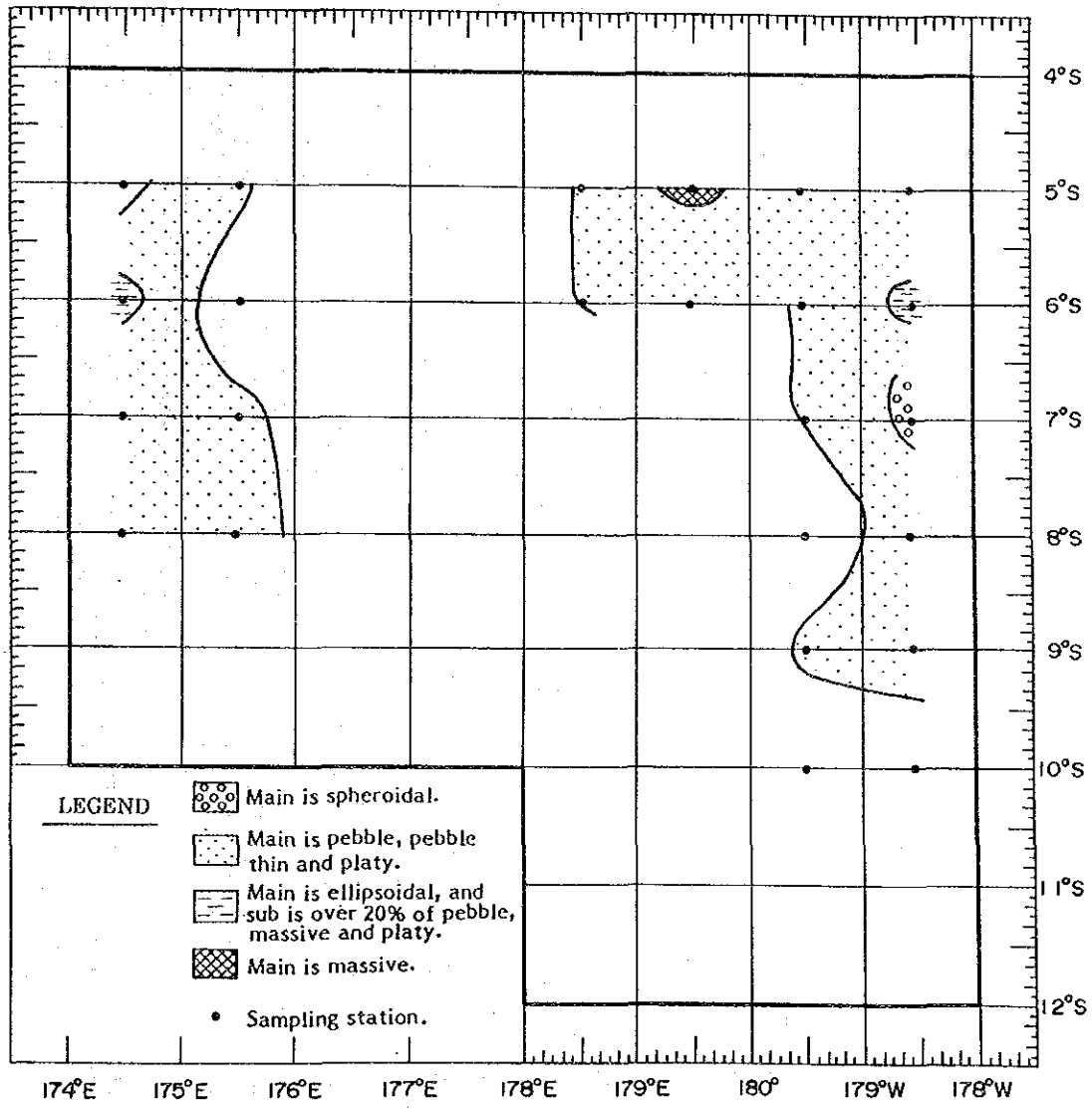

Figure 3-5-4 Morphology Distribution of Manganese Nodules

(2) Size distribution of manganese nodules

The size distribution of manganese nodules is shown in Fig. 3-5-5. There is one locality in the northwestern fringe of the western sea, where the average size of the manganese nodules exceeds 10 cm; at one locality in the northern part of the eastern sea, it is 6~8 cm. Otherwise, the average size is predominantly 2~4 cm. The average size calculated from the collected samples are 6.0cm in the western sea, 4.7 cm in the eastern sea and 5.1 cm for the whole survey area.

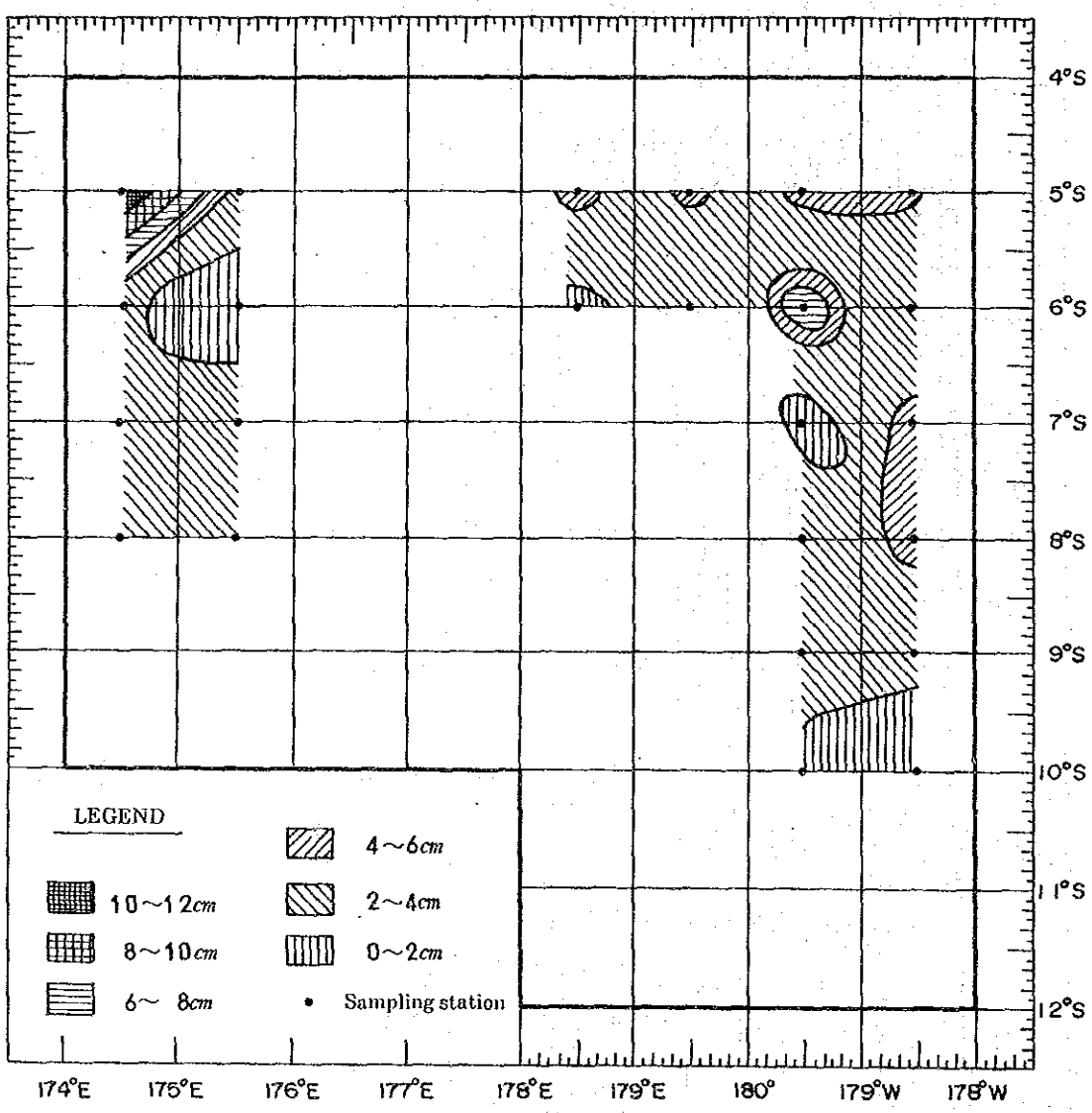

Figure 3-5-5 Size Distribution of Manganese Nodules

(3) Size and morphology

The relation between the size and the type of manganese nodules is shown in Fig. 3-5-6. The larger the size of manganese nodules, the pebble type decreases and the massive and the ellipsoidal types increase. Up to 4~6 cm, the spheroidal type increases with the size. Ellipsoidal fat type first appears at 8~16 cm. At sizes over 16 cm, all the nodules are irregular other types which cannot be categorized in (1).

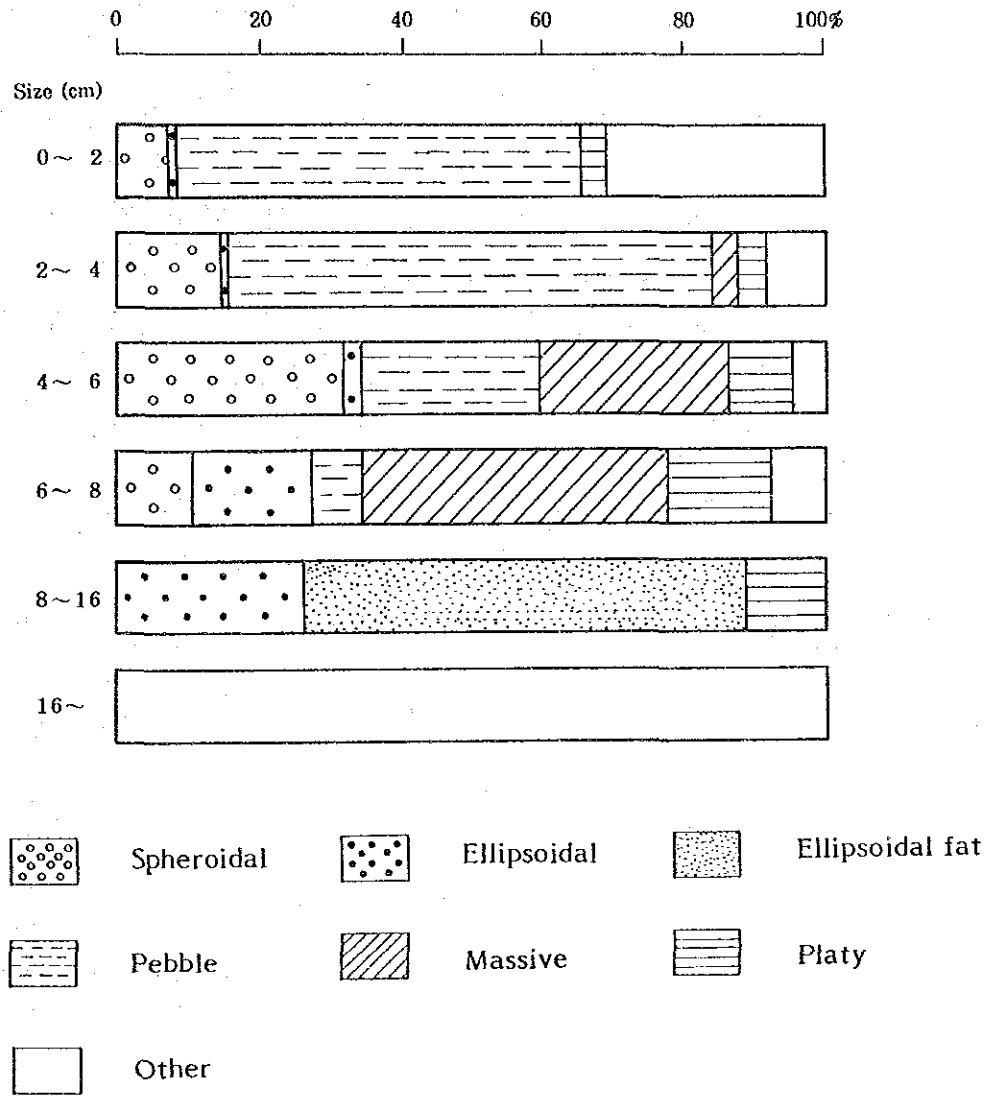

Figure 3-5-6 Relation between Size and Morphology

(4) Local topography and morphology

The morphological distribution of manganese nodules is shown in Fig. 3-5-4, and the relationship between micro-topography and morphology is shown in Fig. 3-5-7. The pebble type is predominant in the survey area and this occurs in all types of micro-topography. In the plains, pebble is followed by massive, spheroidal and ellipsoidal types. In the knoll zone, plate and other types are characteristic. In the seamounts, pebbles are predominant with minor amounts of ellipsoidal types.

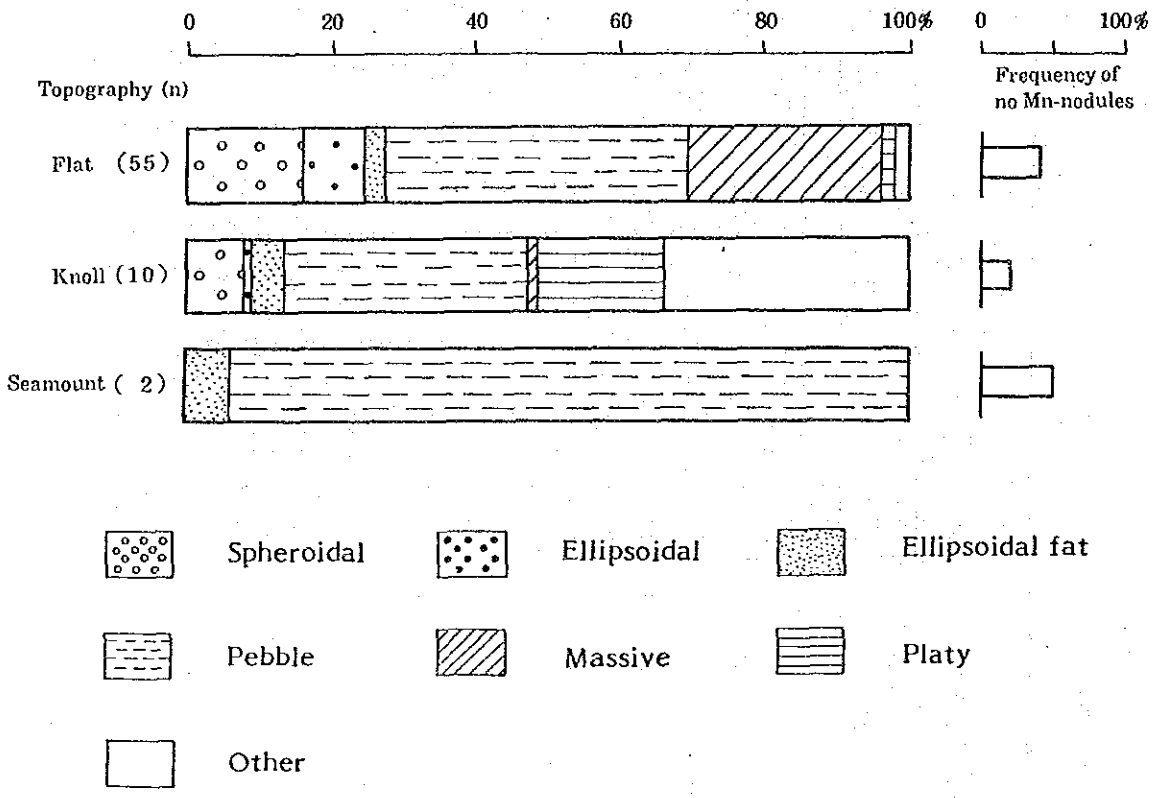

Figure 3-5-7 Relation between Local Topography and Morphology

(5) SBP type and morphology

The relation between SBP type and morphology, the relation between upper transparent layer thickness and morphology are shown in Fig. 3-5-8 and Fig. 3-5-9 respectively. These figures indicate that pebble type occurs generally in this area and that the following holds for other types. The distribution ratios

of the pebble, spheroid and ellipsoid type are high in types b and e_1 while that of massive and plate are low, with clear transparent layers. On the other hand, the distribution ratios of the pebble and massive types are high, but that of the spheroid and ellipsoidal is low in type c, d_1 and d_2 which have no transparent layers. Type ds differs from other opaque layers that the main nodule types are pebbles and spheroids. In the present survey, however, the samples from the non-transparent layer zones are limited and whether the above trend really reflects the actual mode or not could be controversial. The distribution ratios of the spheroid and pebble types are high where the thickness of the upper transparent layer is between 0~10 m. Particularly, the

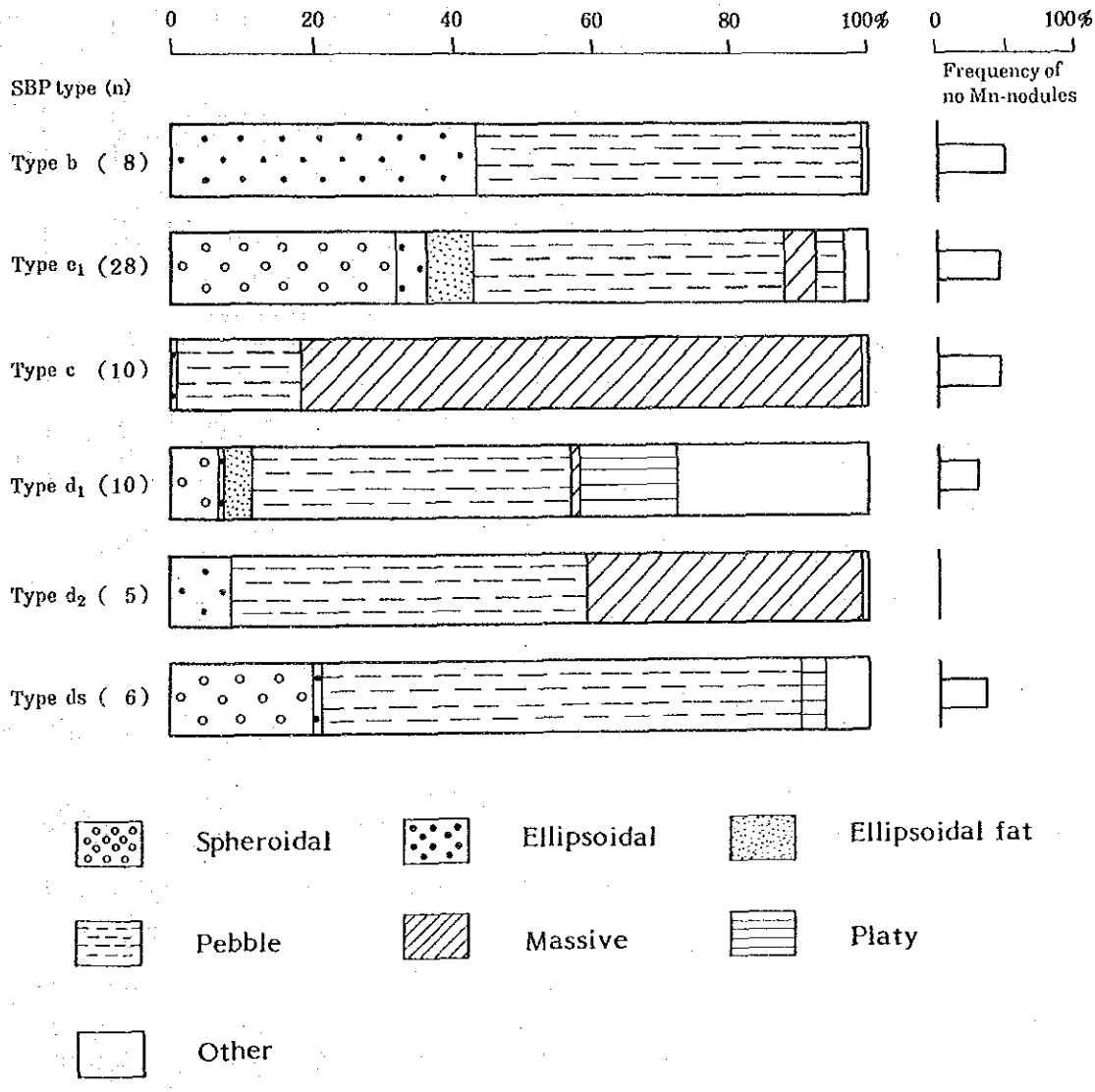

Figure 3-5-8 Relation between SBP Type and Morphology

plate type is observed only where the upper transparent layer do not exist. The distribution ratios of the spheroidal type as well as pebble is high where the thickness of the upper transparent layer is between 20~30 m. This corresponds to SBP type b and e_1. Where the thickness of the upper transparentlayer is 40 m, the ratio of massive and plate type is high, while the pebble, spheroids and ellipsoidal fat types do not occur. When it is 50 m, the ratio of others becomes high.

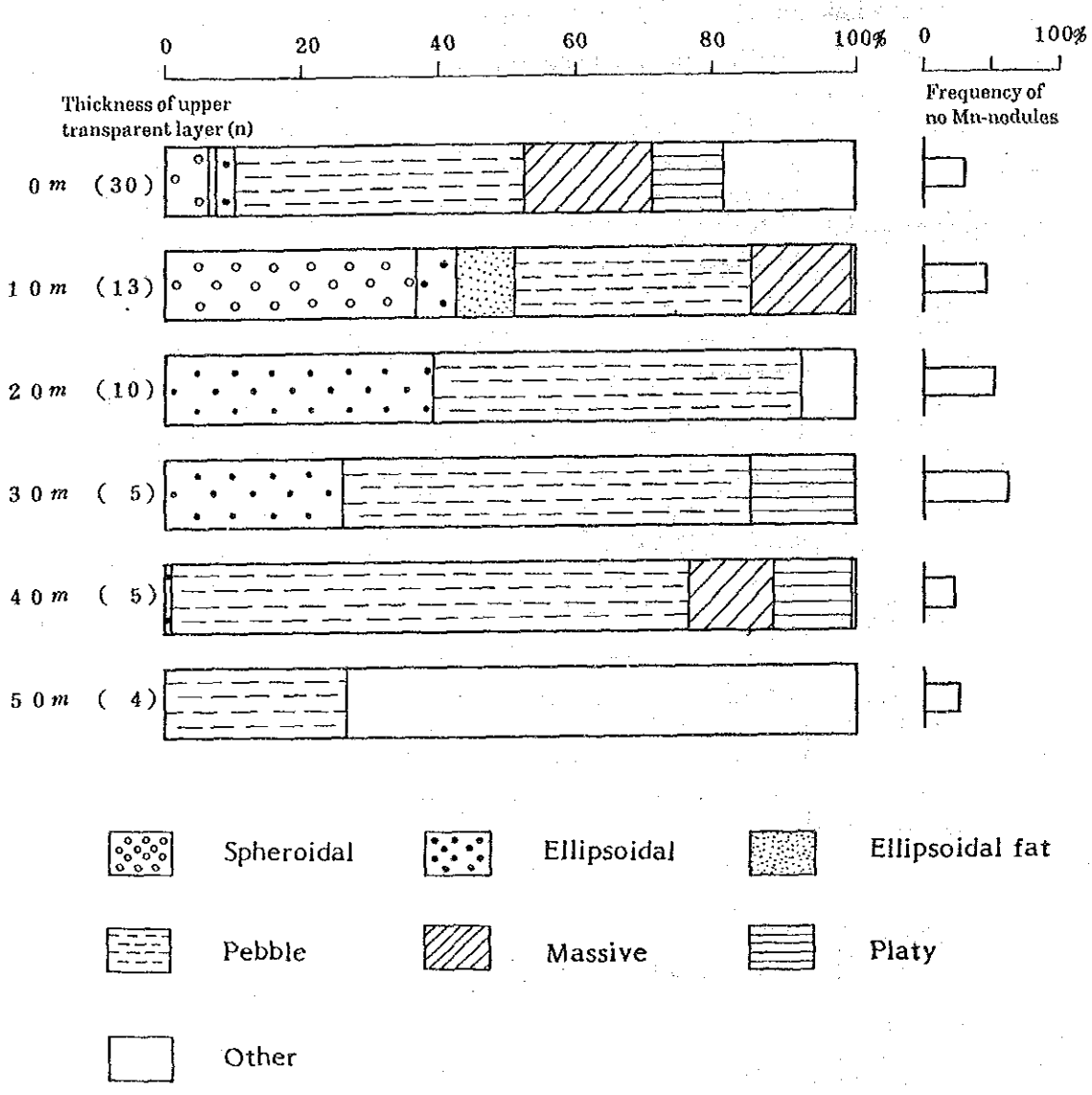

Figure 3-5-9 Relation between Upper Transparent Layer Thickness and Morphology

(6) Bottom materials and morphology

The relationship between the bottom materials and morphology is shown in Fig. 3-5-10. It is seen that the distribution ratio of pebbles is high in brown clay with occurrences of spheroids, massive types and plates. In the case of missing of bottom materials, other types are predominant with a few occurrences of ellipsoids, pebbles and masives.

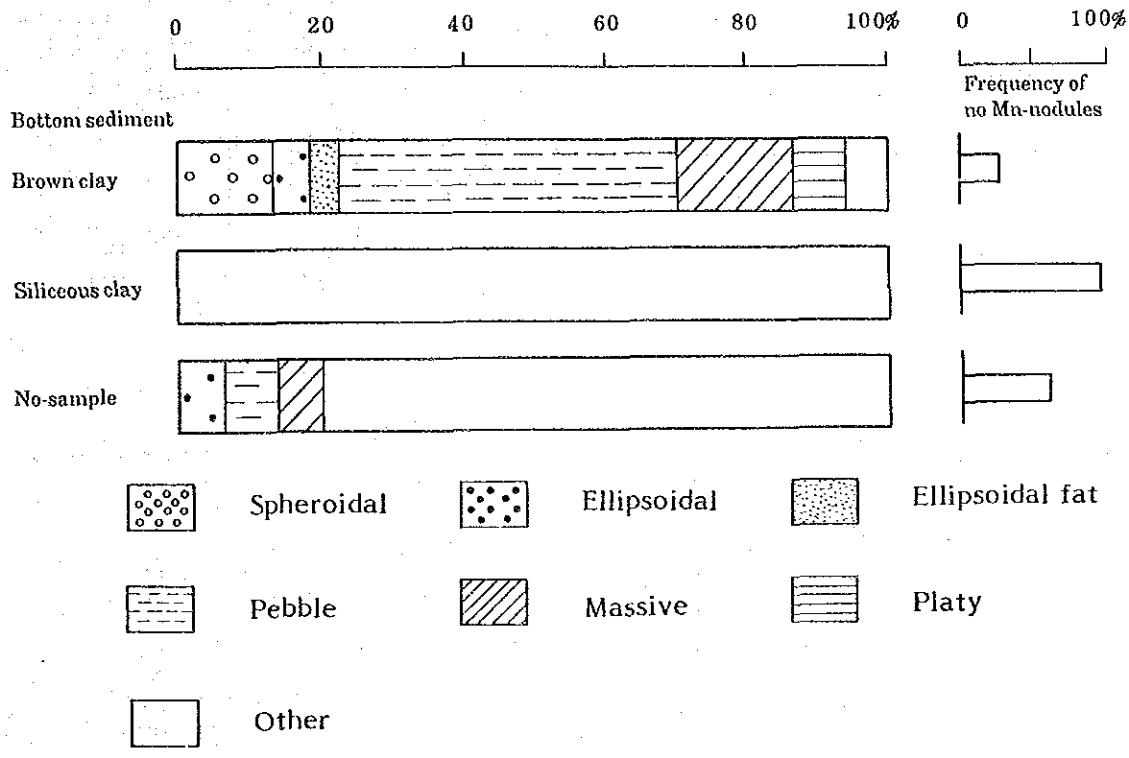

Figure 3-5-10 Relation between Bottom Sediments and Morphology

(7) Abundance of manganese nodules

Annexed Fig. 7 is a map showing the abundance of manganese nodules in the survey area. The average abundance of the area is 2.40 kg/m^2 in western sea, 2.91 kg/m^2 in eastern sea and the whole area with 24 stations averages 2.74 kg/m^2. The maximum value of sampling points is 19.22 kg/m^2, but none of the stations averaged excess of 10 kg/m^2. This shows that this area has low manganese nodules potential. There are several points with relatively high values (over 7.5 kg/m^2), but the areal extents are small and they occur sporadically. These are mostly in knolls and seamount zones and the nodules have high content of pebbles, spheroids and massive types.

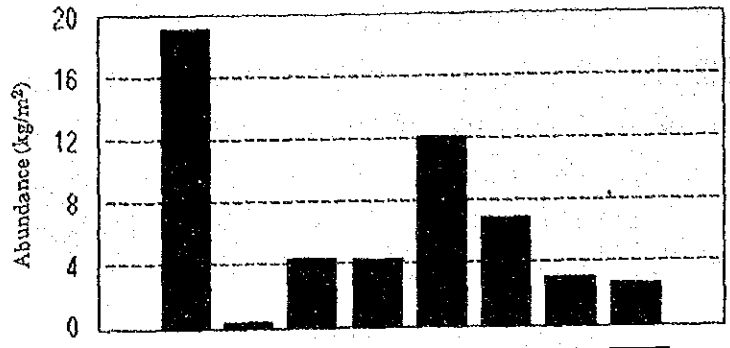

Morphology	Sp	E	Ef	P	M	Pl	Ot	Total
Average Abundance (kg/m²)	19.22	0.60	4.78	4.16	12.31	7.02	3.25	2.86
Appearance ratio (%) of ≧ 10 kg/m²	100	0	0	23.80	66.67	50.0	25.0	14.93
Standard deviation	–	1.20	–	5.94	3.54	9.90	5.72	5.38
Number of Samples	1	6	1	21	3	2	8	67

LEGEND

Morphology

Sp Spheroidal
E Ellipsoidal
Ef Ellipsoidal fat
Pt Pebble thin
P Pebble
M Massive
Pl Platy
Ot Other

Abundance

1 0.0 ~ 2.5 kg/m2
2 2.5 ~ 5.0
3 5.0 ~ 7.5
4 7.5 ~ 10.0
5 10.0 <

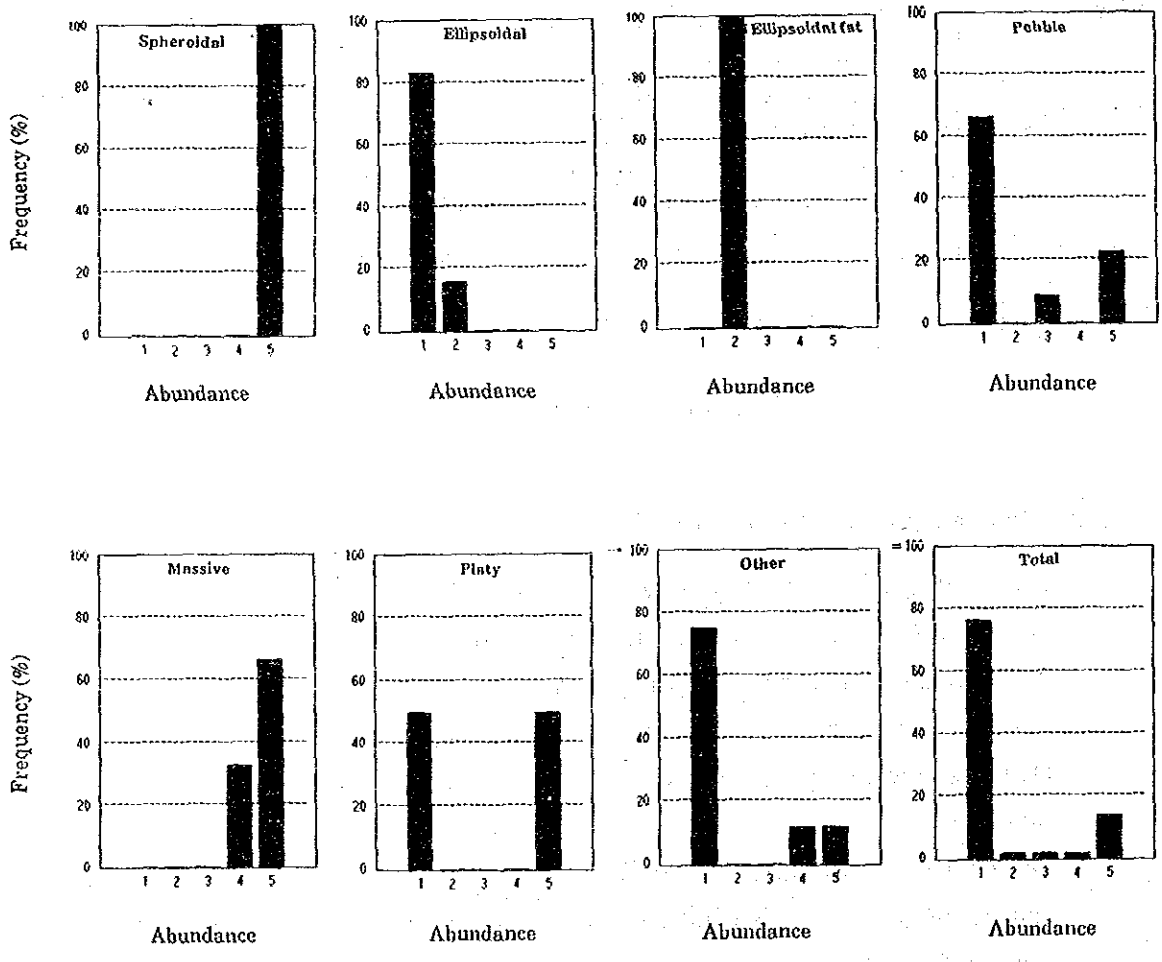

Figure 3-5-11 Relation between Morphology and Abundance

Three free fall grabs were thrown in at each station, but it was very rare when all three grabs collected manganese nodules. The distribution of manganese nodules in this marine area is not good.

The average abundance for each morphological type and the frequency of the abundance are shown in Fig. 3-5-11. It should be noted, however, that the number of samples used for this processing is small. The average abundance is high for spheroidal and massive types at 19.22 kg/m^2 and 12.31 kg/m^2 respectively. But only one spheroid and three massive type samples were collected and the figure may not reflect the real conditions. The average abundance of other morphological types is in the vicinity of 4 kg/m^2 and the occurance rate of those with over 10 kg/m^2 is about 20%.

Regarding the relation between the abundance and bottom materials, manganese nodules were not collected from the calcareous clay zone and it is not possible to discuss the problem with reference to brown clay.

3) Chemical Properties

Fluorescent X-ray analysis for five components (Ni, Cu, Co, Mn and Fe) of each grain size division, was done on board. Analysis of auxiliary components of representative samples selected from the above samples was done on shore. Some manganese nodules were divided into several pieces considering their concentric structure and each of these pieces was analyzed by fluorescent X-ray method. The chemical properties of manganese nodules will be described according to these results. Statistical results derived from small number of samples should be treated with care.

(1) Five principal components and their distribution

Fig. 3-5-12 shows the frequency distribution of the five principal components of manganese nodules in the surveyed area. Fig. 3-5-13 and Table 3-5-2 show the scatter diagram of each component and the statistics of the average grade and other factors of manganese nodules respectively. The average values of Ni, Cu and Co are 0.54%, 0.47% and 0.20% respectively and they are low. The average values of Mn and Fe are 17.01% and 12.73% and the average Mn/F ratio is 1.34. These average values are the reflection of the grade of the pebble, ellipsoid and other types of nodules collected in higher amounts. Annexed Fig. 8~10 shows grade distribution of Ni, Cu and Co.

This figure shows that the high Ni and Cu part occur in the western fringe of the western sea.

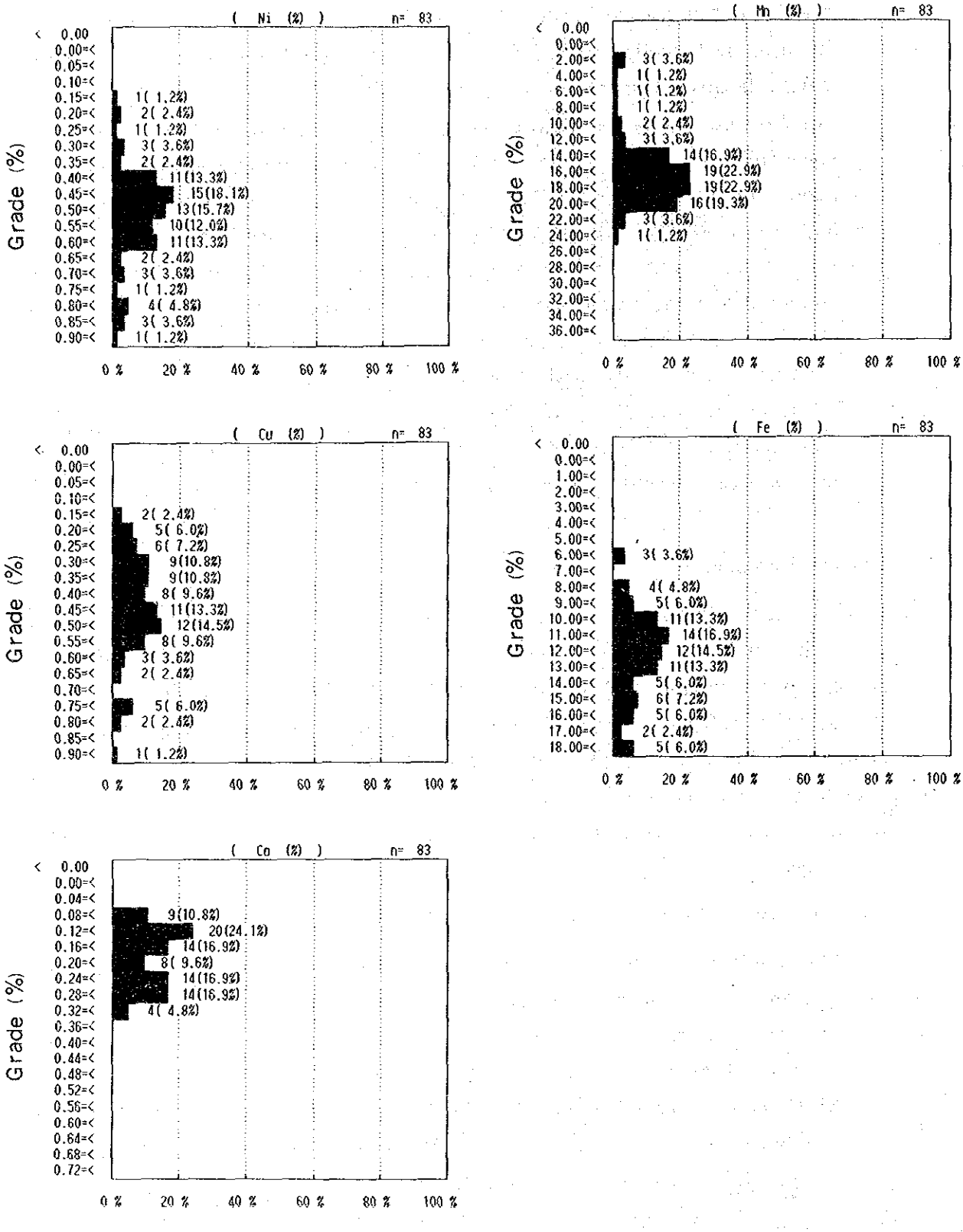

Figure 3-5-12 Frequency Distribution of Five Principal Chemical Components

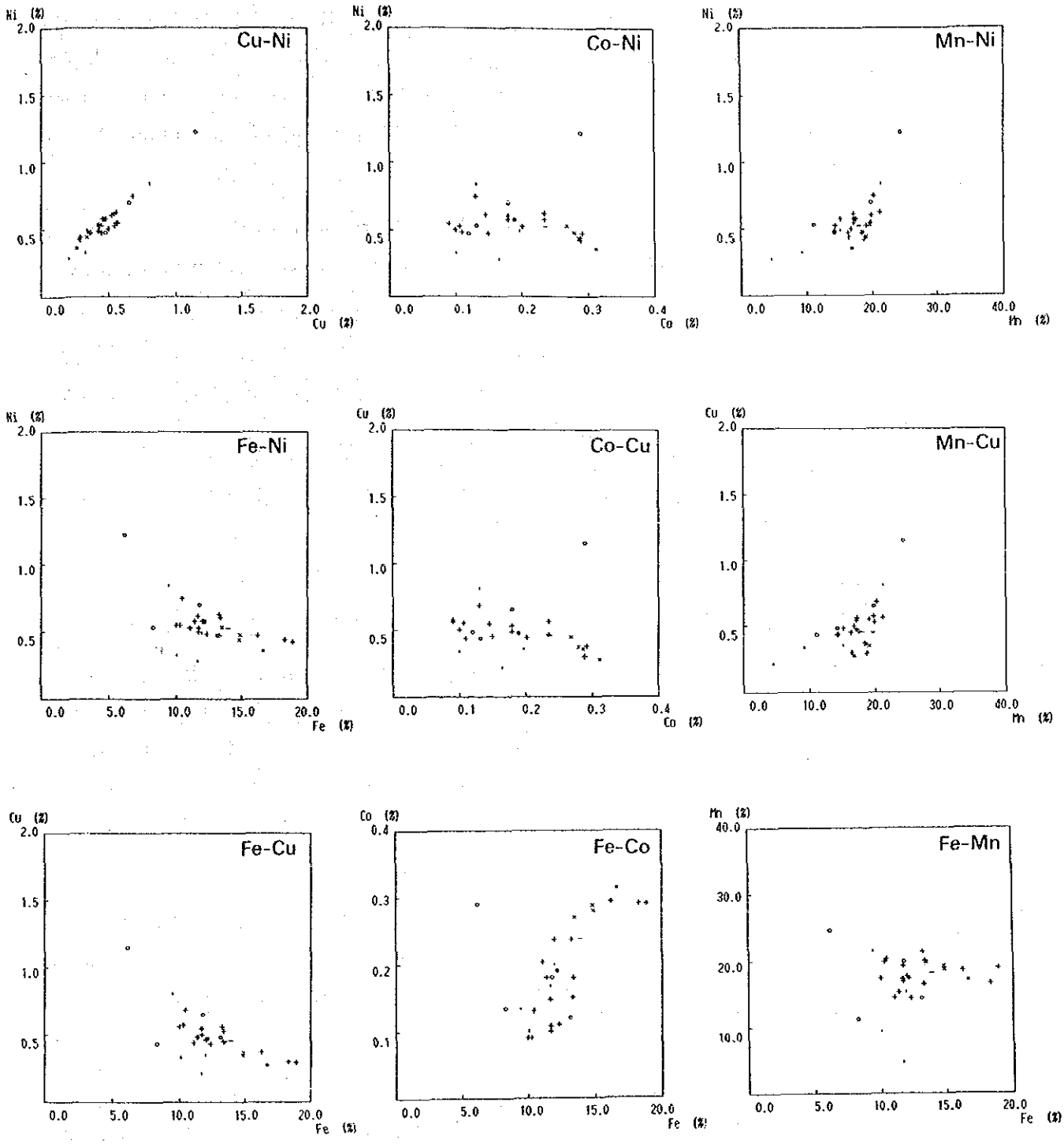

Legend ■ Spheroidal ○ Ellipsoidal ● Ellipsoidal fat
+ Pebble × Massive − Platy | Other (n = 30)

Figure 3-5-13 Scatter Distribution Diagram among Respective Components

Other above-average-grade parts are at the southern part of the western sea and the eastern part of the eastern sea. On the other hand, Co is high in the western to the northern and southeastern part of the western sea and in the northwest and southeastern part of the eastern sea. This corresponds to the high abundance zone of nodules. The grade distribution of each element is as follows (Annexed Figs. 8~12).

Table 3-5-2 Chemical Properties of Manganese Nodules

	Statistics (%)				Correlation Coefficient				
	Average	Standard deviation	Maximum	Minimum	Fe	Mn	Co	Cu	Ni
Ni	0.54	0.17	1.22	0.17	-0.47	0.70	-0.19	0.96	1.00
Cu	0.47	0.17	1.15	0.18	-0.58	0.64	-0.36	1.00	
Co	0.20	0.07	0.33	0.09	0.70	0.27	1.00		
Mn	17.01	4.44	24.45	2.98	0.14	1.00			
Fe	12.73	3.00	19.89	6.06	1.00				

(n=83)

[Ni]

The maximum grade of Ni is 1.22%, the minimum 0.17% and the average 0.54. The distribution of Ni grade shown in Annexed Fig. 8, denotes higher content in western fringe of the western sea. The parts with above-average Ni content occur sporadically in the southern part of the western sea and the eastern part of the eastern sea. These correspond to high manganese nodule abundance zones.

[Cu]

The maximun grade of Cu is 1.15%, the minimum 0.18% the average 0.47%. The distribution of Cu grade shown in Annexed Fig. 9, has similar tendency to that of Ni. The correlation coefficient between Ni and Cu is high at 0.96 as shown in Table 3-5-2.

[Co]

The maximum content of Co is 0.33%, the minimum 0.09% and the average 0.20%. Annexed Fig. 10 shows the equal-grade chart of Co. There are high Co localities in the western to the northern part and the southeastern part of the western sea and also in the northwestern and southeastern part of the eastern sea. These correspond to the high abundance zones of manganese nodules.

[Mn and Fe]

The maximum grade of Mn is 24.45%, the minimum 2.98% and the average 17.01. The maximum grade of Fe is 19.89%, the minimum 6.06% and the average 12.73%. The distribution of Mn and Fe is shown in Annexed Figs. 11,12. The grade of Mn shows fair positive correlation with Ni and Cu. It is high in the western margine of the surveyed sea. On the other hand, the grade of Fe shows fair negative correlation with Ni and Cu.

(2) Auxiliary components

Total analysis and minor element analysis were made on five representative samples selected from those used for the on-board, five principal component analysis, in order to investigate the auxiliary components of manganese nodules. Table 3-5-7 shows the results of both the total and minor element analysis along with the five principal components values. The TiO_2, CaO, Pb, V, Y and Sr contents of the manganese nodules in the surveyed areas are higher than the average content(*1) in the Clarion-Clipperton Prime Area by Mckelvey et al., (1979). On the contrary, SiO_2, Al_2O_3, BaO, Na_2O, K_2O, P_2O_5, Zn and Mo content is lower than the average of the Clarion-Clipperton Prime Area.

Total analysis and minor element analysis based on morphological classification show similar values and do not indicate extreme differences.

(3) Grade characterisics

i) Correlation among the elements

Table 3-5-2 shows the correlation coefficients of five elements. It is evident that the correlation is positive among Ni-Cu-Mn system and between Fe-Co system. It is also evident that the correlation is negative between the former and the latter systems. Fig. 3-5-14 shows the relation between the grade of five main elements and water depth. Clear correlation between water depth and element is not observed. Nevertheless, the Fe grade tends to decrease slightly in proportion to the water depth.

(*1) 7.81% Si, 0.61% Ti, 2.84% Al, 1.89% Mg, 1.47% Ca, 0.32% Ba, 1.87% Na, 0.82% K, 0.23% P, 0.048% Pb, 0.066% Mo, 0.048% V, 0.016% B, 0.13% Zn, 0.01% Y.

ii) Grade and morphology of manganese nodules

Table 3-5-3 shows the grade properties classified by the shape of the manganese nodules. They are summarized in the following four points.

Table 3-5-3 Morphology and Chemical Properties of Manganese Nodules

Morphology	(n)	Ni (%)				Cu (%)				Co (%)			
		Average	Standard deviation	Maximum	Minimum	Average	Standard deviation	Maximum	Minimum	Average	Standard deviation	Maximum	Minimum
Spheroidal	5	0.53	0.21	0.85	0.32	0.44	0.21	0.77	0.24	0.26	0.06	0.33	0.16
Ellipsoidal	9	0.63	0.23	1.22	0.47	0.56	0.24	1.15	0.38	0.19	0.06	0.29	0.12
Ellipsoidal fat	3	0.47	0.06	0.51	0.40	0.37	0.08	0.44	0.29	0.21	0.08	0.29	0.14
Pebble	42	0.57	0.13	0.88	0.32	0.50	0.13	0.79	0.27	0.19	0.07	0.30	0.09
Massive	7	0.42	0.09	0.52	0.27	0.33	0.08	0.43	0.20	0.30	0.03	0.33	0.25
Platy	8	0.53	0.23	0.86	0.17	0.45	0.24	0.83	0.21	0.22	0.06	0.29	0.13
Others	9	0.45	0.19	0.84	0.21	0.39	0.22	0.83	0.18	0.15	0.05	0.25	0.09

Morphology	(n)	Mn (%)				Fe (%)				Cu/Ni	Mn/Fe
		Average	Standard deviation	Maximum	Minimum	Average	Standard deviation	Maximum	Minimum		
Spheroidal	5	18.92	2.17	21.32	16.48	14.44	3.31	16.76	8.94	0.81	1.42
Ellipsoidal	9	16.71	3.92	24.45	10.05	10.68	2.31	13.18	6.20	0.89	1.69
Ellipsoidal fat	3	13.66	3.05	15.97	10.21	10.44	3.81	13.02	6.06	0.79	1.37
Pebble	42	17.99	2.77	22.80	9.23	12.79	2.85	19.66	8.38	0.86	1.46
Massive	7	17.66	2.38	19.65	12.79	14.47	1.10	15.89	12.99	0.78	1.22
Platy	8	17.16	6.61	23.49	3.05	14.55	3.78	19.89	9.61	0.86	1.27
Others	9	12.11	7.85	21.42	2.98	11.34	2.43	15.42	6.62	0.84	1.10

(a) Ellipsoidal and ellipsoidal fat types have high Ni, Cu and Mn, and low Co and Fe content.

(b) On the other hand, spheroidal and massive types have high Co and Fe and low Ni, Cu and Mn grade.

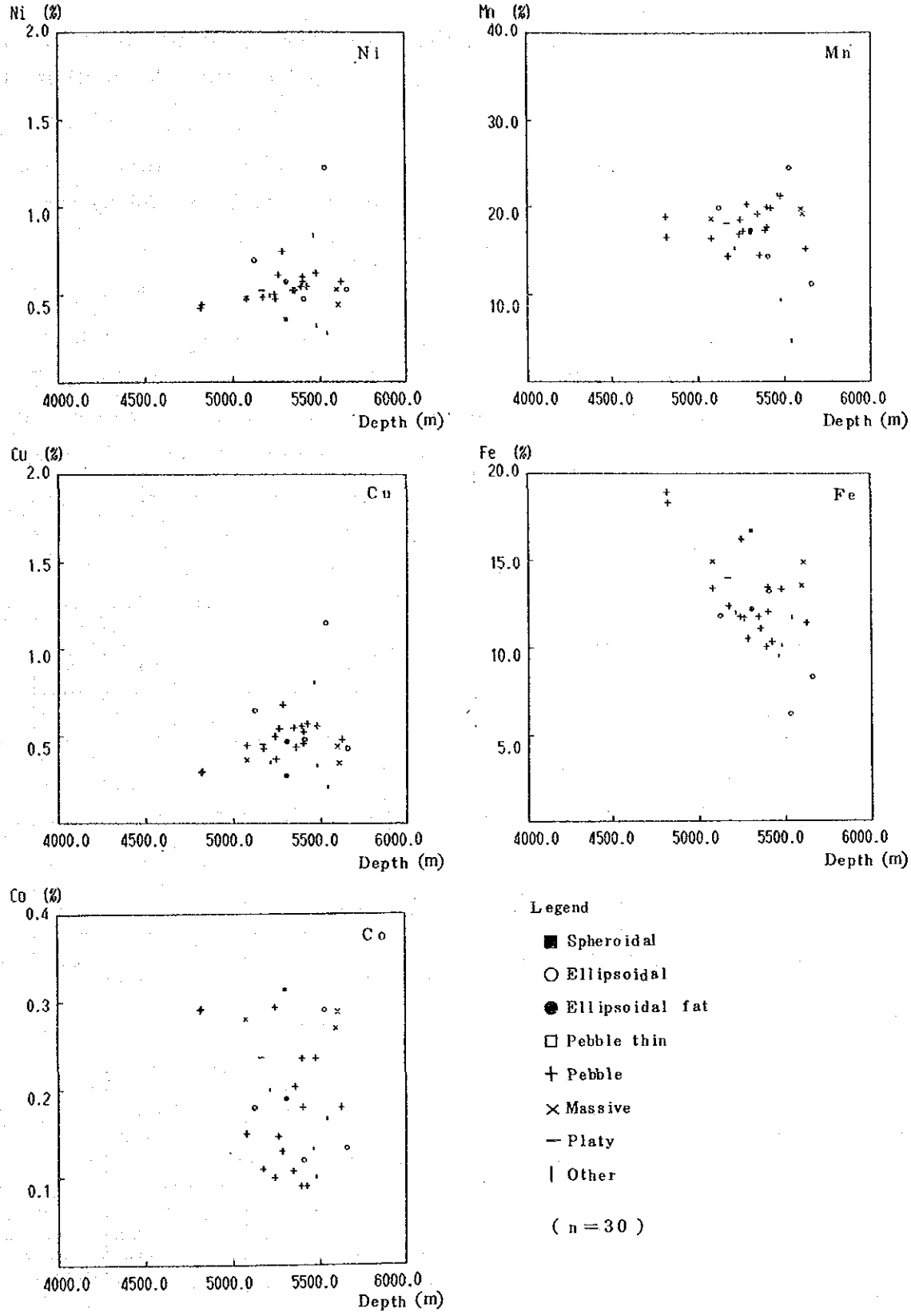

Figure 3-5-14 Relation between Each Five Principal Chemical Components and Water Depth

(c) The plate type shows intermediate behaviour between the above two groups, namely high Co, Mn and Fe and somewhat lower Ni and Cu content.

(d) Those nodules in the "other type" category have lower content of the useful metals and this is believed to be caused by the rock fragments constituting the core.

iii) Grade and grain size

The grade characteristies of grain-size groups are shown in Table 3-5-4. Tendency that the grade of Ni and Cu increases and the ratio of Cu/Ni and Mn/Fe decreases as the grain size decreases is observed. It is observed that Mn grade slightly decreases with larger grain size and that the Fe grade is higher in the medium size nodules (4~6 cm).

Table 3-5-4 Size and Chemical Properties of Manganese Nodules

Size	(n)	Ni (%)				Cu (%)				Co (%)			
		Average	Standard deviation	Maximum	Minimum	Average	Standard deviation	Maximum	Minimum	Average	Standard deviation	Maximum	Minimum
2 – 2	15	0.62	0.18	0.88	0.21	0.54	0.18	0.79	0.18	0.19	0.07	0.29	0.09
2 – 4	30	0.56	0.17	1.22	0.32	0.50	0.17	1.15	0.23	0.19	0.07	0.30	0.09
4 – 6	18	0.49	0.13	0.86	0.23	0.41	0.15	0.83	0.18	0.23	0.07	0.33	0.12
6 – 8	14	0.52	0.16	0.84	0.27	0.44	0.19	0.83	0.20	0.23	0.08	0.33	0.09
8 – 16	5	0.41	0.14	0.51	0.17	0.34	0.09	0.44	0.21	0.18	0.07	0.29	0.13
16 –	1	0.48	–	0.48	0.48	0.34	–	0.34	0.34	0.20	–	0.20	0.20

Size	(n)	Mn (%)				Fe (%)				Cu/Ni	Mn/Fe
		Average	Standard deviation	Maximum	Minimum	Average	Standard deviation	Maximum	Minimum		
2 – 2	15	17.85	5.04	22.80	2.98	12.21	2.99	17.94	8.39	0.86	1.54
2 – 4	30	17.55	3.83	24.45	4.39	12.51	2.88	18.89	6.20	0.88	1.49
4 – 6	18	17.19	4.17	23.49	3.06	14.10	2.70	19.89	9.61	0.82	1.26
6 – 8	14	17.06	4.15	22.80	6.69	12.97	3.31	19.07	6.62	0.82	1.37
8 – 16	5	10.82	5.09	15.97	3.05	10.17	2.89	13.02	6.06	0.88	1.12
16 –	1	15.06	–	15.06	15.06	12.05	–	12.05	12.05	0.71	1.25

iv) Grade and topography

Table 3-5-5 shows the grade properties classified by topography. The Ni and Cu grade decreases in the order of flat to knoll to seamount topography, while that of Co and Fe shows the opposite trend.

Table 3-5-5 Sea Floor Topography and Chemical Properties of Manganese Nodules

Topography	(n)	Ni (%)				Cu (%)				Co (%)			
		Average	Standard deviation	Maximum	Minimum	Average	Standard deviation	Maximum	Minimum	Average	Standard deviation	Maximum	Minimum
Flat	21	0.57	0.19	1.22	0.32	0.52	0.19	1.15	0.27	0.18	0.08	0.31	0.09
Knoll	8	0.49	0.11	0.69	0.28	0.41	0.14	0.65	0.21	0.21	0.07	0.29	0.10
Seamount	1	0.42	–	0.42	0.42	0.29	–	0.29	0.29	0.29	–	0.29	0.29

Topography	(n)	Mn (%)				Fe (%)			
		Average	Standard deviation	Maximum	Minimum	Average	Standard deviation	Maximum	Minimum
Flat	21	17.65	3.50	24.45	9.23	11.89	2.40	16.70	6.20
Knoll	8	15.46	4.72	19.80	4.62	13.36	2.62	18.33	11.08
Seamount	1	18.87	–	18.87	18.87	18.92	–	18.92	18.92

v) Grade and surficial sediments

Only two types of surficial sediments were found in the survey area, brown clay and calcareous clay. Manganese nodules could not be collected at the sites of calcareous clay occurrence and thus it is not possible to discuss the relationship (Table 3-5-6).

Table 3-5-6 Bottom Sediments and Chemical Properties of Manganese Nodules

Sediment	(n)	Ni (%)				Cu (%)				Co (%)			
		Average	Standard deviation	Maximum	Minimum	Average	Standard deviation	Maximum	Minimum	Average	Standard deviation	Maximum	Minimum
Brown clay	28	0.55	0.17	1.22	0.32	0.49	0.18	1.15	0.27	0.19	0.08	0.31	0.09
Siliceous clay	0	–	–	–	–	–	–	–	–	–	–	–	–

Sediment	(n)	Mn (%)				Fe (%)			
		Average	Standard deviation	Maximum	Minimum	Average	Standard deviation	Maximum	Minimum
Brown clay	28	17.55	3.16	24.45	9.23	12.57	2.84	18.92	6.20
Siliceous clay	0	–	–	–	–	–	–	–	–

4) Mineralogy

X-ray diffraction analysis and microscopic observation of polished thin sections were carried out on representative samples in order to investigate the mineral composition and inner structure of the manganese nodules.

(1) X-ray diffraction

Manganese nodules were roughly divided into the outer layer, inner layer and the core, they were further subdivided into serveral smaller parts and X-ray diffraction was carried out. The results of analysis are in laid out in Table 3-5-8 and the X-ray diffraction patterns are in Fig. 3-5-15. A notable result obtained, is that the common manganese minerals 10Å manganite and δ-MnO_2 were not identified by the X-ray diffraction and only an unknown manganese mineral was recognized. The two common minerals, however, were identified by microscopic observation, an the probable explanation for the lack of diffraction pattern of these minerals is that their crystalinity is low.

Phillipsite and other minerals were also identified. Although in small amount, phillipsite occurs in almost all of the samples. Illite-montmorillonite mixed layer mineral with low crystalinity, plagioclase, augite, quartz and magnetite were detected in minor amount.

(2) Microscopic studies

Polished thin sections were prepared for manganese nodule spheroids and observed microscopically by both reflecting and transmitted light. Spheroidal nodule (88SO679FG02, Fig. 3-5-16).

[Observation by unaided eyes]

"S" type manganese nodule with approximately 5cm diameter. The section was cut to include the centre of the nodule and is potato-shaped, almost circular, the long diameter 5.5 cm. The core is about 8×3 mm. The manganese mineral zone has concentric structure.

[Observation by microscope]

The white core is composed almost totaly of montmorillonite, this was confirmed by X-ray diffraction. Phillipsite occurs as ascicular, platy and radial euhedral crystals (0.25~0.1 mm) in the insterstices of the bands of manganese minerals surrounding the core.

The manganese minerals generally have layered structure. Under the reflecting microscope, grayish white and gray bands alternate as

Table 3-5-7 Total and Minor Element Analysis of Manganese Nodules

Sample No.		88S0681 FG03	88S0674 FG03	88S0874 FG01	88S0679 FG02	88S0879 SC01
Topography		(Quasi) Seaknol	(Plain) Seaknol	(Plain) Flat	(Quasi) Flat	(Quasi) Flat
Depth (m)		5,357	5,170	5,400	5,597	5,310
Morphology		Ellipsoidal fat	Spheroidal	Massive	Massive	Spheroidal
Size (cm)		2–4	4–6	2–4	4–6	4–6
Major Metal Contents (%)	Ni	0.52	0.52	0.60	0.52	0.35
	Cu	0.43	0.46	0.53	0.44	0.27
	Co	0.20	0.24	0.18	0.27	0.31
	Mn	14.37	18.02	19.99	19.75	16.91
	Fe	11.08	13.98	13.44	13.53	16.70
Major Element Contents (%)	SiO_2	17.08	13.45	14.95	14.78	16.76
	TiO_2	1.19	1.52	1.22	1.54	2.05
	Al_2O_3	6.26	5.02	4.75	5.66	6.05
	Fe_2O_3	17.89	21.56	17.94	20.06	21.75
	FeO	<0.01	<0.01	<0.01	<0.01	<0.01
	MnO	22.02	22.46	24.27	23.14	19.09
	MgO	2.34	2.19	2.55	2.08	1.98
	CaO	2.48	2.44	2.56	2.44	2.44
	BaO	0.12	0.17	0.12	0.14	0.15
	Na_2O	2.28	2.02	2.25	2.17	2.15
	K_2O	1.27	0.72	0.77	0.87	0.93
	P_2O_5	0.77	0.70	0.52	0.58	0.58
	L.O.I.	20.26	19.01	19.92	20.12	22.78
	Total	93.96	91.26	91.82	93.58	96.71
Minor Element Contents (ppm)	Pb	659	780	643	830	805
	Zn	644	880	884	638	565
	As	103	106	84	93	91
	Sr	825	985	820	956	941
	V	443	436	416	445	418
	Mo	284	246	248	274	178
	B	142	179	146	167	172
	Y	120	135	109	120	125
	Zr	425	522	404	415	389
	Pt	0.1	0.1	0.1	0.1	0.1
	T.R.E.	1719	1925	1396	1966	1992

Table 3-5-8 Result of X-ray Diffraction Analysis of Manganese Nodules

No.	Sample No.	Mn-Mineral		Silicate Mineral						Others			
		Undetermined Mn-Mineral*		Plazioclase	Pyroxene	Olivine	Quartz	Phillipsite	Clay mineral**	Calcite	Apatite	Magnetite	
CM-1	88S0681FG03	•						•					bulk
CM-2	88S0674FG03	•					•	•	•				bulk
CM-3(1)	88S0874FG01	•						•					outer layer
CM-3(2)	88S0874FG01	•		•									inner layer
CM-3(3)	88S0874FG01	•						•					core (rock)
CM-4	88S0679FG02	•						•					bulk
CM-5(1)	88S0879SC01	•						•					outer layer
CM-5(2)	88S0879SC01			•			•	•					inner layer
CM-5(3)	88S0879SC01			•	•		•	○	•			•	core (rock)
CM-6	88S0681FG03									•	◎		core (rock)

◎: Abundant ○: Common •: Little

* δMnO_2 under microscopic observation.

** Probably illite/montmorillonite mixed layer mineral.

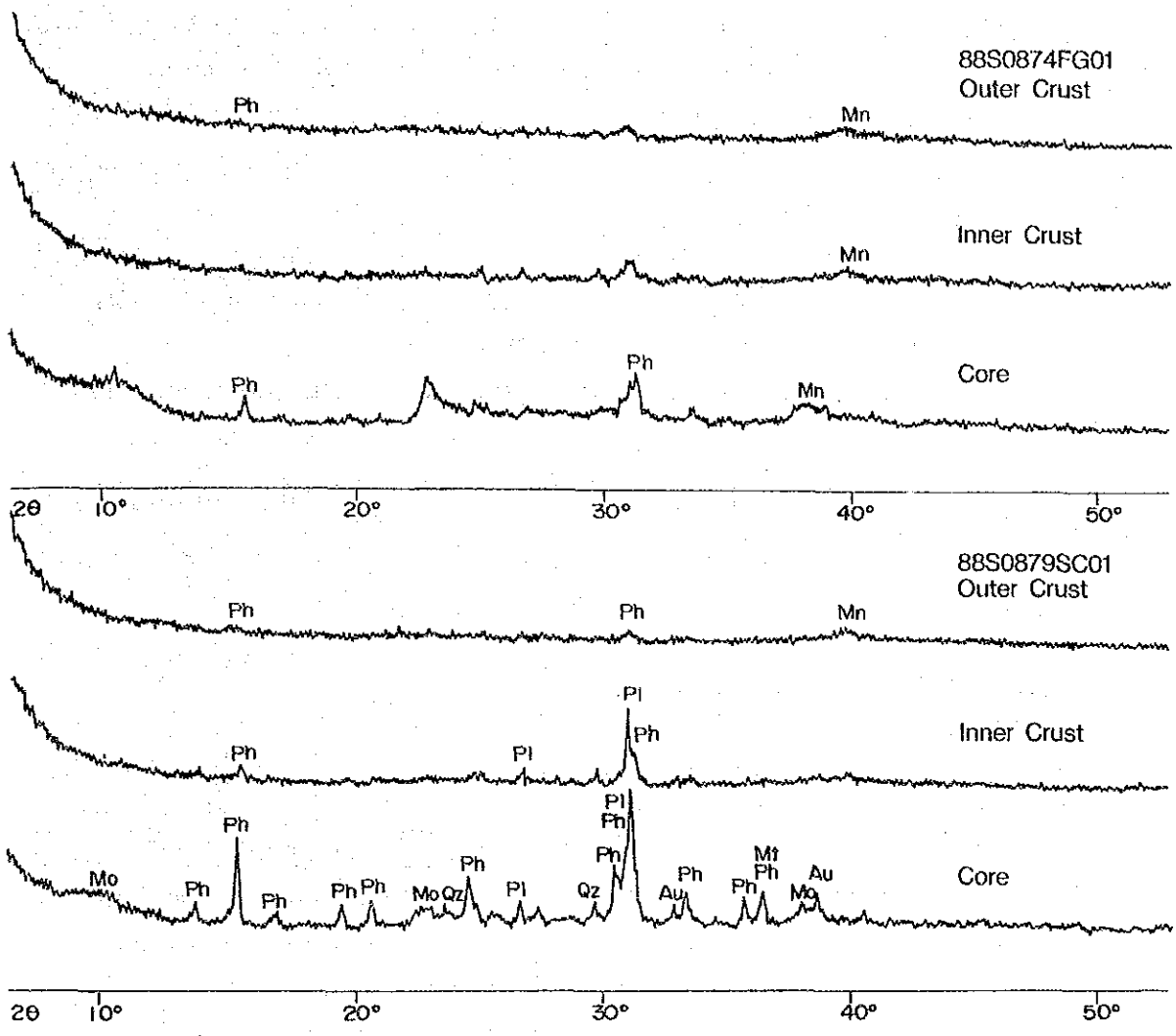

Legend Mn : Mn-mineral Au : Augite Mo : Clay mineral
Mt : Magnetite Ph : Phillipsite Pl : Plagioclase Qz : Quartz

Figure 3-5-15 X-ray Diffraction Pattern of Manganese Nodules

crustification, and these appear respectively as dark brown, reddish brown~yellowish brown bands under tramsmitted light. The former, namely the material with grayish white reflection has high reflectivity, weak anisotropism under reflected light and is hard. It is considered to be 10Å manganite. The latter, gray reflection material, has low reflectivity and is isotropic with low hardness. It is considered to be δ-MnO_2. These two minerals occur in approximately equal amount.

Mineral which is yellowish brown in tramsmitted and dark gray under reflected light occurs in the interstices of the manganese minerals. This is probably amorphous hydrous iron hydroxide.

Clay minerals mainly occur between the bands of manganese minerals, but rarely minute fragments of plagioclase (0.05~0.03 mm, fresh, clear polysynthetic twinning) and siliceous microfossils (probably radiolaria) are observed.

5) Sea-floor Conditions and Abundance

(1) Sea-floor topography and abundance

The relation between the sea-floor topography and manganese nodule abundance at each sampling point is shown in Figs. 3-5-17, 3-5-18.

Difference in abundance was not observed between the plains and quasi plains, it is low with average of 2~3.5 kg/m^2 for both zones. The data for the micro-topographic, mountainous zones are few with only six stations, but the result is barren, 0 kg/m^2. These six stations, however, are not in the micro-topographic seamounts and knolls, but in the flat parts of mountainous zones, as shown in Fig. 3-5-18.

There are, however, clear difference in abundances between the micro-topographic flat parts and knolls in the plain zone. The former is 0.39 kg/m^2 while the latter is somewhat higher at 6.9 kg/m^2. The plain zone and the flat parts of the mountainous zone have smooth sea-floor, and from SBP records, development of turbidites is inferred.

On the other hand, in the quasi plain zone, the difference of abundance between the flat parts and knolls is small at 3 kg/m^2 and 5 kg/m^2. These flat parts of the quasi plain zone are different from the above flat parts of the plains and mountain zones that the relief of the sea floor is fairly large.

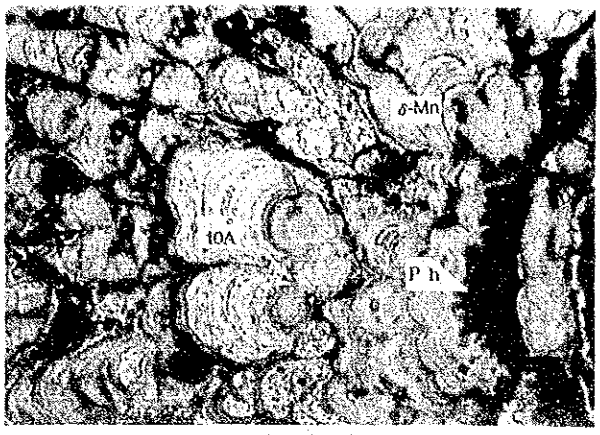

(Inner part) reflected Light

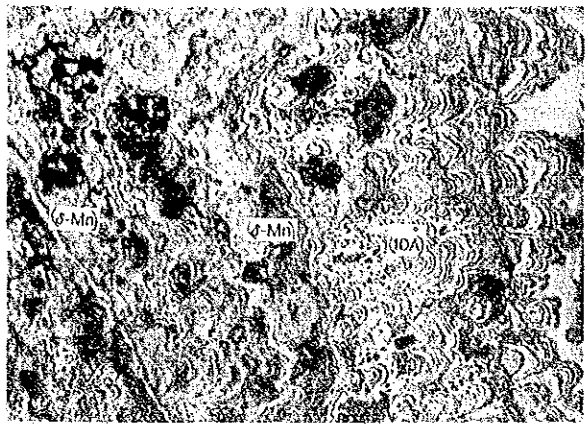

(Outer part) reflected Light

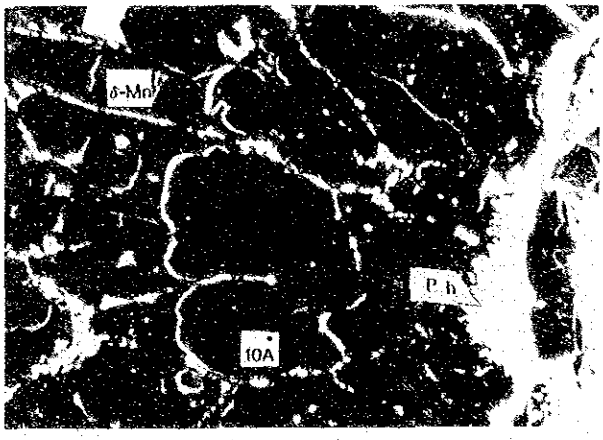

(Inner part) Polarized Light (Open Nicols)

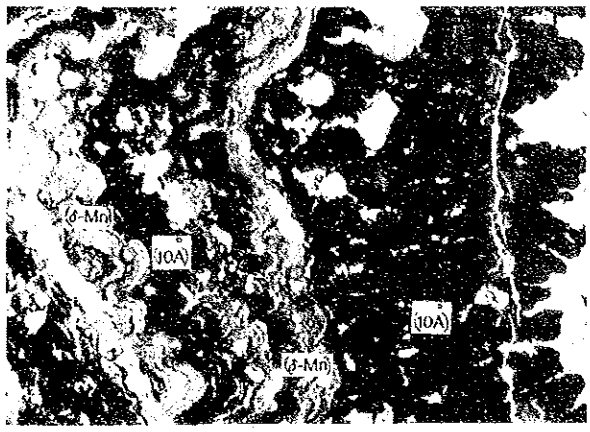

(Outer part) Polarized Light (Open Nicols)

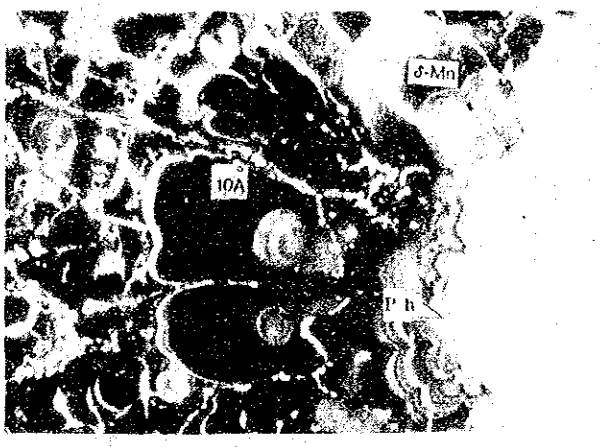

(Inner part) Polarized Light (Crossed Nicols)

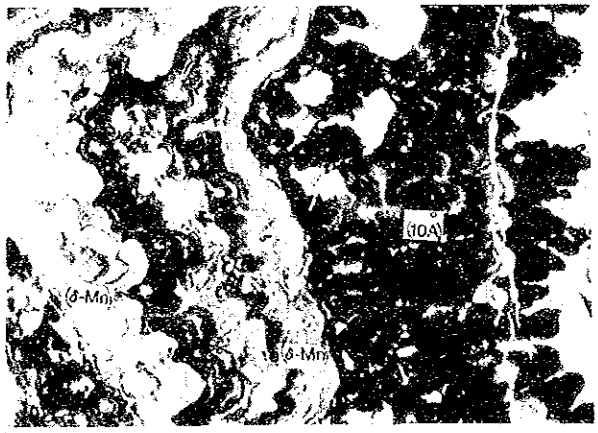

(Outer part) Polarized Light (Crossed Nicols)

Legend 10Å : 10Å Manganite δ-Mn : δ-MnO_2 Ph : Phillipsite

Sample No. 88S0679FG02 Scale : 8.75X

Figure 3-5-16 Macro-Photo and Microscopic Photos of Polished Thin Section of Manganese Nodules

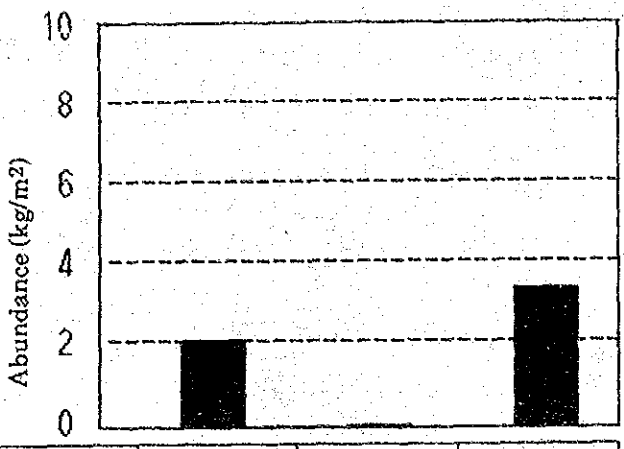

Topography	Plain	Mountainous	Quasi Plan
Average Abundance (kg/m2)	2.02	0.00	3.45
Weight Coefficient (kg/m2)	18.2	–	23.6
Embeded ratio (%)	48.5	–	51.0
Number of Samples	24	6	42

(1) Macroscopic Topography

Figure 3-5-17 Relation between Macroscopic Topography and Abundance of Manganese Nodules

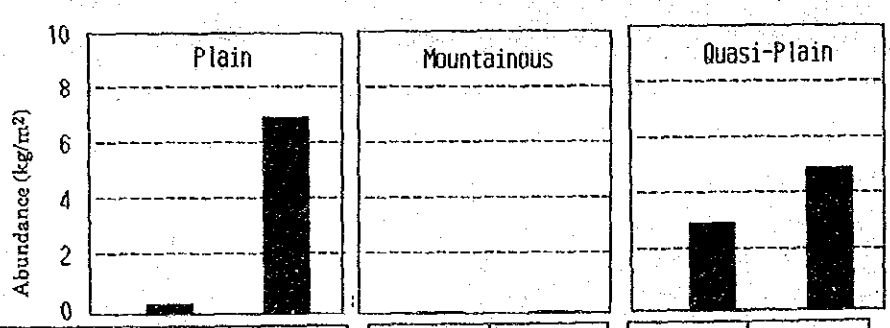

Topography	Flat	knoll	Flat	knoll	Flat	knoll
Average Abundance (kg/m2)	0.39	6.90	0	–	3.05	3.05
Weight Coefficient (kg/m2)	15.2	27.9	–	–	24.8	24.8
Embeded ratio (%)	74.5	37.8	–	–	61.2	61.2
Number of Samples	18	6	6	0	33	33

(2) Microscopic Topography

Figure 3-5-18 Relation between Microscopic Topography and Abundance of Manganese Nodules

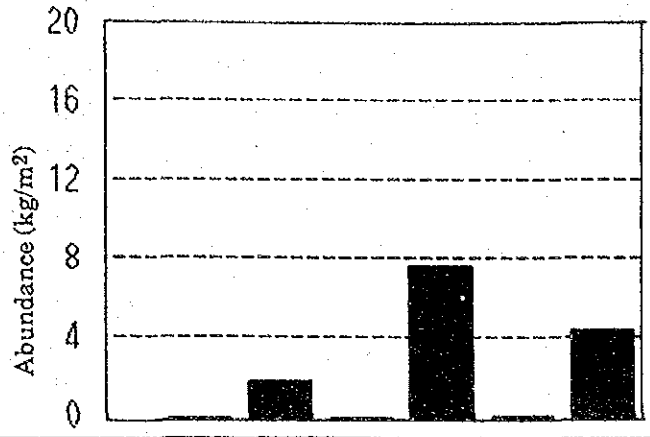

SBP Type	b	e1	c	d1	d2	ds
Average Abundance (kg/m2)	02.1	2.0	0.1	7.9	0.4	4.6
Weight Coefficient (kg/m2)	23.5	14.8	30.0	24.5	20.9	21.6
Embeded ratio (%)	27.4	81.4	49.0	47.2	0.0	55.3
Number of Samples	7	18	14	11	8	14

Figure 3-5-19 Relation between SBP Type and Abundance of Manganese Nodules

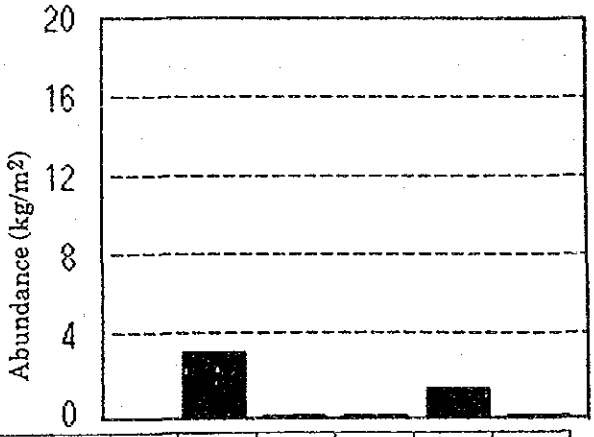

Transparent Layer (m)	10	20	30	40	50<
Average Abundance (kg/m2)	3.2	0.1	0.1	1.6	0.1
Weight Coefficient (kg/m2)	19.1	18.6	14.1	17.3	14.1
Embeded ratio (%)	53.2	-	61.2	75.3	86.2
Number of Samples	9	3	5	5	4

Figure 3-5-20 Relation between Upper Transparent Layer Thickness and Abundance of Manganese Nodules

(2) SBP type and abundance

The relation between the SBP type and abundance is shown in Fig. 3-5-19. It is seen from the figure that the abundance is relatively high in parts with opaque layers at the top and the relief is high, namely d_1 (knoll, seamounts) and ds where the average abundance is 7.9 kg/m^2 and 4.6 kg/m^2 respectively. The parts where the topography is flat, regardless of the existence of opaque upper layers c, d_2 type,is almost invariably barren.

In the types with upper transparent layers, b is mostly barren, but e_1 shows somewhat higher 2 kg/m^2.

The weight coefficient*1 of type e_1 is smaller than other types, indicating smaller grain-diameter. The average embedded ratio is 81.4%, which is considerably higher than other types.

(3) Upper transparent layers and abundance

The relationship between the upper transparent layers and the abundance of manganese nodules is shown in Fig. 3-5-20. It is seen that there is no clear relation between the thickness of the transparent layer and the abundance. This of course, may be due to the insufficient amount of data. The average embedded ratio tends to increase with the thickness of the upper layers

6) Total Metal Content

In assessing the resource potential of manganese nodules, it is necessary to consider the total metal content - particutarly the target metals, Ni, Cu, Co - of the manganese nodules in the survey area. The metal density (the amount of metal in an unit area) was calculated for Ni, Cu, Co for earch station as follows. The results are shown in Annexed Figs. 13~15.

Ni density = abundance × (1 - water content) × Ni grade
Cu density = abundance × (1 - water content) × Cu grade
Co density = abundance × (1 - water content) × Co grade
Cut-off values are not set for abundance and grade

---

*1 weight coefficient (kg) = uplifted weight(kg)/(coverage × grab opening (m^2))
= abundance/coverage

It is seen from this excercise that in the survey area, the zones of high Ni, Cu, Co density nearly correspond with the high manganese nodule abundance zones.
The amount of Ni, Cu, Co in unit area is low and the stations exceeding 20 g/m^2 for individual metal content, bonanza, are few. Thus, for the metal content calculation of this area, the total (Ni+Cu+Co) density was calculated rather than for each metal. The (Ni+Cu+Co) density of each station is shown below.

Average: 22.6 g/m^2
Maximum: 80.0 g/m^2
Minimum: 0 g/m^2

The total (Ni+Cu+Co) content of manganese nodules in the survey area (covering the area of sampling sites, 122,200 km^2) is calculated as follows.

$$22.6\ (g/m^2) \times 122{,}200\ (km^2) = 2.75 \times 106\ (t)$$

Thus the value of 2.76 million tons is arrived at. This figure, however, is solely for rough reference only. This is a very small value compared to other manganese nodule areas of the world.

3-6 Discussions

The characteristics of manganese nodule distribution in the survey area is that the abundance is low and the continuity of the manganese nodule occurrence is poor. Of the 24 stations sampled, only five showed abundance exceeding 7.5 kg/m^2 and none exceeded 10 kg/m^2. The major factors which produced this low manganese nodule distribution is considered to be-

a) Low biological productivity.
b) Sea floor topography, large coverage of the area by seamounts and knolls.
c) Lack of flat area near CCD.

In the area, siliceous sediments which are indicative of high biological productivity were not observed at all, thus the productivity of micro-organisms which play the role of carrier of metals (Mn, Ni, Cu, etc.) to the sea-floor (D.S. Cronan, 1984) is considered to be low.

There are a large number of atolls, seamounts and knolls destributed in the area, causing the development and wide distribution of turbidites. The flat surface is almost invariably covered by these sediments and the low sedimentation rate necessary for the formation of manganese nodules was not maintained. The area with SBP e_1 and d_2 corresponds to this turbidite predominant zone (30~40 m thick). It is said that the most favourable water depth zone for manganese nodule development and the zone where manganese nodule distribution is domimant is between the lithocline level and CCD or near CCD (D.S. Cronan, 1984). But in the survey area, the areal extent of the sea-floor near the estimated CCD (4,900~5,000 m) is small and the localities best suited for manganese nodule development appears to be small.

Aside from these factors, the inflow of the Antarctica Bottom current (ABW) is inferred to be small. The sea-floor topography of the survey area and its vicinity, such as the bank zone to the south and Robbie Ridge (shallow part 3,500 m deep), hinders the flow of ABW into this area. The accurate relationship between these topographic features and the inflow must await further observation and analysis, but it is believed that there is a strong possibility that this is another factor which contributes to the difficulty of maintaining low sedimentation rate necessary for manganese nodule development.

The present survey, as shown above, resulted in evaluating the various hypotheses regarding the genesis of the manganese nodules in a low abundance area. The highly abundant zone which occur locally in the northeast fringe of the area, is not expected to extend very much from the MFES data and also from the fact that the sea becomes

deeper northward. Regarding the grade, the content of four elements, Ni, Cu, Co, Mn is higher than that of the Cook Islands area, but the content of five elements including Fe is lower than in Kiribati waters. The Mn/Fe ratio is 1.34 and is closer to the nature of smooth type rather than the rough type manganese nodule.

Chapter 4. Results of the Survey (Cobalt Crust)

4-1 Seamount Topography

1) Classification

Seamounts of the survey area are classified by their morphology as ahown in Table 4-1-1.

Table 4-1-1 Classification of Topographic Type of Seamount

Classification	Morphological characteristics
Single seamount guyot	The summit is flat and horizontal.
Peaked seamount	The summit is sharp.
Atoll	The summit reaches the surface of the sea and forms atoll.

The seamounts surveyed during the present cruise are five guyots, three peaked ones and two atolls. SB04 and SB08 were counted as two seamounts. The seamount topography is roughly divided into "Top" and "Slope", which are subdivided as follows in order to facilitate the description (Table 4-1-2).

Table 4-1-2 Classification of Topography of Seamount

Classification		Morphological characteristics
The top	Central part	The centre of the summit where it is flat or gently inclined.
	Shoulder	The transitional zone from the central part of the top to the upper part of slope.
The slope	Upper part	The upper part where the slope is steep.
	Middle part	The part between the upper and the lower part of the slope. The inclination is medium.
	Lower part	The lower part where the slope is gentle.

Table 4-1-3 Topographic Feature of Individul Seamount

	Range of Depth (m)	Area (km^2)	Average Slope	Maximum	Minimum	0 - 10°	10 - 20°	20 - 30°	30°<
SB 01 Seamount									
Flat summit	- 1400	2.5	3.6°	1.5°	7.5°	100.0%	0.0%	0.0%	0%
Upper slope	1400 - 2000	54.5	12.4°	3.3°	24.6°	33.9%	56.5%	9.7%	0%
Middle slope	2000 - 3000	183.6	14.7°	2.4°	32.0°	13.5%	74.4%	11.6%	5%
Lower slope	3000 - 4500	709.2	9.7°	.3°	29.0°	55.3%	42.0%	2.7%	0%
SB 02 Seamount									
Flat summit	- 50	590.2	.7°	.3°	10.0°	100.0%	0.0%	0.0%	0%
Upper slope	50 - 400	212.9	10.8°	3.6°	23.2°	48.2%	50.2%	1.6%	0%
Middle slope	400 - 800	664.6	5.5°	.3°	26.0°	86.2%	11.0%	2.8%	0%
Lower slope	800 - 2500	2240.3	7.3°	.3°	28.5°	70.3%	25.1%	4.7%	0%
SB 03 Seamount									
Flat summit	- 1000	317.0	1.4°	.3°	12.3°	99.5%	0.5%	0.0%	0%
Upper slope	1000 - 1400	795.2	4.5°	.3°	20.6°	94.0%	5.9%	0.1%	0%
Middle slope	1400 - 2000	1331.3	4.4°	.3°	18.4°	95.2%	4.8%	0.0%	0%
Lower slope	2000 - 3000	1169.8	4.9°	.7°	18.4°	93.5%	6.5%	0.0%	0%
SB 04 Seamount									
Flat summit	- 50	83.7	4.1°	.4°	23.5°	80.0%	18.0%	2.0%	0%
Upper slope	50 - 400	30.4	21.2°	11.8°	29.5°	0.0%	32.4%	67.6%	0%
Middle slope	400 - 2000	269.6	18.6°	9.2°	33.8°	1.3%	59.2%	37.9%	2%
Lower slope	2000 - 3000	1215.7	4.7°	.3°	16.6°	90.5%	9.5%	0.0%	0%
SB 05 Seamount									
Upper slope	2100 - 2800	137.5	10.1°	.4°	21.1°	56.9%	41.3%	1.9%	0%
Middle slope	2800 - 3300	152.5	9.3°	1.9°	20.5°	62.9%	36.5%	0.6%	0%
Lower slope	3300 - 4500	228.0	8.4°	.3°	17.8°	64.0%	36.0%	0.0%	0%
SB 06 Seamount									
Flat summit *1									
Upper slope	500 - 1500	199.2	24.4°	7.8°	39.7°	0.5%	21.5%	60.7%	17%
Middle slope	1500 - 2500	384.3	15.4°	4.2°	27.9°	10.7%	75.2%	14.1%	0%
Lower slope	2500 - 3500	582.4	11.5°	4.5°	20.6°	33.8%	65.9%	0.3%	0%
SB 07 Seamount (E)									
Upper slope	500 - 1500	105.3	10.7°	1.0°	21.4°	41.8%	56.6%	1.6%	0%
Middle slope	1500 - 2500	314.1	12.8°	1.0°	24.3°	24.7%	73.4%	1.9%	0%
Lower slope	2500 - 3500	287.2	11.3°	3.4°	30.0°	42.8%	54.2%	3.0%	0%
SB 07 Seamount (W)									
Flat summit *1									
Upper slope	500 - 1500	74.2	18.5°	1.6°	36.4°	22.0%	26.8%	43.9%	7%
Middle slope	1500 - 2500	170.8	13.2°	4.5°	22.7°	21.4%	75.5%	3.1%	0%
Lower slope	2500 - 3500	164.0	9.2°	1.6°	17.1°	60.2%	39.8%	0.0%	0%
SB 08 Seamount (S)									
Flat summit	- 1500	39.6	6.2°	0.9°	15.7°	73.9%	26.1%	0.0%	0%
Upper slope	1500 - 2000	65.9	16.1°	5.7°	25.6°	18.9%	55.4%	25.7%	0%
Middle slope	2000 - 3000	208.8	17.5°	5.7°	26.4°	5.6%	69.1%	25.3%	0%
Lower slope	3000 - 4000	411.8	13.2°	1.9°	29.7°	21.7%	72.7%	5.5%	0%
SB 08 Seamount (N)									
Upper slope	1500 - 2000	18.6	14.5°	8.1°	21.9°	4.8%	85.7%	9.5%	0%
Middle slope	2000 - 3000	87.7	18.9°	6.4°	26.3°	4.1%	51.5%	44.3%	0%
Lower slope	3000 - 4000	174.6	17.3°	4.0°	26.0°	2.1%	81.0%	16.9%	0%

*1. Because of an atoll, area and inclination of slope is not determined.

Table 4-1-4 Topographic Feature of Individual Seamount (1)

Seamount	Macroscopic Topography	Microscopic Topography
S B 0 1	Location 4°41'S . 176°35'E Type Guiyot Scale *1 12 ×10 km Range of Water Depth 1,390～5,000m Size of Top 6 × 3 km Inclination of Slope*2 Upper part 12° (3°～25°) Middle part 15° (3°～32°) Lower Part 10° (0°～29°) Others Direction of major axis N 20° W.	SBP Data Acuostic transparent layer is not observed.Many side-echo is observed in southern and northern slope. Area(Water depth) (less than 2,500m 123 km²) 0 ～1,400m 18 km² 1,400 ～2,000m 54 Km² 2,000 ～3,000m 183 Km² 3,000 ～4,500m 709 km² Others At the summit,rise and pinnacle is observed
S B 0 2 Westside	Location 12°00'S .179°35'W Type Guiyot Scale *1 70 × 50 km more Range of Water Depth 30～3,500 m Size of Top 50 × 12 km more Inclination of Slope*2 Upper part 11° (4°～23°) Middle part 6° (0°～26°) Lower Part 7° (0°～29°) Others Direction of major axis N 45°W.	SBP Data Acoustic transparent layer is observed on gentle slopes. Range of the thickness10～30m. Area(Water Depth) (less than 2,500m 3708 Km²) 0～ 50m 590 Km² 50～ 400m 212 Km² 400～ 800m 664 Km² 800～2,500m 2240 km² Others At northwest,the bank (water depth20m)exsist.
S B 0 3	Location 11°20'S .179°05'W Type Guiyot Scale *1 75 × 44 km more Range of Water Depth 830m～3,000m Size of Top 15x6,15x14 Km more Inclination of Slope*2 Upper part 5° (0° ～21°) Middle part 4° (0° ～18°) Lower Part 5° (1° ～18°) Oters Direction of major axis N 70°W.	SBP Data Acoustic transparent layer is observed on the summit and gentle slope.the range of thickness 10 ～50m. Area(Water Depth) (less than 2,500m 3301 Km²) 0 ～1,400m 317 Km² 1,400 ～2,000m 54 Km² 2,000 ～3,000m 183 Km² 3,000 ～4,500m 709 km² Others two summits are observed .their water depth is about 1,000m.
S B 0 4	Location 10°40'S .179°10'W Type Guiyot(Macaw bank) Scale *1 24 × 28 km Range of Water Depth 20 ～3,500m Size of Top 9 × 8 km Inclination of Slope*2 Upper Part 21° (12° ～30°) Middle Part 19° (9° ～34°) Lower Part 5° (0° ～17°) Oters Nearly cone shape.	SBP Data Acoustic transparent layer is not observed. Area(Water Depth) (less than 2,500m 709 km²) 0 ～ 50m 84 km² 50～ 400m 30 km² 400～2,000m 269 km² 2,000 ～3,000m 1215 km² Others The slope is gentle.

*1 Contour line at 2,500m in water depth.
*2 Subdivision of slope refer table 4-1-3.

Table 4-1-4 Topographic Feature of Individual Seamount (2)

Seamount	Macroscopic topography	Microscopic topography
S B 0 5	Location 8°20'S .177°10'E Tpye Peaked seamount scale *1 22 × 3 km more Range of Water Depth 1,950～4,000m Size of Top 23 ×0.2 km more Inclination of Slope*2 Upper Part 10° (0°～21°) Middle Part 9° (2°～21°) Lower Part 8° (0°～18°) Others Direction of the major axis N 0°W. Ridge like seamount extend over23km	SBP Data Acoustic transparent layer is not observed.Many side-echo is observed on western slope. Area (less than 2,500m 66 km²) 0～2,100m 4 km² 2,100～2,800m 137 km² 2,800～3,300m 152 km² 3,300～4,500m 228 km² Others This seamount has two summits. Eastern slope is steep and western slope undulate.
S B 0 6	Location 8°30'S . 179°08'E Type Atoll (Funafuti) Scale *1 30 × 26 km Range of Water Depth 0 ～4,500m Size of Top 22 × 14 km Inclination of Slope*2 Upper Part 24° (8°～40°) middle Part 15° (4°～28°) Lower Part 12° (5°～21°) Others There are no direction. The shape of summit is nealy pear.	SBP Data Acoustic transparent layer is not observed.Side-echo is not observed on gentle slope. Area(Water Depth) (less than 2,500m 906 km²) 0～2,100m 322 km² 2,100～2,800m 137 km² 2,800～3,300m 152 km² 3,300～4,500m 228 km² Others The slope is steep.
S B 0 7 (E)	Location 7°27'S.179°30'E Type Peaked seamount Scale *1 15×12km, 16×14km Range of Water Depth 450 ～3,500m Size of Top 6 × 2 km Inclination of Slope*2 Upper Part 11° (1°～21°) middle Part 13° (1°～24°) Lower Part 11° (3°～30°) Others Two summit exsist at the east and the west.	SBP Data Acoustic transparent layer is not observed. Area(water depth) (less than 2,500m 419 km²) 500～1,500m 12 km² 1,500～2,500m 314 km² 2,500～3,500m 287 km² Others Pinnacles and side-echo are observed at the summit.
S B 0 7 (W)	Location 7°29'S .178°41'E Type Atoll(Vaitupu) Scale *1 23 × 11 km more Range of Water Depth 0 ～3,500m Size of Top 6 ×3 km more Inclination of Slope*2 Upper Part 19° (2°～36°) Middle part 13° (5°～23°) Lower Part 9° (2°～17°) Others Direction of the major axis N50°W.	SBP Data Side-echo and acoustic transparent layer is not observed. Area(water depth) (less than 2,500m 268 km²) 500 ～1,500m 18 km² 1,500 ～2,500m 170km² 2,500 ～3,500m 164km² Others The upper part of slope extends to the northeast direction. The slope of the east-side is more steeper than the westside slope.

Table 4-1-4 Topographic Feature of Individual Seamount (3)

Seamount	Macroscopic topography	Microscopic Topography
S B 0 8 (S)	Location 5°31'S . 179°31'E Type Guiyot Scale *1 23 × 8 km Range of Water Depth 1,230 ~4,500m Size of Top 5 × 7 km Inclination of Slope*2 Upper part 16° (6° ~25°) Middle Part 18° (6° ~26°) Lower Part 13° (2° ~30°) Others Direction of the major axis N35°W.	SBP Data Acoustic transparent layer is observed on the top of the sea mount. The maximum thickness is 70m. Area (water depth) (less than 2,500m 203 km²) 0 ~1,500m 39 km² 1,500 ~2,000m 65 km² 2,500 ~3,000m 208 km² 3,000 ~4,000m 411 km² Others The pinnacle with relative height 70m is observed on the summit.
S B 0 8 (N)	Location 5°13'S.179°17'E Type Peaked seamount Scale *1 7.5 ×7 km Range of Water Depth 1,450 ~4,500m Size of Top 1 × 1 km Inclination of Slope*2 Upper Part 15° (8° ~22°) Middle Part 19° (6° ~26°) Lower Part 17° (4° ~26°) Others There are no direction. The shape of the summit is quadrilateral.	SBP Data Acoustic transparent layer is not observed. Area (Water Depth) (less than 2,500m 58 km²) 1,500 ~2,000m 1 km² 2,000 ~3,000m 87 km² 3,000 ~4,000m 174 km² Others The slope is steep.

Previously, we had shown the standard depth of the top and slope parts, but in this survey area, the depths vary with individual seamounts and thus the water-depth classification was done for each seamount (Table 4-1-3).

2) Topographic Features

The topographic features of individual seamounts are shown in Table 4-1-4. The topographic maps and the typical cross sections are laid out in Annexed Fig. 17. The inclination, SBP profile and a birds-eye-view are shown in Annexed Fig. 18 Figs. 4-1-1 and 4-1-2 respectively. These features are as follows.

SB01 (Annexd Fig. 17-1)

Flat top guyot, summit depth 1,500 m, relative height 3,000 m, summit area 6×3 km. There are protrusions of 1,390 m water depth in the central part of the summit and the western shoulder, these are the shallowest part. The area deeper than 2,500 m is small at 123 km^2. The long axistrends N20°W. The average inclination of the slope is about 14° and it is steep at the eastern side of the middle and lower slope.

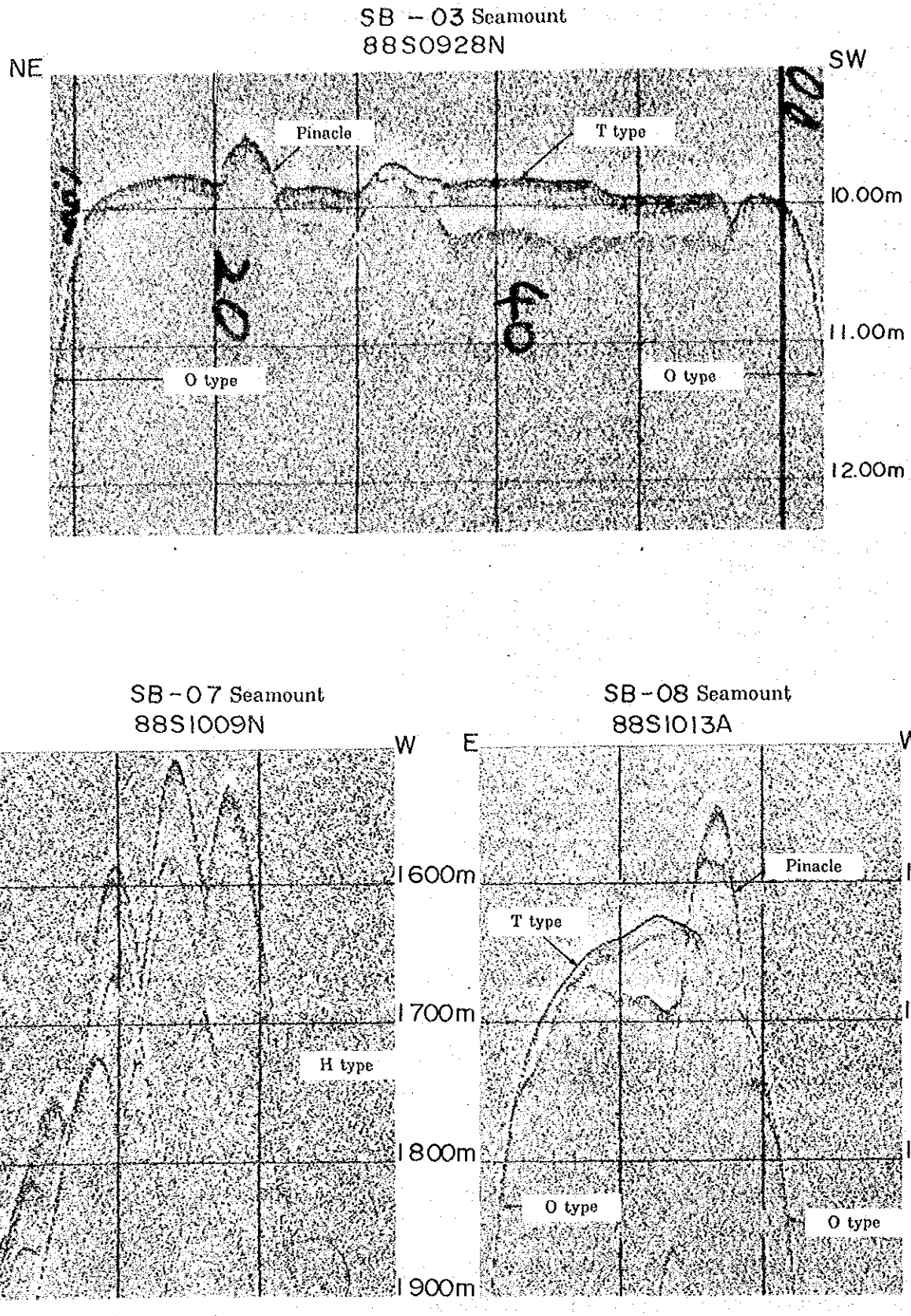

Figure 4-1-1 SBP Profile of Seamounts

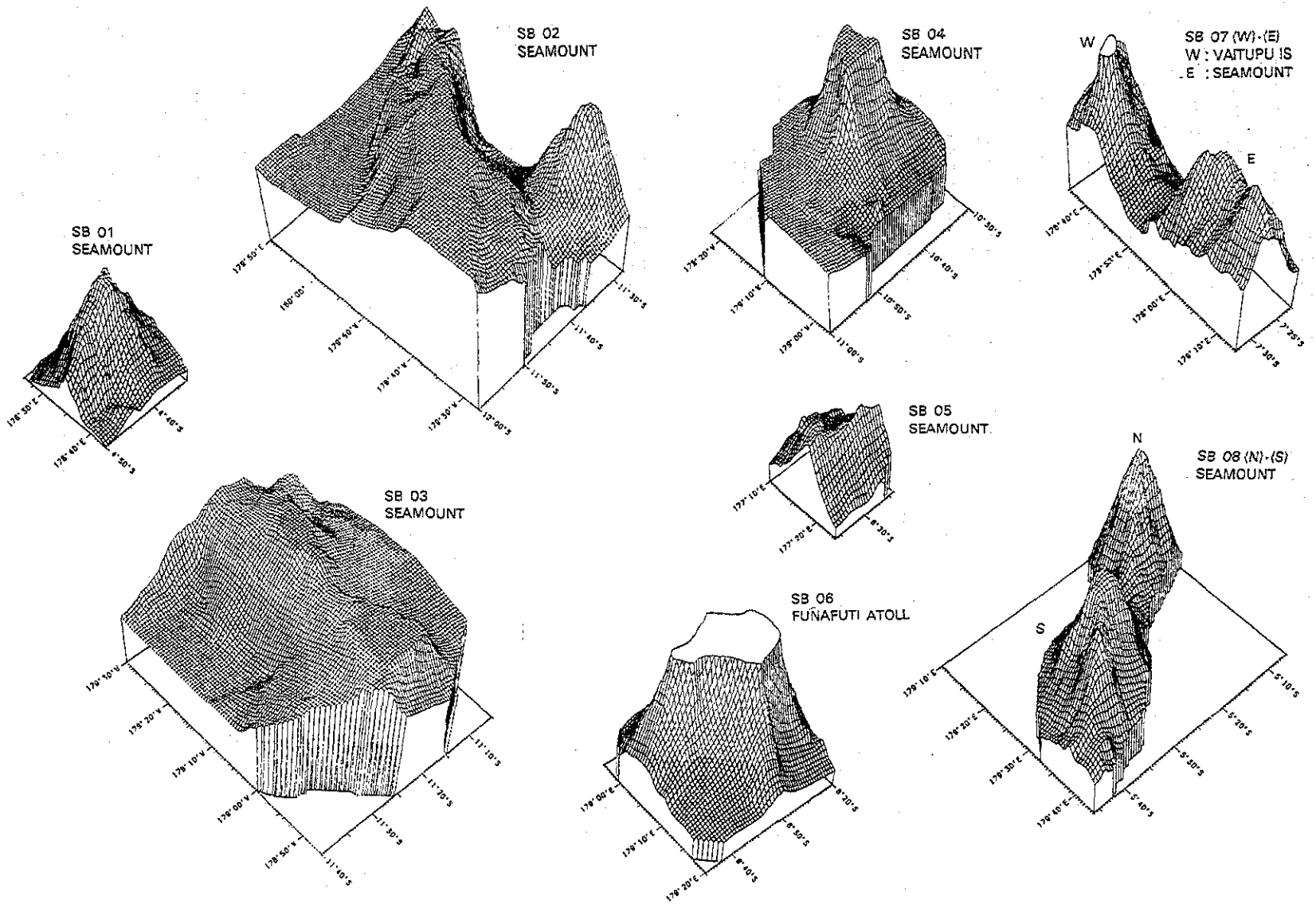

Figure 4-1-2 Bird's-eye View of Seamounts

SB02 (Annexed Fig. 17-2)

A large flat top guyot with gentle slope. The summit depth is very shallow at 40 m and the flat summit is very wide. The relative height is about 3,500 m. The long axis trends N45°W. Three or four small knolls are found in the northwestern edge of the summit. Several pinnacles occur on the summit. The eastern slope is steep 20° at the northeastern side, but the southeastern side is gentle at about 10°. The western slope between 1,000~2,000 m water depth is average 10°.

SB03 (Annexed Fig. 17-3)

Large flat top guyot, summit depth 1,000 m. Two summits connected in east-west direction. Two pinnacles of 830~910 m depth on the flat summit. Long axis trends N70°W. Relative height small at 2,000 m. The inclination of the whole slope is gentle at about 5°.

SB04 (Annexed Fig. 17-4)

Flat top guyot. The summit depth is very shallow at about 20 m and the summit area is 9×8 km, relative height 3,500 m. The flat summit has square shape without significant direction. The slope above 2,500 m depth is very gentle at about 5°.

SB05 (Annexed Fig. 17-5)

Peaked seamounts with two peaks of 2,000 m and 1,950 m connected in north-south direction. Thesummit is deep and the size of the seamount is 22×3 km and the relative height approximately 2,000 m. The area above 2,500 m is 66 km^2, very small. The long axis trends north-south. The southern body extends further south. The eastern slope is steep, but on the western side small knolls occur sporadically and has strong relief.

SB06 Funafuti Atoll (Annexed Fig. 17-6)

The atoll is 22×14 km with water depth of 500 m and is pear-shaped. Several ridges extend from the atoll. Aside from these ridges, the slope is monotonous. The average upper slope (500~1,500 m) is steep at 24°, that of middle slope (1,500~2,500 m) 15° and the lower part (2,500~3,500 m) 12°.

SB07(E) (Annexed Fig. 17-7)

Peaked seamount with two peaks of 450 m and 1,290 m connected in east-west direction. The summit area is 6×2 km and the relative height 3,000 m. The summit has strong relief with spire-like topography and pinnacles, but these

occupy small areas. The inclination is relatively gentle at 10°~12° throughout the slope. The part below 2,000 m has high relief.

SB07(W) Vaitupu Atoll (Annexed Fig. 17-7)

The size of the atoll is 6×3 km with oblong shape. Closer to table reef than atoll. The upper slop extends in N40°W direction. The slope is 15° average to the depth of 2,500 m, but the upper part is steep at 18°. The slope is monotonous with low relief.

SB08(S) (Annexed Fig. 17-8)

Flat top guyot. Summit depth 1,500 m, summit area 7×5 km, relative height 3,000m. The shallowest part is 1,230 m and pinnacles are developed on the summit. The size of the whole seamount is 23×8 km, the area below 2,500 m is 203 km^2, and it is relatively narrow. The summit is elongated in N35°W direction in ridge-like topography and the sides of this ridge has nearly symmetrical form. The average slope above 2,500 m is steep at more than 15°. The upper slope and the lower part between 1,500 and 3,000 m are particularly steep. Below 3,000 m, the slope is gentle with rich relief.

SB08(N) (Annexed Fig. 17-8)

This is the smallest peaked seamount found in the surveyed area. The summit is somewhat deep at 1,450 m. The size is 7.5×7 km. The long axis when considered as related to SB08(S) is in N35°W, if considered as an independent seamount, it has square shape without particular trend. The average slope above 2,500 m is 15°, but the steeper parts exceed 20°. Generally, the slope is steep with low relief and is monotonous.

4-2 Seamount Geology

1) Geology

The geology of all seamounts are shown in Annexed Fig. 18 (1)~(8). All the seamounts surveyed has basalt and basaltic pyroclastics as the basement and the development of the overlying calcareous material varies by whether the seamount is an atoll, a bank or a submerged seamount.

The rock samples collected from atolls SB06, SB07(W) and banks SB02, SB03, SB04, are almost all limestone and very few basalt was obtained. On the other hand, from submerged seamounts, SB01, SB07(E), SB08, basalt and hyaloclastite were commonly collected. Phosphorite was collected from SB01 and SB08 as unit layers or as matrix of hyaloclastite.

The geology of individual seamounts is summarized in Table 4-2-1. Significant features are reported below.

a) The massive, compact basalt samples excluding hyaloclastites are mostly fresh and the effect of submarine alteration is very weak. The age of the vitreous pillow lava from SB02 was determined to be 0.2 Ma. It is noted, however, that SB08 in the northern part of the survey area, samples strongly altered to brown colour was collected, the age of this rock is difficult to determine.

b) The lithology of limestone varies. For example, the age varies from very old appearing rocks to very young semi-consolidated material. The mode of occurrences of these limestones is not clear.

c) Phsophorites were not collected from atolls and banks, while their development was generally confirmed in the submerged seamounts, particularly on SB01 and SB08 in the northern part.

d) In this survey area, foraminifera sand and foraminifera ooze is generally well developed. It is well documented in the SBP data (Table 4-1-4, Fig. 4-1-1). Generally these sediments are observed in the middle to lower slope of the seamounts together with the development of acoustically transparent layers. In some seamounts, however, such as SB03 and SB08, these are developed even in the summits with thickness of 10~70 m. Ripple marks were often observed on the surface of these sediments and information regarding the direction of bottom currents was obtained (Fig. 4-3-4).

Table 4-2-1 Geology of Individual Seamount

Seamount		Sampling Data
SB01	Lithology	Limestone, basalt, hyaloclastite, foraminifera sand.
	Distribution	Basalt, hyaloclastite on southern to eastern slope. Limestone on slope in almost all directions. Foreminifera sand on the whole surface of the seamount.
SB02	Lithology	Limestone (coral fossils, foraminifera). Basalt (vitreous and fresh).
	Distribution	Flat-top seamounts with shallow banks. Limestone on slope in all directions except north-east. Basalt on northeastern and northwestern slope. Foraminifera sand generally abundant.
SB03	Lithology	Limestone (foraminifera, coral fossils), foraminefera sand (soft mud).
	Distribution	Two peaked flat-top seamount. Only limestone distributed, no other rocks. Large amount of foraminifera sand, covers limestone.
SB04	Lithology	Limestone (foraminifera, coral fossils), foraminifera sand (soft mud).
	Distribution	Very shallow bank. Only limestone sampled, lack other rocks. Foraminifera sand and soft mud cover, thick and wide.
SB05	Lithology	Limestone, hyaloclastite.
	Distribution	Peaked seamount, elongated N-S, two peaks. Hyaloclastite in northeastern, western, southwestern parts. Limestone in northwestern, western, southeastern slope.
SB06	Lithology	Limestone, hyaloclastite, sedimentary rocks (mudstone).
	Distribution	Atoll (Funafuti Atoll). No basalt. Limestone predominant on slope in all directions. Mudstone on eastern slope Hyaloclastite collected at one locality each on east, west and northern slope.
SB07	Lithology	Limestone (coral fossils), hyaloclastite, basalt, foraminifera sand.
	Distribution	Atoll (Vaitupu Atoll) on the west and two peaks to the east. Hyaloclastite predominant in the east, only basalt in the eastern edge, limestone on southern slope of the eastern part and on west.
SB08	Lithology	Hyaloclastite, limestone, basalt, phosphorite, tuff breccias, tuff, tuffaceous sandstone, foraminifera sand.
	Distribution	Southern summit flat, northern summit peaked. Basalt on northwest slope of the southern part and on southeastern slope. Limestone mostly in southern part, and in one locality on northeast slope of the northern part. Hyaloclastite on both summits, phosphorite on northern slope of the southern part characteristic, foraminifera less than other seamounts.

2) Description of Substrates

The results of descriptive work on various substrates are summarized in various tables. The results of macro and microscopic observation are laid out in Table 4-2-2, representative photographs in Fig. 4-2-1, microphotographs in Fig. 4-2-2, mineralogical composition in Table 4-2-3 and the chemical composition in Table 4-2-4.

3) Age Determination

The sample was basalt with porous innerside. The surface was composed of compact chilled phase and thus the porous central part was used. The results are shown in Table 4-2-5.

The following decay constant for 40K by Stieiger and Jaeger (1977) was used.

$$\lambda e = 0.581 \times 10^{-10}/y$$
$$\lambda \beta = 4.962 \times 10^{-10}/y$$

The used ratio of 40K was

$$^{40}K/K = 0.01167 \text{ atm\%}$$

Calibration was done by method of Nagao et al., (1984).

The measurement was done twice. The age is correlated to Quaternary Pleistocene. The content of stable Ar (air content) is high at 98.2~96.8% and rendered high the error of age determination.

Relatively young (several Ma) basalts may contain excess argon in the glass of the matrix and care must be taken for age determination by considering the collected depth and whether the gas has been completely eliminated.

Table 4-2-5 Result of Age Determination of Substrate

Sample No.	Portion	Kwt %	Rad. ^{40}Ar (10^8 cc/g)	K-Ar Age (Ma)	Air Cont (%)
88SB02CB07	Whole	2.58	1.67 ± 1.44 2.30 ± 1.06	0.17 ± 0.14 0.23 ± 0.11	98.2 96.8

Table 4-2-2 Substrates of Cobalt Crusts (1)

Rock type	Macroscopie observation	Microscopic observation
Basalt	Pillow lava and pyroclastic rocks are observed. The lava varies from compact to vesicular, and most of them are fresh. At SB02, black glassy basalt was collected and it is believed to be the crust of pillows. Those which suffered further weathering and have turned brown were collected from SB08. Plagioclase phenocrysts and vesicles have all suffered carbonatization or phosphatization. The amount of collected basalt samples were small and the detailed mode of occurrence is unkonwn. The age of the glassy lave was determined to be 0.2 Ma. Transitional with lava. Hyaloclastite is most common, normally it consists of basaltic breccias and irregular fragments of several millimeters to several centimeters. It is more vesicular than lava and is brown due to sea-floor weathering. Matrix consists of fine-grained hyaloclastite, calcareous material and phosphatic matter (Example, SB01AD03, SB05AD03, SB06AD11, SB08AD09). Hyaloclastite includes all material named tuff breccial, and tuff are included in hyaloclastite.	Aphyric balast (A), vesicular basalt (B), and nepheline basanite (C) are observed. (C) contains large amount of nepheline and small amount of plagioclase and minor amount of olivine and aegirine. The nepheline is zeolitized and apatized. In (A) and (B), pyroxene and olivine are observed, but nepheline does not occur. Some of the vesicular basalt contain large amount of clinopyroxene in the matrix (SB07AD08-2). Example of (A): SB02CB07 " (B): SB07AD08-2 SB08AD11 " (C): SB07AD08-1 Generally vesicular and glassy, some show glassy flow structure (SB08AD10A). Some contain or the pyroxene phenocrysts (SB06AD01-1, SB08AD10A). These types are usually not observed in deep-sea tholeites. Chalcedony, chlorite and phillipsite occur in the vesicles. Collophane was identified in samples which suffered phosphatization (SB05AD03).
Limestone	Various types such as accumulation of coral fossils, of finer-grained fossils, compact and hard, soft and semi-consolidated materials occur. Semi-consolidated types are similar to forminifera sand (SB06AD08, SB02CB04, SB03AD09, SB07AD14). Colour becomes yellowish as phosphatization progresses and becomes more effervescent by hydrochloric acid.	The coral of the coral limimestone (SB07AD06) a kind of "Alveopora" which belongs to "Hexacorallia". "Lithophaga curta" bore numerous holes in these corals. Both of these live in shallow seas of several tens of meters deep. Limestone has foraminifera (0.05~0.6 mm) in microcrystalline calcite. Some contain large amount of hyaloclastites. They are in various state of collophanization.

Table 4-2-2 Substrates of Cobalt Crusts (2)

Rock type	Macroscopie observation	Microscopic observation
Phosphorites	Yellowish (creamy colour) compared to limestone. Also many are compact without structure. Phosphorite mass was collected only at SB01 (SB01AD03, AD06, CB10), but it is found at various localities in the matrix of clastic rocks (SB01AD03, SB07AD01, SB08AD07, SB08AD08, etc.). In SB05AD05, it occurs as a core of nodular crust. It appears to be more abundant in the northern seamounts SB01 and SB08.	Strongly collophanized material is called phosphorite (SB06AD08, SB08AD10-A). Although SB05AD05 and SB08AD08 appeared strongly phosphatized by the unaided eyes, they were found to be weakly collophanized under the microscope.
Others	Although Co crustics not developed, foraminifera sand, foraminifera mud and pumice are observed on the surface of some seamounts.	

Table 4-2-3 Mineral Assemblage of Substrates

	Rock Name	Volcanic Rock																				Sedimentary Rock												
		Phenocryst						Groundmass										Vesicle				Fragment					Mineral and Fossil							
		Plazioclase	Ortho-Pyrox.	Clino-Pyrox.	Olivine	Mafic Min.	Nepherine	Plazioclase	Ortho-Pyrox.	Clino-Pyrox.	Aegirine	Olivine	Nepheline	Magnetite	Titanite	Glass	Apatite	Chlorite	Zeolite	Chalcedney	Chlorite	Andesite	Basalt	Plazioclase	Clino-Pyrox.	Glass	Calcite	Collophane	Zeolite	Chlorite	Clay Min.	Micro Fossil	Shell Fossil	Mn-Fe Min.
SB02CB07	Aphyric Basalt	●		●				△		○				△		○																		
SB05AD03	Hyaloclastite	○	○*	○*	△			○								◎				△														
SB05AD03	Coll. Limestone																										●	◎	△			◎		△
SB05AD05	For. Limestone																										◎	△				◎		○
SB06AD08A	Coll. Limestone																							●			○	◎				◎	●	
SB06AD01-1	Hyaloclastite	○	○			○										◎			△		●						◎		○	●				●
SB07AD06	Coral Limestone																										◎						◎	
SB07AD08-1	Nepheline Basite	△			●		◎	△			●		○			◎	●																	△
SB07AD08-2	Basalt	?	○*	○*	○*			△		◎					●	○	●	△	◎															
SB07AD12	Hyaloclastite	?	△*	△*	△*											◎			△	△									◎					
SB08AD02A	For. Limestone																										◎	○				◎		△
SB08AD02C	For. Limestone																					△	△		●		◎	○	○		○	○		●
SB08AD06C	Hyaloclastite	△						△								◎		○	△		●													
SB08AD06C	Limestone																									◎	◎	△	◎					△
SB08AD08B	Hyaloclastite	△														◎				●	△			△			◎	●				◎		△
SB08AD10A	Hyaloclastite	△	△		△			●								◎				△														
SB08AD10A	Coll. Limestone																						△	●			○	◎	△			△		△
SB08AD11B	Basalt	?	○*	○*	△			◎	●*	●*		●				◎			○	△														△

◎ : Abundant ○ : Common △ : Little ● : Very Little ? : Uncertain Coll. : Collaphanized For. : Foraminifella Pyrox. : Pyroxene

* : Intensely altered, minerals are inffered from their remained shape.

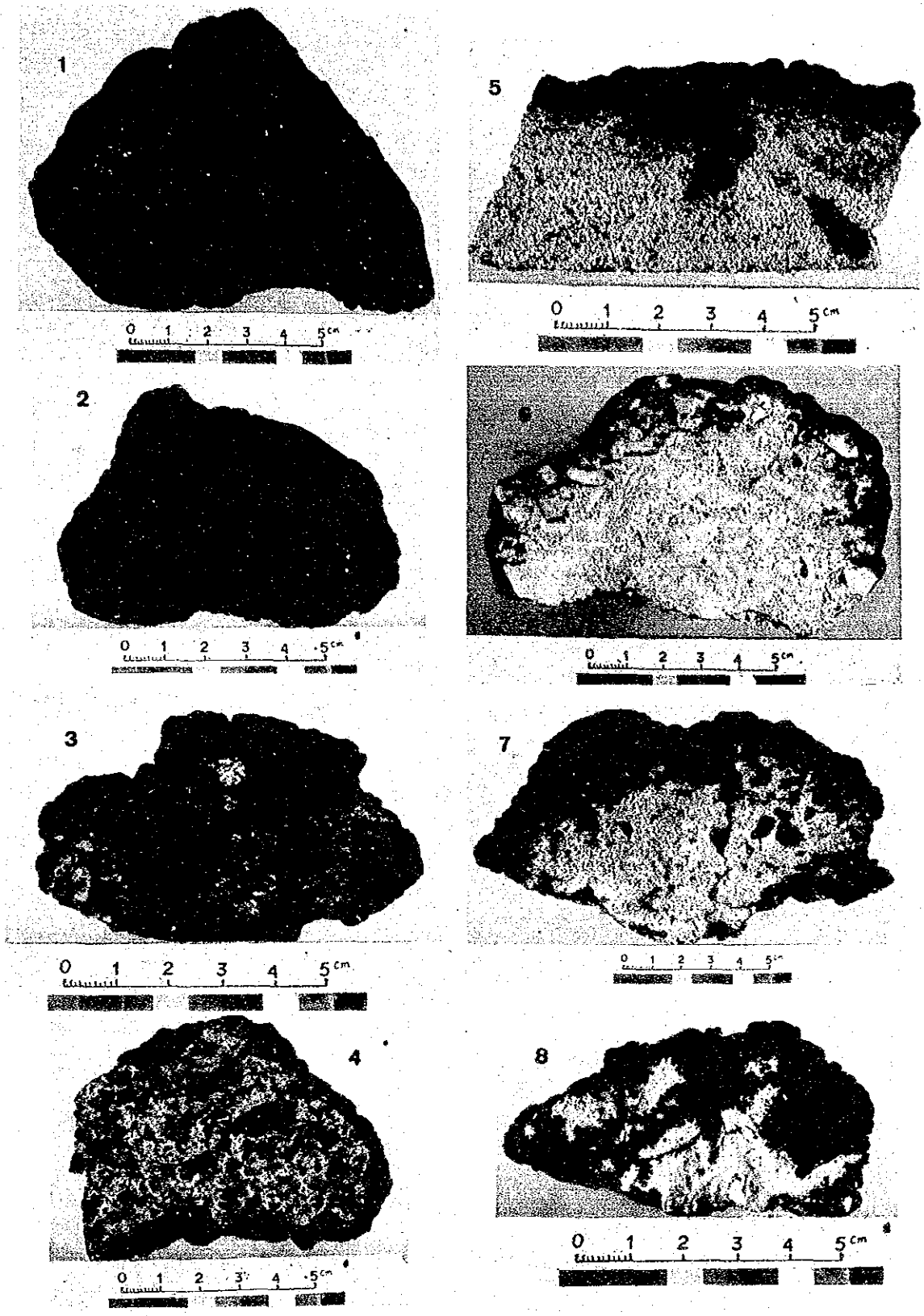

1) SB01AD03, Basalt
2) SB08AD11(A), Basalt
3) SB07AD01(A), Breccia basalt with phosphoritic matrix
4) SA08AD12, Hyaloclastite
5) SB03AD09(B), Foraminifera limestone
6) SB01AD07, Coral limestone
7) SB03CB02, Foraminifera limestone
8) SB08AD09, Phosphorite with basalt fragment and dissemination.

Figure 4-2-1 Photos of Representative Rocks

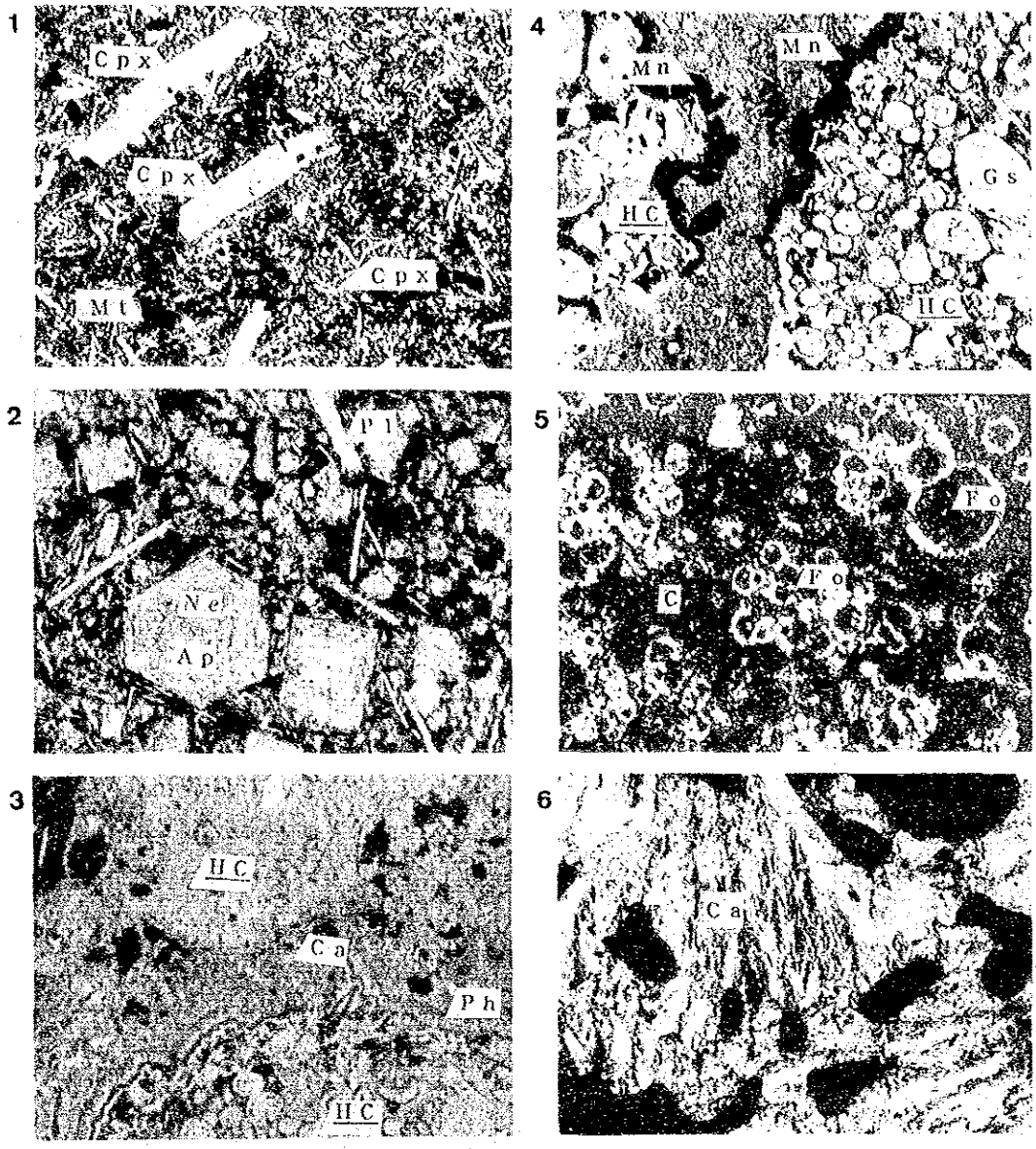

Ap	:	Apatite	Mt	:	Magnetite	Sh	:	Shell
C	:	*Collophane*	Ne	:	*Nephelline*	CQ_2	:	Chalcedney
Ca	:	Calcite	Ol	:	Olivine	Bs	:	Basalt
Fo	:	Foraminifera	Ph	:	Phillipsite	BL	:	Fossile limestone
Gl	:	Glass	Pl	:	Plazioclase	CL	:	Collophanized limestone
Gs	:	Gass cavity	Px	:	Pyroxene			
Mf	:	Mafic mineral	CPx	:	Clino-pyroxene	HC	:	Hyaloclastite
Mn	:	δMnO_2	OPx	:	Ortho-pyroxene			

1. SB02CB07, open nical, X20, aphyric basalt, age determined
2. SB07AD08-1, single nical, X16, *nephelline basite*
3. SB08AD10A, single nical, X8, collophanized limestone with hyaloclastite
4. SB05AD03, single nical, X8, hyaloclastite mixed limestone
5. SB06AD08-A, cross nicol, X8, foraminifera limestone
6. SB07AD06, cross nical, X8, coral limestone

Figure 4-2-2 Microscopic Photos of Substrates of Cobalt Crusts

Table 4-2-4 Chemical Composition of Substrates

No.	Sample No.	SiO_2 wt %	TiO_2 wt %	Al_2O_3 wt %	Fe_2O_3 wt %	FeO wt %	MnO wt %	MgO wt %	CaO wt %	BaO wt %	Na_2O wt %	K_2O wt %	P_2O_5 wt %	LOSS wt %	Total wt %
R-1	88SB02CB07	41.09	2.97	16.68	4.62	5.47	0.24	4.83	10.03	0.15	5.76	3.37	1.09	1.27	97.57
R-2	88SB06CB03	43.15	2.27	14.68	10.95	0.06	0.65	2.99	3.71	0.05	3.38	3.89	0.53	13.30	99.61
R-3	88SB07AD12	43.31	2.37	13.98	12.72	0.03	0.26	2.04	1.65	0.01	4.04	3.96	0.09	15.41	99.87
R-4	88SB07AD14	0.27	0.02	0.13	0.04	0.05	0.01	1.38	51.43	<0.01	0.33	0.02	0.20	45.82	99.70
R-5	88SB08AD02A	0.42	0.02	0.25	0.03	0.13	0.09	0.27	52.26	0.01	0.96	0.08	28.13	16.54	99.19
R-6	88SB08AD02C	32.91	2.54	10.95	9.96	<0.01	1.68	2.36	13.89	0.03	3.01	3.37	7.91	11.06	99.67
R-7	88SB08AD06C	0.62	0.07	0.35	0.60	<0.01	0.61	0.30	50.75	0.30	0.84	0.12	17.35	27.13	99.04
R-8	88SB08AD10C	24.45	2.61	11.53	9.41	<0.01	0.73	1.24	22.63	0.07	2.54	1.27	15.23	7.76	99.47
R-9	88SB08AD12	39.38	2.94	15.84	10.52	0.81	0.35	1.90	6.91	0.03	3.20	2.86	2.39	11.62	98.75

(Rock Type)
R-1: Basalt, fresh and glassy, age determined.
R-2: Basalt, d. brown, whethered.
R-3: Hyaloclastite, buff colour, whethered and phosphatized.
R-4: Coral limestone, many shells.
R-5: Phosphollite, cleamy colour.
R-6: Hyaloclastite, fine, whethered, and phosphatized.
R-7: Limestone, phosphatized.
R-8: Hyaloclastite, phosphatized.
R-9: Hyaloclastite.

4-3 Mode of Cobalt Crust Occurrences

1) Distribution and Occurrence

(1) Occurrence

The distribution of cobalt crusts at each seamounts are shown in the Annexed Figs. 18 (1)~(5).

The cobalt crusts occur at the top and along the slope of seamounts in water depth of 800~2,800 m. They also have various forms and shape. As mentioned earlier, the morphology of the seamounts surveyed during the present cruise is largely divided into the summit and slope (upper,middle, lower), crusts were collected from and the distribution confirmed in all sections of the seamounts with the exception of the tops of atolls. The development of the crust generally ceases in the lower slope.

Many of the dredged samples have only very thin film of manganese oxide coating on the substrates and it was clear that the crust is not developed in this survey area. In the four seamounts SB01, 02, 04 and 06, the average thickness of the crust is less than 1mm. On the other hand, that of SB08 is 10.2mm and it is seen that the thickness is unstable and varies considerably from seamount to seamount. Even within a single seamount, the change of thickness is very large, for example, in the above SB08, the maximum is 65mm and the average 10.2 mm.

The occurrence of crusts is classified into seven group listed in Table 4-3-1. This was done on the basis of the sampling and FDC photographs. Photographs of typical samples of crust from the area are shown in Figs. 4-3-1 and 4-3-2. The occurrence is summarized in Table 4-3-2.

(2) Thickness of the crusts

The average thicknesses of the crusts at each sampling station of the seamounts SB01-08 are shown in Table 4-3-3. Also the frequency distribution of the thickness of analysed samples is laid out in Fig. 4-3-3. The maximum for stations is 52 mm of Station 08 of SB08. That for individual samples is 65 mm of a slab type collected at SB08AD08.

Regarding the consideration of thickness, all samples were measured when collected, and the range of thickness was determined. Then the representative crusts from each station were studied and measured in detail and the average thickness determined. The thickness is very unstable as mentioned above and it often varies from 1mm to 10 mm in a single specimen.

Table 4-3-1 Classification of Types of Cobalt Crusts

	Name	Mark	Characteristics and Distribution
Crust type-group	Crust type	C	(Characteristics) The crust directly covers rocks such as basalt, volcano-clastic rocks and sedimentary rocks. The crust is distributed continuously and present large scale mode of occurrence.
			(Distribution) Distributed on SB01, SB02, SB03, SB05, SB06, SB07, SB08.
	Slab type	S	(Characteristics) The crust is angular and flat-shaped. It covers the whole surface. Partly exfoliated material is included.
			(Distribution) Seen on SB03, SB05, SB08 and others.
	Pavement type	P	(Characteristics) This is a kind of crust shape. The crusts which were originally nodule shape or cobble shape were combined with each other and formed pavement-like appearance.
			(Distribution) This is seen on sea bottom photographs, but the occurrence is rare.
Nodule type-group	Massive type *1	M	(Characteristics) Crust developed over a core of rock fragments, external form is angular and irregular. Size varies.
			(Distribution) Observed on SB01, SB02, SB05, SB06, SB08.
	Cobble type	B	(Characteristics) Crust developed over a core of rock fragments, external form is rounded. The diameter is more than 10cm±.
			(Distribution) SB01, SB02, SB05, SB06, SB07, SB08.
	Nodule type	N	The mode of occurrence of this shape is the same as that of manganese nodule. This size ranges between pebble and fist-size (10 ± in diameter).
			(Distribution) Distribution is local, SB03, SB05 and others.
Other	Film type or coating type	F	The crust is covering the substrate as thin film whose thickness is less than about 1mm.
			(Distribution) Abundant in atolls and banks of SB01, SB02, SB04, SB06, SB07.

*1 Statistically included in Cobble type

Table 4-3-2 Occurrences of Cobalt Crusts at Individual Seamount (1)

Seamount	Occurrence		Average grade(%) Arith. av. of n samples
SB01	Morphology	Flat top	Co 0.81±0.06
	Geology	Limestone, basalt, pyroclastics	Ni 0.47±0.04
	Depth range	1,470~2,530m	Cu 0.05±0.01
	Type	Pebble > crust > coating	Mn 22.26±0.80
	Substrate	Basalt, limestone, pyroclastics	Fe 18.23±0.66
	Structure	Almost all mono-layered	
	Continuity	ref. section on FDC survey for all seamounts	
	Coverage	〃	
	Thickness	0.4mm	
	Number of samples	10(averaged n=4)	
SB02	Morphology	Flat top	Co 0.95±0.57
	Geology	Limestone (reefal. ls.) predominant, some basalt	Ni 0.40±0.16
	Depth range	810-1,815m	Cu 0.13±0.15
	Type	Coating > pebble	Mn 19.10±1.57
	Substrate	Basalt, limestone	Fe 16.23±2.79
	Structure	Almost all mono-layered	
	Continuity	-	
	Coverage	-	
	Thickness	0.4mm	
	Number of samples	7(n=3)	
SB03	Morphology	Flat top	Co 0.57±0.28
	Geology	Limestone (reefal ls.) predominant	Ni 0.39±0.06
	Depth range	920~1,780m	Cu 0.06±0.01
	Type	Crust>nodule>slab>coating	Mn 19.33±1.71
	Substrate	Limestone, foraminifera sand	Fe 20.55±1.83
	Structure	Almost all mono-layered	
	Continuity	-	
	Coverage	-	
	Thickness	4.1mm	
	Number of samples	8(n=8)	

Table 4-3-2 Occurrences of Cobalt Crusts at Individual Seamount (2)

Seamount	Occurrence		Average grade(%) Arith. av. of n samples
SB04	Morphology	Flat top	Co 0.70
	Geology	Limestone (reefal ls.) abundant, foraminifera sand coated	Ni 0.34
			Cu 0.05
	Depth range	940-2,580m	Mn 19.12
	Type	Coating>crust	Fe 19.73
	Substrate	Limestone, foraminifera sand	
	Structure	Almost all filmy and mono-layered	
	Continuity	-	
	Coverage	-	
	Thickness	0.1mm	
	Number of samples	4(n=1)	
SB05	Morphology	Peaked seamount (Ridge type)	Co 0.33±0.20
	Geology	Limestone, basalt, pyroclastics	Ni 0.47±0.22
	Depth range	2,340~2,930m	Cu 0.13±0.06
	Type	Pebble>nodule>crust>coating>slab	Mn 21.77±1.68
	Substrate	Pyroclastics, limestone, basalt	Fe 19.89±1.02
	Structure	Many crust, nodular types are 2-layered	
	Continuity	-	
	Coverage	-	
	Thickness	3.8mm	
	Number of samples	5(n=4)	
SB06	Morphology	Atoll (Funafuti)	Co 0.62±0.05
	Geology	Limestone, pyroclastics, sedimentary rocks	Ni 0.41±0.04
	Depth range	950~2,650m	Cu 0.06±0.01
	Type	Pebble>crust>coating	Mn 19.91±1.72
	Substrate	Limestone, pyroclastics, corals, sediment	Fe 18.29±1.29
	Structure	Almost all mono-layered	
	Continuity	-	
	Coverage	-	
	Thickness	0.4mm	
	Number of samples	11(n=4)	

Table 4-3-2 Occurrences of Cobalt Crusts at Individual Seamount (3)

Seamount	Occurrence		Average grade(%) Arith. av. of n samples
SB07	Morphology	(W) Atoll (Vaitupu), (E) Peaked seamount	Co 1.08±0.43
	Geology	Limestone (reefal ls.) and pyroclastics predominant with basalt	Ni 0.61±0.14
			Cu 0.07±0.02
	Depth range	(W) 805~2,220m	Mn 23.89±3.34
	Type	Coating>pebble>crust	Fe 16.41±2.20
	Substrate	Limestone, pyroclastics, coral fossils	
	Structure	Almost all mono-layered	
	Continuity	-	
	Coverage	-	
	Thickness	1.9mm	
	Number of samples	15(n=7)	
SB08	Morphology	(N) Peaked seamount, (S) Flat seamount	Co 0.89±0.27
	Geology	Limestone, basalt, pyroclastics, minor phosphorite	Ni 0.62±0.13
			Cu 0.11±0.06
	Depth range	1,875~2,800m	Mn 23.28±3.14
	Type	Slab>pebble>crust>coating	Fe 16.84±1.70
	Substrate	Tuff breccia, limestone, pyroclastics	
	Structure	Many slabs 2 layered, pebbles 3 layered	
	Continuity	-	
	Coverage	-	
	Thickness	10.2mm	
	Number of samples	14(n=12)	

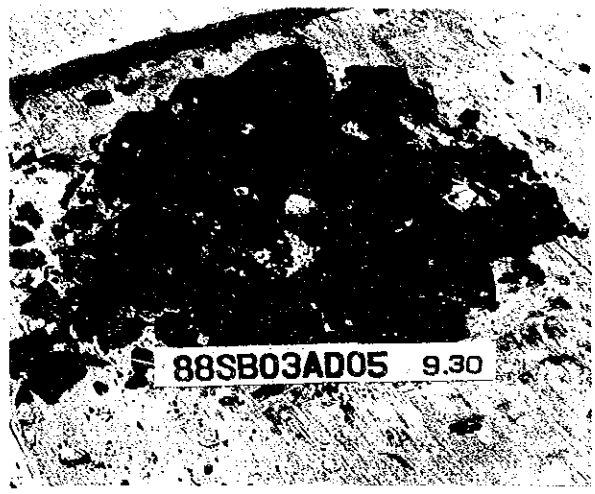

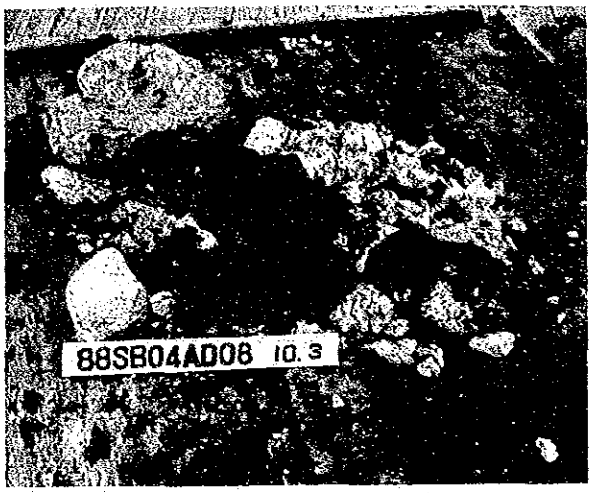

1) SB03AD05, 37.0 kg
crust, 1.5~15 mm thickness
2) SB04AD08, 68.5 kg
coating~crust, 0~3 mm thickness
3) SB05AD05, 101.0 kg
nodule, cobble, 0.1~30 mm thickness
4) SB06FP13, 225.0 kg limestone,barren
5) SB07AD06, 148.0 kg limestone with
crust coating 0.1 mm±
6) SB08AD08, 152.1 kg large slub with
crust at top and bottom,0.5~65.0 mm

Figure 4-3-1 Representative Cobalt Crust Types (On Board)

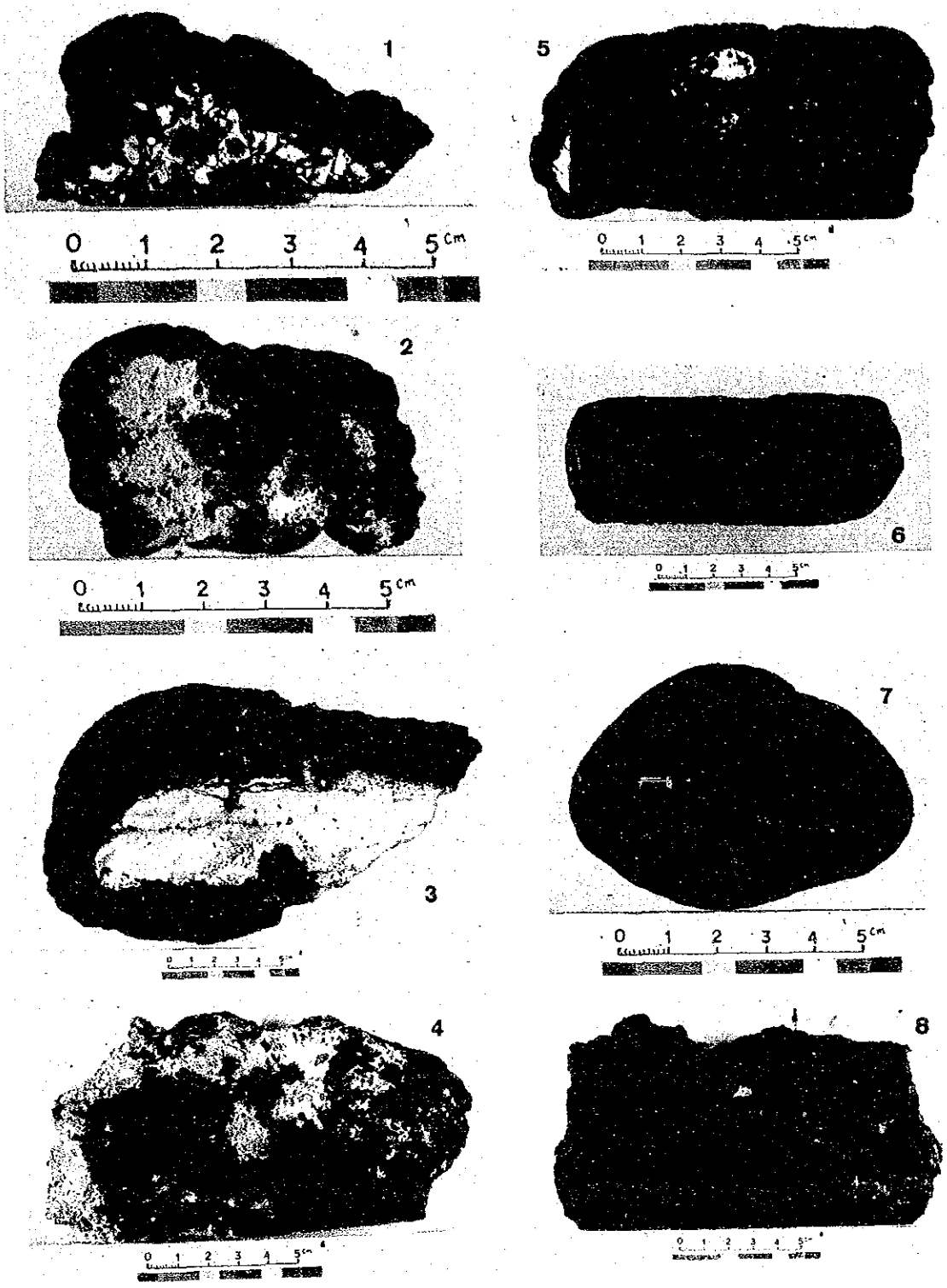

1) SB06AD10(A), crust
2) SB03CB01, crust
3) SB08AD02(A), cobble
4) SB07AD15, coating
5) SB08AD11, cobble
6) SB01AD06, slub
7) SB05AD05, nodule
8) SB08AD08, crust surface

Figure 4-3-2 Representative Cobalt Crust Types (Section)

Table 4-3-3 Average Thickness of Cobalt Crust at Each Seamount

Seamount	Sampling Sites	Crust Thickness (mm)	
		Average	Standard Deviation
SB 01	10	0.42	0.91
SB 02	7	0.36	0.34
SB 03	8	4.11	2.51
SB 04	4	0.12	0.02
SB 05	5	3.8	4.2
SB 06	11	0.38	0.56
SB 07	15	1.93	2.29
SB 08	14	10.2	15.3
Total	74	3.17	7.59

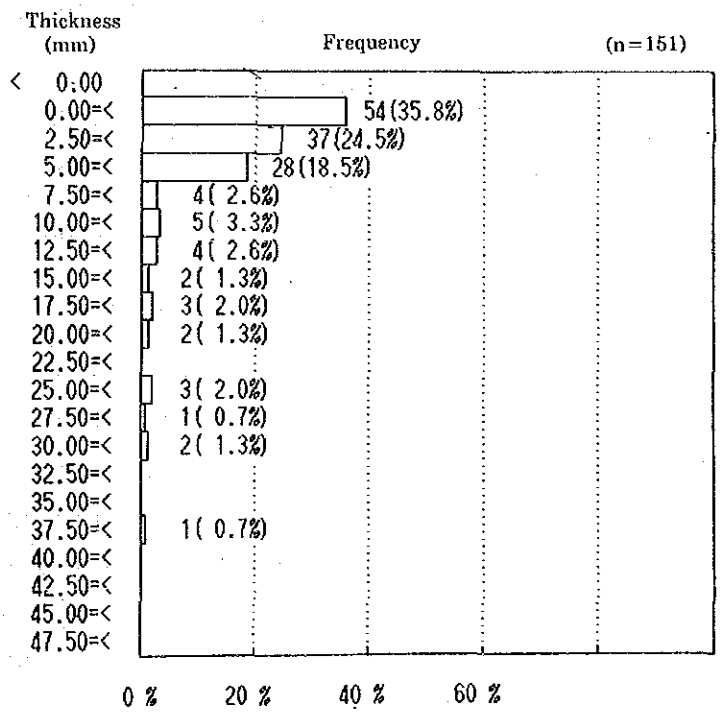

Figure 4-3-3 Frequency Distribution of Thickness of Cobalt Crusts

(3) Surfcace conditions

The surface state of the crusts was classified into three groups, namely smooth, rough and botryoidal.

The smooth surface is mostly observed on extremely thin coating of crusts and the frequency of occurrence is not very high, it constitutes 7% of the analysed samples. There are cases, when the surface of thick crusts have very smooth surface with pitchblend-type lustre.

The rough surface texture is caused by small irregularities of the surface. This occurs widely from slightly thick coating to typical thick crusts. The shark-skin and cokes types are also included in this category. This comprises 46.5% of the samples.

The botryoidal surface is composed of aggregates of semispheres with 5~15 mm diameter. The section of these crusts, however, show that the inner part grew harmonious with the substrate surface and do not have botryoidal structure. The crusts with this surface are generally thick. But in some cases, these surfaces begin to appear in crusts as thin as 2 mm and with 5 mm typical botryoidal material start to occur. These crusts are very common in the survey area and occupy 46.5% of the samples, similar to the rough surface type.

(4) Inner structure

In general, the inner structure of crusts thinner than 10 mm is homogeneous without changes and the only variation is the existence of somewhat porous layer in the central part. But relatively thick crusts (over 20 mm) are composed of two layers-outer and inner-and the thick crusts can often be divided into three layers-outer, intermediate, inner-or more. For example, 88SB08AD02-A can be divided into five layers.

The outer layer is generally 5~25 mm thick, black to blackish brown and has weak submetallic lustre. It is homogeneous and slightly porous. The intermediate layer is 10~20 mm thick, blackish brown to black and is extremely porous. The inner layer is 5~20 mm thick, black to grayish black with strong submetallic lustre and is homogeneous and extremely compact. The fracture of the inner layer has pitchblend lustre. The inner layer has clear boundary with the substrate, but sometimes contain small pebbles of the substrate, and in some cases phosphate minerals grow in dendritic manner along the boundary.

(5) Substrates

The mode of occurrence of the crusts and the lithology of the substrates and the core material is shown in Table 4-3-4. The rocks constituting the substrates and the core are most often limestone and pyroclastics, they constitute approximately 70% of the total material. In cases of phosphatic substrates, fragments of crusts or rocks with crusts are sometimes contained in the substrates and also there are cases where manganese oxide layers are formed at the boundary of pebbles and phosphatized matrix (ex. 88SB08AD08-A).

Table 4-3-4 Bearing Rates of Different Rock Types in Each Crust Types

(Based on analized samples)

Crust Type \ Rock Type	Basalt	Clastic Rocks*	Limestone	Others	No Substrate	Total
Crust	2	15	29	2	11	59
Slub	0	2	2	0	1	5
Cobble	8	4	2	1	1	16
Nodule	0	2	2	1	1	6
Coating	1	3	10	0	0	14
Total	11	26	45	4	14	100

(* include hyaloclastite)

2) FDC Survey

During the present cruise, sea-floor observation by FDC was conducted along six track lines, recorded on video tape and a total of 756 photographs were taken. The distribution and the mode of occurrence of the crusts were studied on the basis of these records, and the crust coverage was calculated. The FDC survey of the seamounts is listed in Table 4-3-5. FDC route-map is shown in Fig. 4-3-4 and some FDC photographs are shown in Fig. 4-3-5. The crust coverage of some parts of the survey area is very high, but the average coverage of each track line is low (Table 4-3-6). This is caused by the wide distribution of unconsolidated sediments (foraminifera sands, mud) over the crust and basement of the flat sea-floor comprising the seamount summits, terraces of slopes and so on.

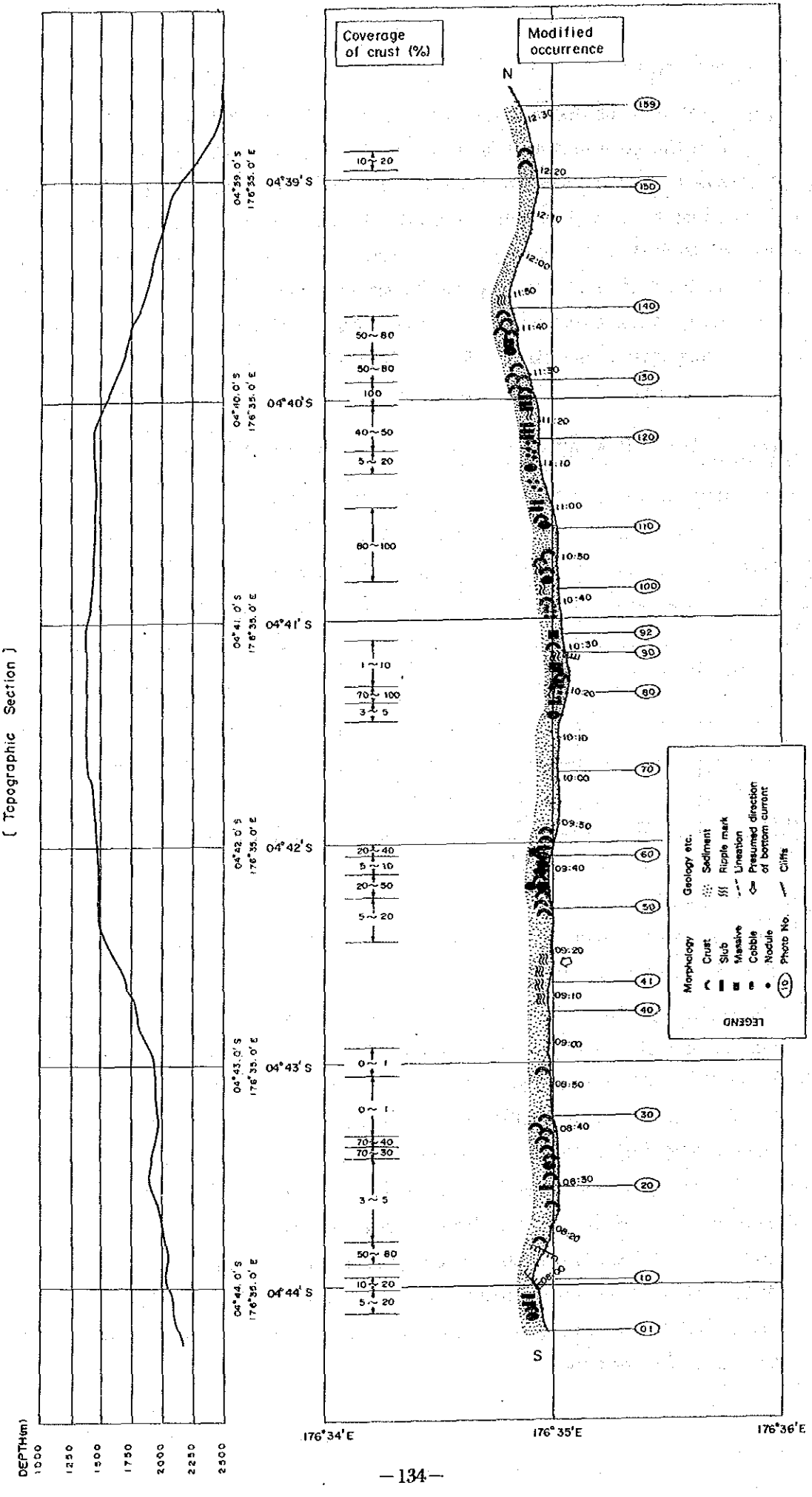

Figure 4-3-4 Modified Distribution of Cobalt Crusts along FDC-Survey Line (1)

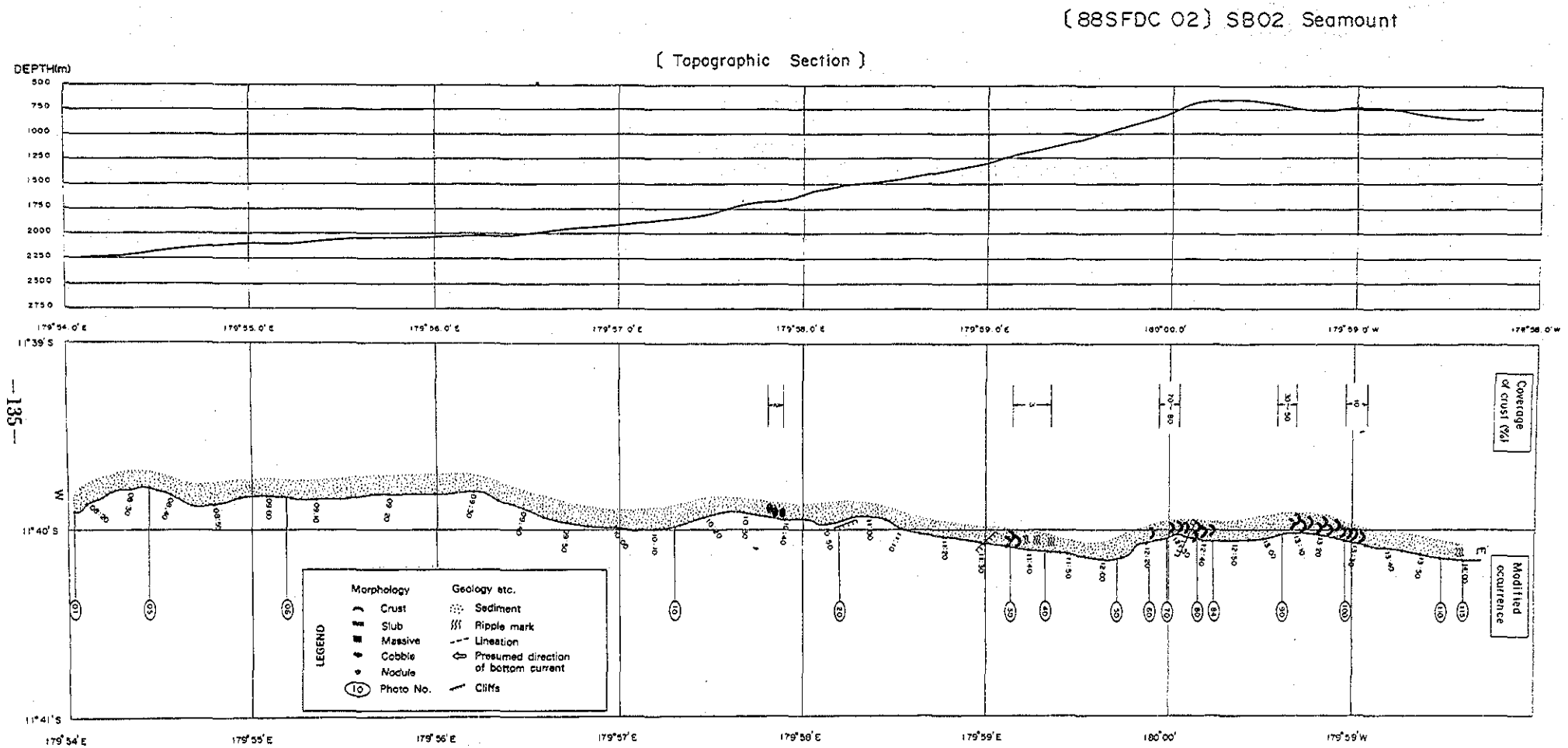

Figure 4-3-4 Modified Distribution of Cobalt Crusts along FDC-Survey Line (2)

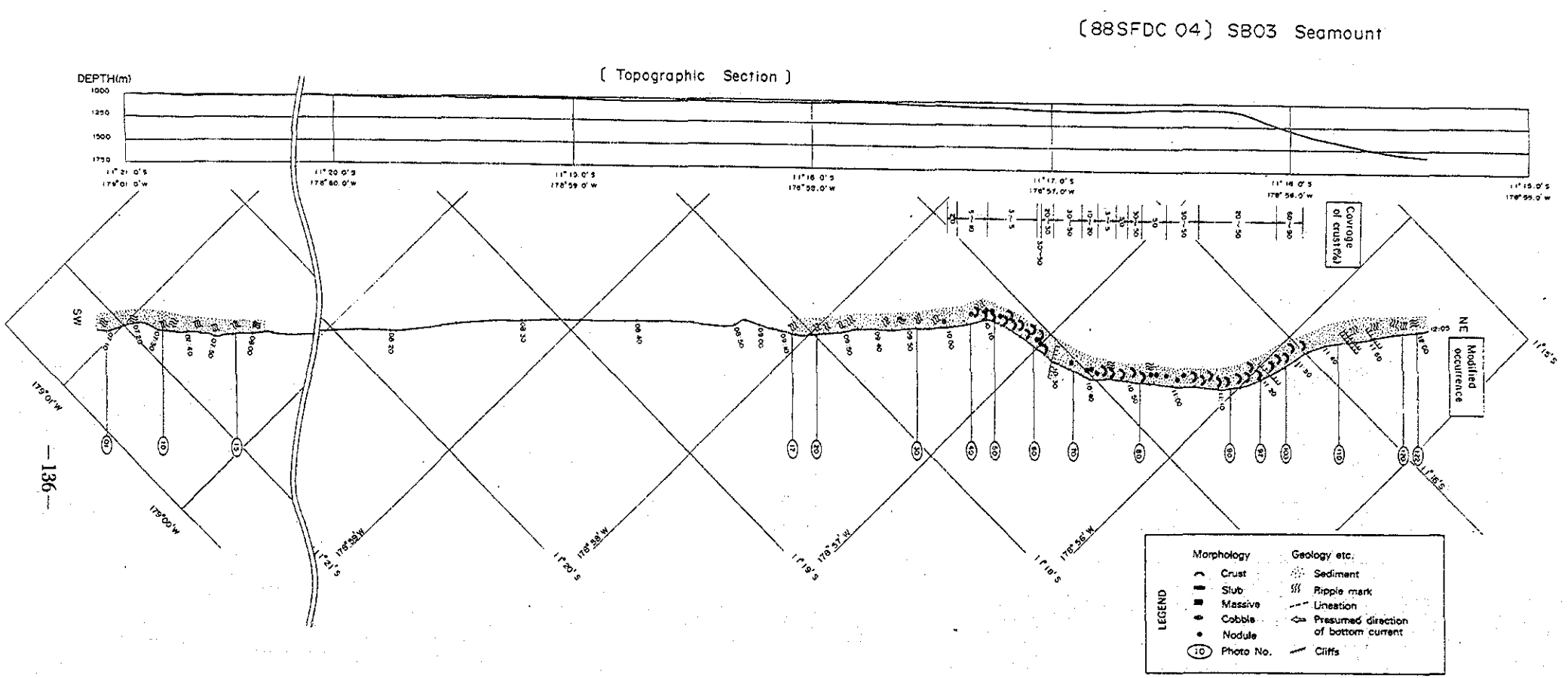

Figure 4-3-4 Modified Distribution of Cobalt Crusts along FDC-Survey Line (3)

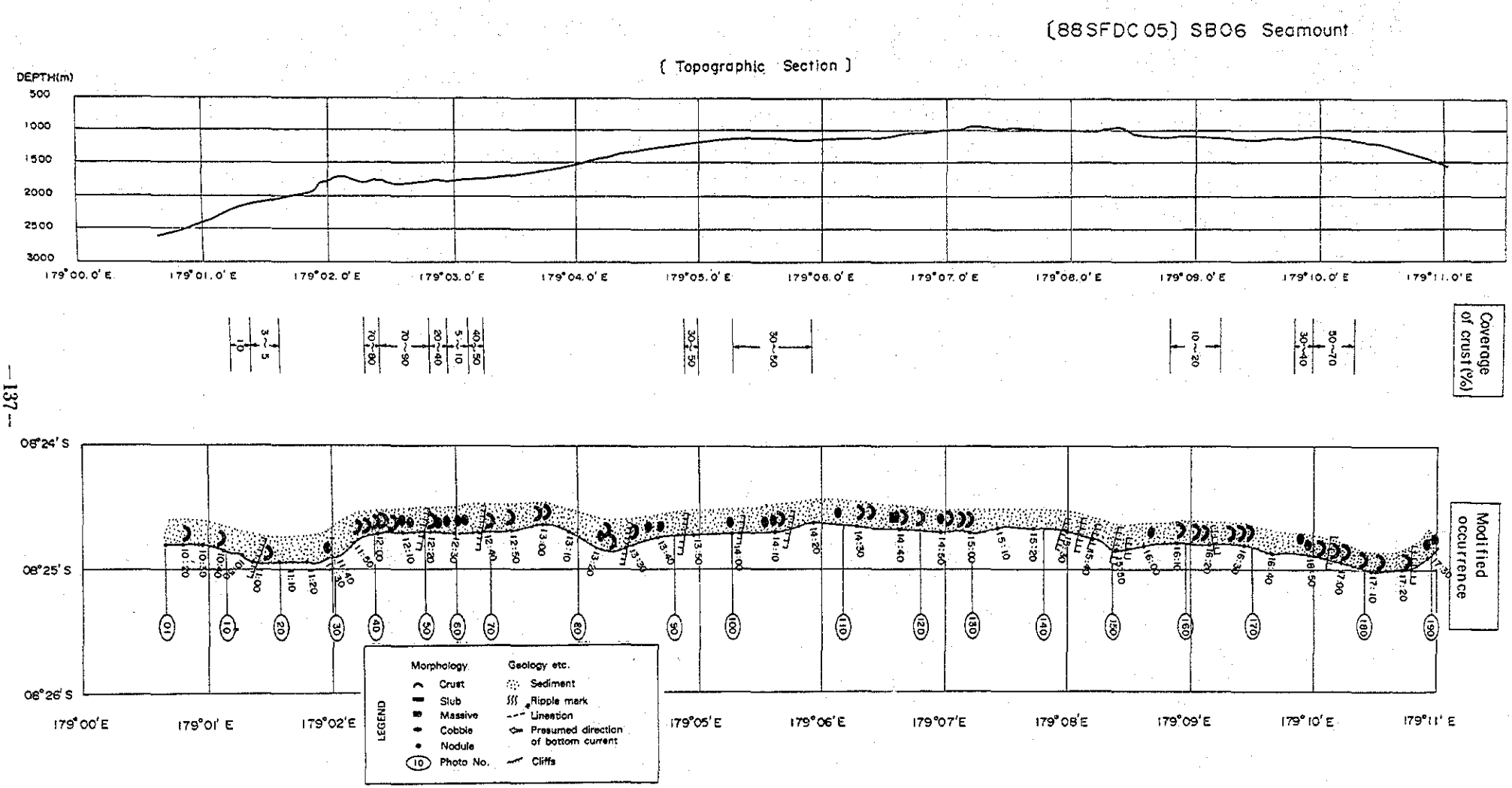

Figure 4-3-4 Modified Distribution of Cobalt Crusts along FDC-Survey Line (4)

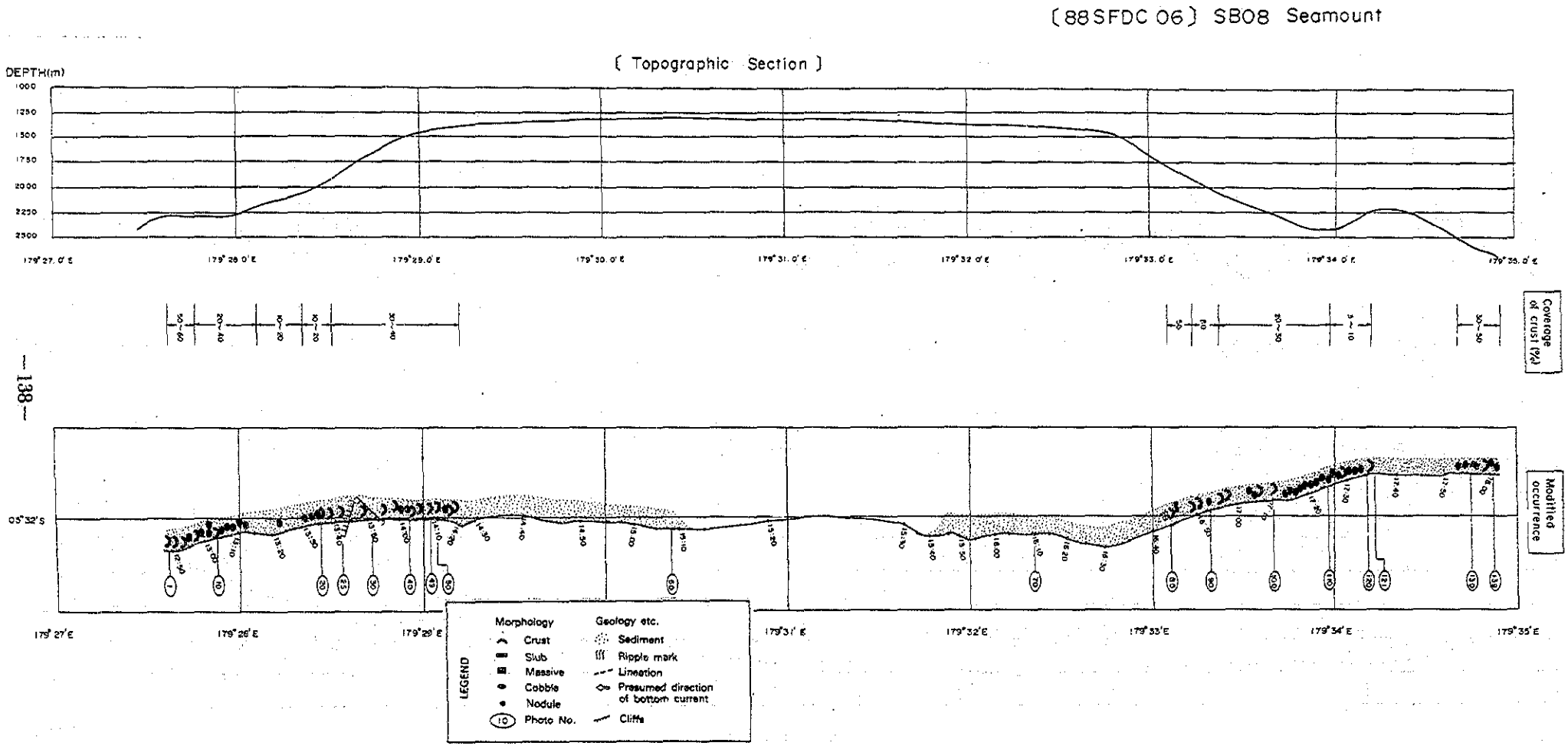

Figure 4-3-4 Modified Distribution of Cobalt Crusts along FDC-Survey Line (5)

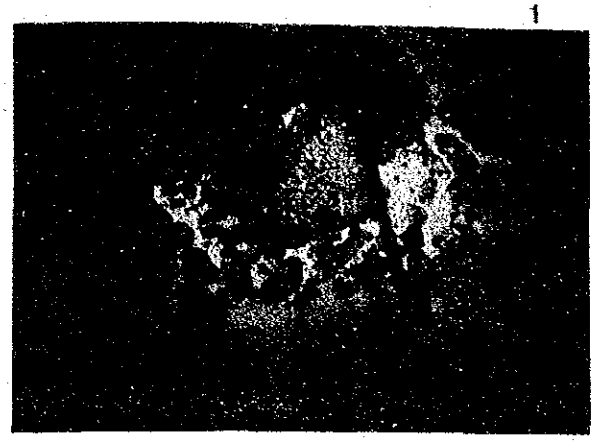

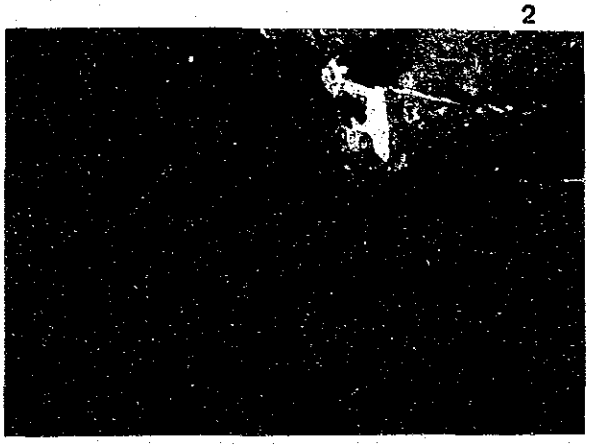

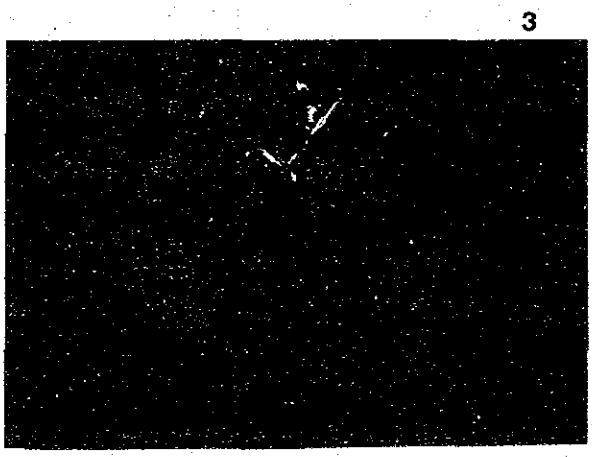

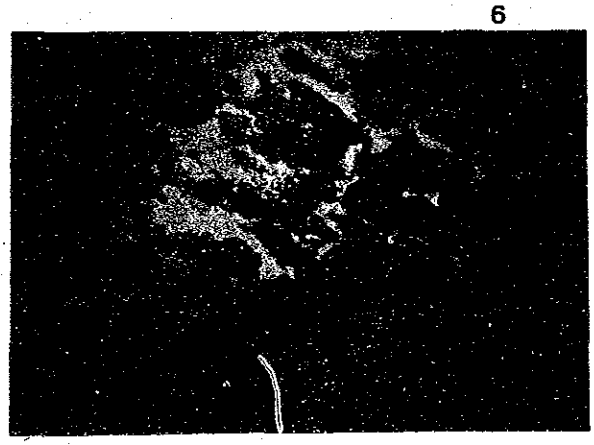

1) FDC01-92, at top of SB01 seamount, 1,385 m.
   Cobble and massive crust with thin crust layer.
2) FDC02-84, at middle slope of SB02 seamount, 650 m.
   Crust.
3) FDC02-100, at middle slope of SB02 seamount, 700 m.
   Limestone(?) with thin crust coating.
4) FDC06-25, at middle slope of SB08 seamount, 1,800 m.
   Botryoidal crust surface.
5) FDC06-49, at upper slope of SB08 seamount, 1,450 m.
   Botryoidal crust surface.
6) FDC06-121, at middle slopoe of SB08 seamount, 2,286 m.
   Botryoidal crust surface.

Figure 4-3-5 Sea Bottom Pictures by FDC Survey

Table 4-3-5 FDC Observation of Cobalt Crust at Each Seamount

	FDC 01	FDC 02	FDC 04	FDC 05	FDC 06
Date	Sep. 06	Sep. 25	Sep. 29	Oct. 06	Oct. 13
Seamount	SB 01 Northern edge	SB 02 Southern edge	SB 03(E) Southern edge	SB 06 Central part	SB 08(S) Northern edge
Seamount Type	Flat top	Flat top	Flat top	Atoll	Flat top
Track Direction	S ⇨ N Mid-slope(Crossing summit)	W ⇨ E (Crossing ride on western sope)	SW ⇨ SE (Down northern slope)	W ⇨ E (Northern slope)	W ⇨ E (Crossing summit)
Topography	Mid-slope ~ upper summit ~ mid-slope	Lower ~ mid-slope	Summit ~ upper ~ mid-slope	Lower ~ upper slope	Mid-slope ~ summit ~ mid-slope
Water Depth	2,150 m - 1,380 m - 2,500 m (P D R)	2,318 m - 643 m - 799 m (C T D)	899 m - 1,430 m (C T D)	2,709 m - 941 m - 1,291 m (C T D)	2,700 m - 581 m - 2,414 m (C T D)
Geology	Sediments predominant with minor exposure at5 ~ 6 localities along cliffs. Otherwise sedimentary cover of varying thickness. Ripple marks observed at some localities, but mostly contain boulders ~ pebbles, slumping sediments without bedding. Granules sometimes arranged in bands where ripple marks are observed.	Sediments predominant, exposure extremely rare in mid-lower slope. Exposures mostly on ridge shoulders, but in some mid slope localities, sedimentary cover in stepwise fashion. Agglomerates of boulders also found. Sediments are white, brown, without ripple marks consist of foraminifera mud, coral fossil sand. Sediments predominant on flat zones of ridges.	Sediments predominant on flat summit with no exposures or pebbles. Ripple marks cleare. Smooth exposures appear downward from the flat zone. Bedrock predominant on the summit shoulder. Sediments again predominant below 1,300m depth.	Sediments predominant. Bedrock appear stepwise or locally. Small extent and intermittent. Bedrock covered by sediments varying thickness. Bedrock exposed on steep topography, gentler slopes sediments cover it thick. Upper slope covered by slumping sediments with boulder and cobble mixture, foraminifera sands and coral fossil sands also abundant.	Slumping sediments with boulders ~ pebbles predominate in the mid slope although bedrock are exposed places. There are many cliffs in the upper slope, bedrock predominant with samll amount of sediments. Summit shoulder consists of bedrock and pebbles, and sediments cover the surface. Sediments become thicker with water depth. Flat surface is predominantly sediments, with clear ripple marks.
Crust Occurrence	Crust found in the exposed bedrock exposed in the cliff at upper northern slope. Other areas are poor.	Crust only found on shoulders of ridges on mid slope. Occurrence not good.	Black lustrous bedrock exposed at 1,090 - 1,210m depth in upper slope with crust development, but otherwise crust poor.	Co crust occurrence poor. Parts of lower slope exposed with black lustre and Co crust developed.	All the exposed bedrocks are black with strong lustre. Co crust is promising. The best occurrence of Co crust among the five seamounts.

Table 4-3-6 Cobalt Crust Coverage along FDC Survey Lines

Survey Line (Seamount)	Position *1	Depth (m)	Coverage (%) ( ) Estimated Average	Calculated Coverage (%) *2
FDC 01 (SB 01)	Top Upper slope Middle slope	<1,400 1,400 ~ 2,000 2,000 ~	0 ~ 100 (20) 0 ~ 70 (15) 0 ~ 80 (15)	19
FDC 02 (SB 02)	Middle slope Lower slope	400 ~ 800 800 ~	0 ~ 70 (10) 0 ~ 5 (1)	4
FDC 03 (SB 02)	Top	<50	0	0
FDC 04 (SB 03)	Top Upper slope	<1,100 1,100 ~ 1,400	0 ~ 50 (5) 0 ~ 90 (10)	8
FDC 05 (SB 06)	Upper slope Middle slope	500 ~ 1,500 1,500 ~ 2,500	0 ~ 70 (10) 0 ~ 90 (20)	11
FDC 06 (SB 08)	Top Upper slope Middle slope	<1,500 1,500 ~ 2,000 2,000 ~	0 30 ~ 80 (50) 10 ~ 50 (15)	13

*1: Based on Table 4-1-3.
*2: Considering exposed (observed) distance.

By the present survey, FDC observation covered six traverses over five seamounts-essentially five traverses-, but there was only one track line for each seamount and the resulted in a single linear observation of a large seamount. For accurate determination of the coverage, it will be necessary to increase the FDC survey for the seamounts and observe the crust distribution in a planar dimension.

3) Chemical Properties

Of the 89 dredgings for the eight seamounts, 49 dredge samples were analysed for the five major elements on board. The samples excluded from analysis were those consisting only of substrates, those with crusts not sufficiently thick for analysis and other unsuitable material. The total analysed elements amount to 169. The method used was X-ray fluorescence.

The analytical data are annexed. Six analyses were excluded from the statistical processing because the amount of the crust was small and there was the possibility of substrate mixture.

The results of various studies on the chemical properties of the cobalt crust are laid out in the following tables.

Table 4-3-7 Average cobalt crust grade of individual seamounts.
4-3-8 Cobalt crust grade of different parts of seamounts.
4-3-9 Grade of cobalt crust with different surface structures
4-3-10 Cobalt crust grade with different substrates.
4-3-11 Grade of different parts of cobalt crust.
4-3-12 Grade of different types of cobalt crust.
4-3-13 Grade of cobalt crust from different water depth.
4-3-14 Total analysis and minor element analysis of cobalt crust.
4-3-15 Total analysis and minor element analysis of different parts of cobalt crust.
4-3-16 Chemical correlation of cobalt crust.
4-3-17 Average grades of cobalt crusts collected in various surveys.

Fig. 4-3-6 Frequency Distribution of Major Chemical Components
4-3-7 Correlative Diagram among Major Chemical Components

The grade characteristics of cobalt crusts in the survey area are summarized from the above data as follows.

a) Average grade of all 43 observation stations used for statistical processing is; Co 0.78%, Ni 0.50%, Cu 0.09%, Mn 21.86%, Fe 18.03%, and Mn/Fe ratio 1.21.

b) The highest cobalt grade of the samples collected from the area was from SB07, station 13, and Co=1.07%.

c) Comparison of grades by seamounts is as follows;

Co: SB07>02>08>01>04>06>03>05
Ni: SB08>07>01=05>06>02>03>05
Cu: SB02=05>08>07>03=06>01=04
Mn: SB07>08>01>05>06>03>04>02
Fe: SB03>05>04>06>01>08>07>02

d) Topographically, high Co in the summit and uppe slope, high Ni, Mn in the summit and low Cu, Mn, Fe content in the lower slope is clearly indicated. Particularly for Mn, clear simple change of values is observed. The Cu and Fe content decreases at the summit.

Table 4-3-7 Average Grade of Cobalt Crusts at Each Seamount

Seamount	Obtained sample weight (kg)	Thickness (mm)		Average Grade (%)					
		Range	Average	H_2O	Co	Ni	Cu	Mn	Fe
SB-01	38.037	0-6	0.42	38.20	0.81	0.47	0.05	22.26	18.23
(13/4)	494.483		0.91	13.99	0.06	0.04	0.01	0.80	0.66
SB-02	13.021	0-2	0.36	42.54	0.95	0.40	0.13	19.10	16.23
(9/3)	117.190		0.34	9.68	0.57	0.16	0.15	1.57	2.79
SB-03	21.28	0-20	4.11	38.11	0.57	0.39	0.06	19.33	20.55
(10/8)	212.845		2.51	4.10	0.28	0.06	0.01	1.71	1.83
SB-04	51.219	0-3	0.12	44.65	0.70	0.34	0.05	19.12	19.73
(9/1)	460.967		0.02						
SB-05	20.276	0-30	3.8	39.27	0.33	0.47	0.13	21.77	19.89
(5/4)	101.378		4.2	4.10	0.20	0.22	0.06	1.68	1.02
SB-06	25.417	0-12	0.38	41.56	0.62	0.41	0.06	19.91	18.29
(13/4)	330.426		0.56	2.03	0.05	0.04	0.01	1.72	1.29
SB-07	49.00	0-17	1.93	35.49	1.08	0.61	0.07	23.89	16.41
(16/7)	784.078		2.29	5.05	0.43	0.14	0.02	3.34	2.20
SB-08	13.828	0-65	10.2	36.25	0.89	0.62	0.11	23.82	16.84
(14/12)	193.585		15.3	4.49	0.27	0.13	0.06	3.14	1.70

(14/12)
- 14: Number of sampling sites used for average calculation.
- 12: Number of total sampling sites.

Table 4-3-8 Cobalt Crust Grade and Topographic Position of Seamount

	n	Average Thickness (mm)	Co (%)	Ni (%)	Cu (%)	Mn (%)	Fe (%)	Mn/Fe
Top	2	1.50	1.01	0.71	0.10	22.73	16.72	1.36
Upper Slope	27	7.75	0.74	0.52	0.08	22.45	18.23	1.23
Middle Slope	56	5.67	0.72	0.52	0.10	22.15	18.25	1.21
Lower Slope	6	0.58	1.21	0.52	0.05	20.34	14.59	1.39

Table 4-3-9 Cobalt Crust Grade and Surface Structure

	n	Average Thickness (mm)	Co (%)	Ni (%)	Cu (%)	Mn (%)	Fe (%)	Mn/Fe
Botryoidal	41	9.88	0.75	0.53	0.10	22.37	18.28	1.22
Rough	41	3.11	0.73	0.51	0.08	22.08	18.21	1.21
Smooth	6	1.59	1.17	0.62	0.09	21.82	14.09	1.55

Table 4-3-10 Cobalt Crust Grade and Substrates

	n	Average Thickness (mm)	Co (%)	Ni (%)	Cu (%)	Mn (%)	Fe (%)	Mn/Fe
Basalt	16	1.69	0.94	0.50	0.06	22.18	17.37	1.28
Tuff Breccia	9	25.38	0.93	0.68	0.09	24.16	16.15	1.50
Tuff	1	4.00	0.74	0.50	0.07	23.25	19.44	1.20
Coral	1	0.10	0.25	0.23	0.25	14.38	15.27	0.94
Limestone	49	4.43	0.65	0.46	0.08	20.26	18.95	1.07
Calcareous Sandstone	5	2.46	0.45	0.38	0.06	18.23	19.27	0.95
Phospholite	1	0.40	0.51	0.45	0.06	19.75	19.01	1.04
Hyaloclastite	25	5.27	0.81	0.54	0.10	22.44	17.33	1.26
Others	6	14.75	0.78	0.57	0.11	23.44	16.47	1.42

Table 4-3-11 Cobalt Crust Grade from Different Layer

	n	Average Thickness (mm)	Co (%)	Ni (%)	Cu (%)	Mn (%)	Fe (%)	Mn/Fe
Bulk	134	5.97	0.75	0.51	0.09	21.79	18.17	1.20
Outer Crust	4	8.05	0.70	0.60	0.12	24.10	18.71	1.29
Middle Crust	2	20.00	0.79	0.77	0.17	28.51	14.82	1.92
Lower Crust	3	17.00	0.56	0.60	0.14	20.99	15.69	1.34
Bottom	4	14.45	1.22	0.79	0.11	24.95	15.62	1.60

Table 4-3-12 Cabalt Crust Grade and Types

	n	Average Thickness (mm)	Co (%)	Ni (%)	Cu (%)	Mn (%)	Fe (%)	Mn/Fe
Crust	55	6.37	0.73	0.50	0.09	20.07	18.45	1.09
Slub	5	15.42	0.76	0.64	0.10	22.66	16.81	1.35
Cobble	18	5.43	0.81	0.54	0.09	22.47	17.66	1.27
Nodule	6	5.13	0.56	0.57	0.14	22.28	18.53	1.20
Coating	6	0.26	1.14	0.55	0.05	20.92	14.67	1.43

Table 4-3-13 Cobalt Crust Grade and Water Depth

Depth (m)	n	Average Thickness (mm)	Co (%)	Ni (%)	Cu (%)	Mn (%)	Fe (%)	Mn/Fe
0 - 1000	7	0.80	1.24	0.59	0.06	20.94	14.72	1.42
1000 - 1500	14	4.44	0.62	0.41	0.06	19.67	19.65	1.00
1500 - 2000	21	5.08	0.78	0.54	0.07	22.91	18.02	1.27
2000 - 2500	25	5.63	0.72	0.55	0.10	22.34	17.63	1.27
2500 - 3000	24	8.97	0.75	0.53	0.11	23.02	18.25	1.26

Table 4-3-14 Analysis of Total and Minor Element of Cobalt Crust

Sample No.		88SB03 CB01	88SB03 CB02	88SB03 AD06	88SB05 AD05B	88SB05 AD05E	88SB05 AD05G
Location		Upper slope	Upper slope	Upper slope	Upper slope	Upper slope	Upper slope
Water Depth (m)		1,300	1,300	1,350	2,400	2,400	2,400
Morphology		Crust	Crust	Crust	Crust	Nodule	Nodule
Analized Portion		Bulk	Bulk	Bulk	Bulk	Bulk	Bulk
Thickness (cm)		0.5	0.5	1.1	2.0	0.5	1.3
Major Metal Contents (%)	Co	0.76	0.61	0.39	0.84	0.53	0.59
	Ni	0.39	0.35	0.28	0.48	0.55	0.64
	Cu	0.05	0.07	0.07	0.10	0.15	0.15
	Mn	21.40	18.17	15.60	22.81	22.20	23.69
	Fe	20.83	19.17	21.43	20.63	18.42	18.45
Major Element Contents (%)	SiO_2	4.81	7.82	8.07	7.30	9.74	12.14
	TiO_2	1.27	1.24	1.35	1.95	1.49	1.67
	Al_2O_3	1.76	2.97	2.51	1.88	2.82	3.64
	Fe_2O_3	23.12	25.76	28.87	26.74	25.91	24.72
	FeO	<0.01	<0.01	<0.01	<0.01	<0.01	<0.01
	MnO	20.02	19.17	19.87	22.53	22.92	20.44
	MgO	1.91	1.79	1.65	1.61	1.64	1.66
	CaO	11.54	7.67	5.46	3.86	2.93	4.06
	BaO	0.11	0.11	0.13	0.16	0.16	0.17
	Na_2O	1.77	1.79	1.64	1.52	1.80	2.00
	K_2O	0.34	0.43	0.46	0.50	0.57	0.75
	P_2O_5	4.45	1.15	1.14	0.74	0.76	1.42
	Loss	22.78	24.20	23.48	24.40	23.29	22.10
	Total	93.88	94.10	94.63	93.19	94.03	94.77
Minor Element Contents (ppm)	Pb	1,272	1,121	1,146	884	750	670
	Zn	586	643	619	620	682	693
	As	209	194	204	146	172	156
	Sr	1,541	1,368	1,535	1,365	1,361	1,299
	V	610	584	597	490	591	540
	Mo	302	245	272	267	393	305
	B	153	168	187	158	169	155
	Y	226	263	182	164	121	156
	Zr	731	437	536	639	120	97
	Pt	0.2	0.2	0.3	0.5	0.3	0.3
	T.R.E.	1,452	1,284	1,462	2,084	1,396	1,551

Table 4-3-15 Analysis of Total and Minor Element from Different Layer of Cobalt Crust

Sample No.		88SB08AD08A		88SB08AD02A			
Location		Upper slope		Middle Slope			
Water Depth (m)		1,800		2,500			
Morphology		Slub		Massive (Slub like)			
Analized Portion		Outer	Inner	Outer	Middle	Inner	Back
Thickness (cm)		2.8	2.3	1.3	2.5	1.8	0.5
Major Metal Contents (%)	Co	0.87	0.66	0.67	1.05	0.35	1.59
	Ni	0.63	0.70	0.49	0.65	0.60	0.79
	Cu	0.06	0.08	0.08	0.14	0.15	0.11
	Mn	26.63	21.40	23.61	27.84	16.95	28.63
	Fe	17.07	10.55	20.53	16.02	10.36	13.27
Major Element Contents (%)	SiO_2	5.30	2.44	4.91	3.72	4.33	3.64
	TiO_2	1.42	1.69	1.71	2.04	1.66	1.99
	Al_2O_3	1.15	0.53	0.96	0.75	1.02	0.70
	Fe_2O_3	22.63	16.04	20.27	18.46	16.64	17.71
	FeO	<0.01	<0.01	<0.01	<0.01	<0.01	<0.01
	MnO	28.19	28.15	29.03	29.51	23.99	30.10
	MgO	1.73	1.58	1.71	1.70	1.51	1.88
	CaO	3.11	10.30	3.14	5.06	13.21	3.87
	BaO	0.18	0.22	0.18	0.23	0.21	0.18
	Na_2O	2.00	1.85	2.07	2.01	1.78	2.04
	K_2O	0.55	0.48	0.53	0.55	0.52	0.58
	P_2O_5	0.82	5.18	0.66	1.74	7.20	1.15
	Loss	25.35	23.87	26.36	25.84	21.37	26.64
	Total	92.43	92.33	91.53	91.61	93.44	90.48
Minor Element Contents (ppm)	Pb	1,152	954	1,059	1,032	764	1,139
	Zn	695	793	739	823	772	791
	As	176	141	133	129	130	134
	Sr	1,596	1,715	1,498	1,596	1,626	1,392
	V	667	615	598	617	527	521
	Mo	519	553	519	541	396	460
	B	150	118	153	127	118	130
	Y	132	197	132	175	459	156
	Zr	526	72	494	299	239	463
	Pt	0.3	0.4	0.2	0.4	0.5	0.3
	T.R.E.	1,816	2,253	2,081	2,524	2,969	2,364

Table 4-3-16 Mutual Relations among Major Chemical Composition of Cobalt Crust

	Depth (m)	Crust Thickness (mm)	Co	Ni	Cu	Mn	Fe
Depth (m)	–	0.16	-0.48	0.04	0.39	-0.04	0.26
Crust Thickness (mm)		–	0.04	0.22	0.12	0.33	-0.42
Co			–	0.49	-0.27	0.55	-0.72
Ni				–	0.24	0.67	-0.60
Cu					–	0.14	-0.05
Mn						–	-0.51
Fe							–

Table 4-3-17 Comparison of Cobalt Crust Compositions

	0	1	2	3	4	5
Element (Wt %)	This Work	Kiribati Area	Kiribati and Tuvaru Area	Hawaiian Islands Archipelago	Central Pacific Basin Seamount	Pacific Seamount Average
	n=43*1	n=33*2	n=50	n=32	n=26~46	n=251~803
Co	0.78	0.78	0.945	0.90	0.79	0.73
Ni	0.50	0.66	0.650	0.44	0.49	0.47
Cu	0.09	0.11	0.095	0.06	0.065	0.16
Mn	21.86	25.38	25.69	23.3	24.6	23.1
Fe	18.03	14.48	14.73	15.6	14.5	16.1
Mn/Fe	1.21	1.75	1.90	1.50	1.70	1.43
Average Depth (m)	1,819	2,256	2,198	1,546	2,179	.....

Both of *1 and *2 represents survey stations. Number of analized samples are 172 (*1) and 98 (*2) respectively.

1. JICA and MMAJ (1987)
2. De Carlo et. al., (1987)
3. De Carlo et. al, (1987)
4. Halbach and Manheim (1984)
5. Manheim (1986)

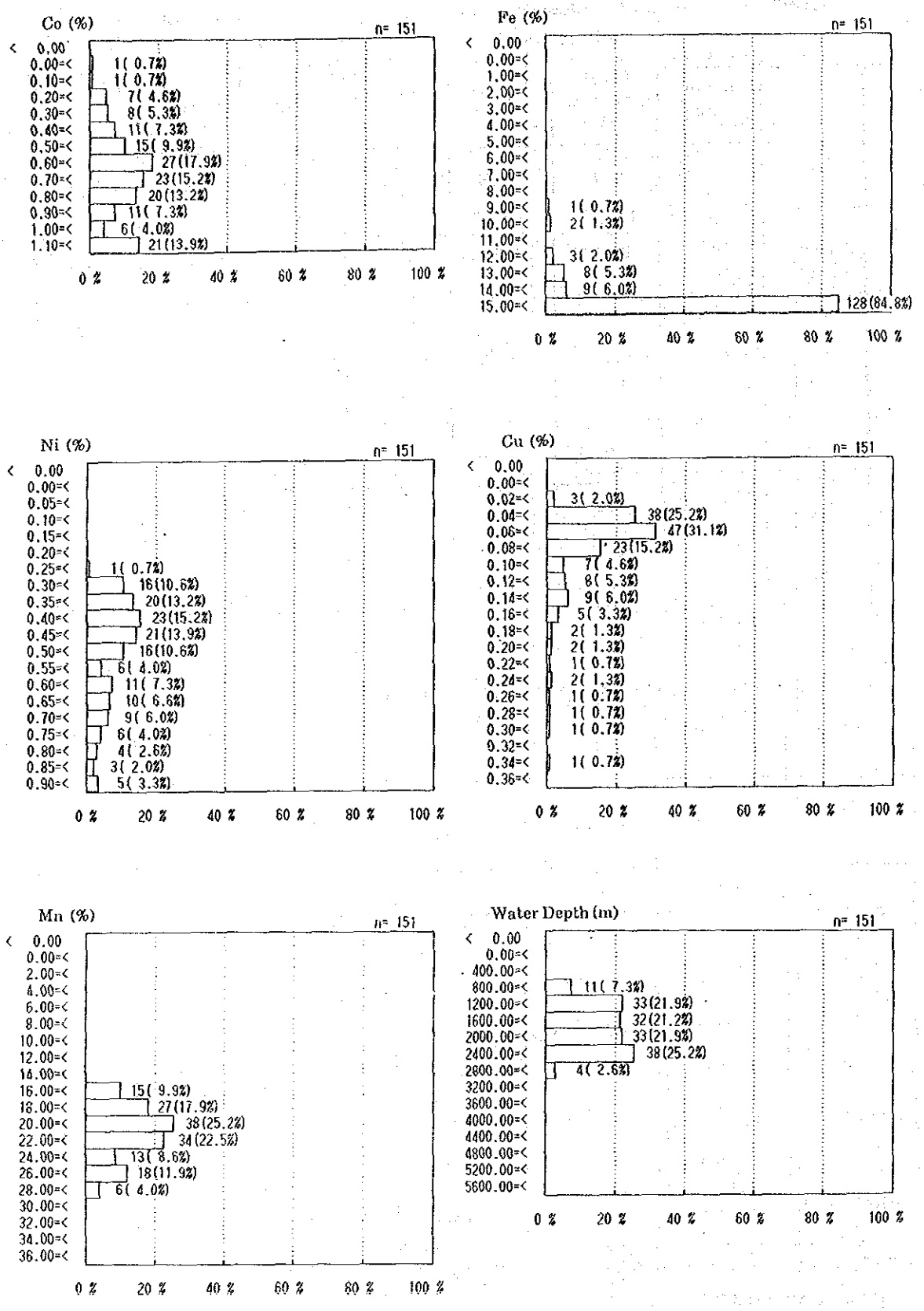

Figure 4-3-6 Frequency Distribution of Major Five Chemical Components

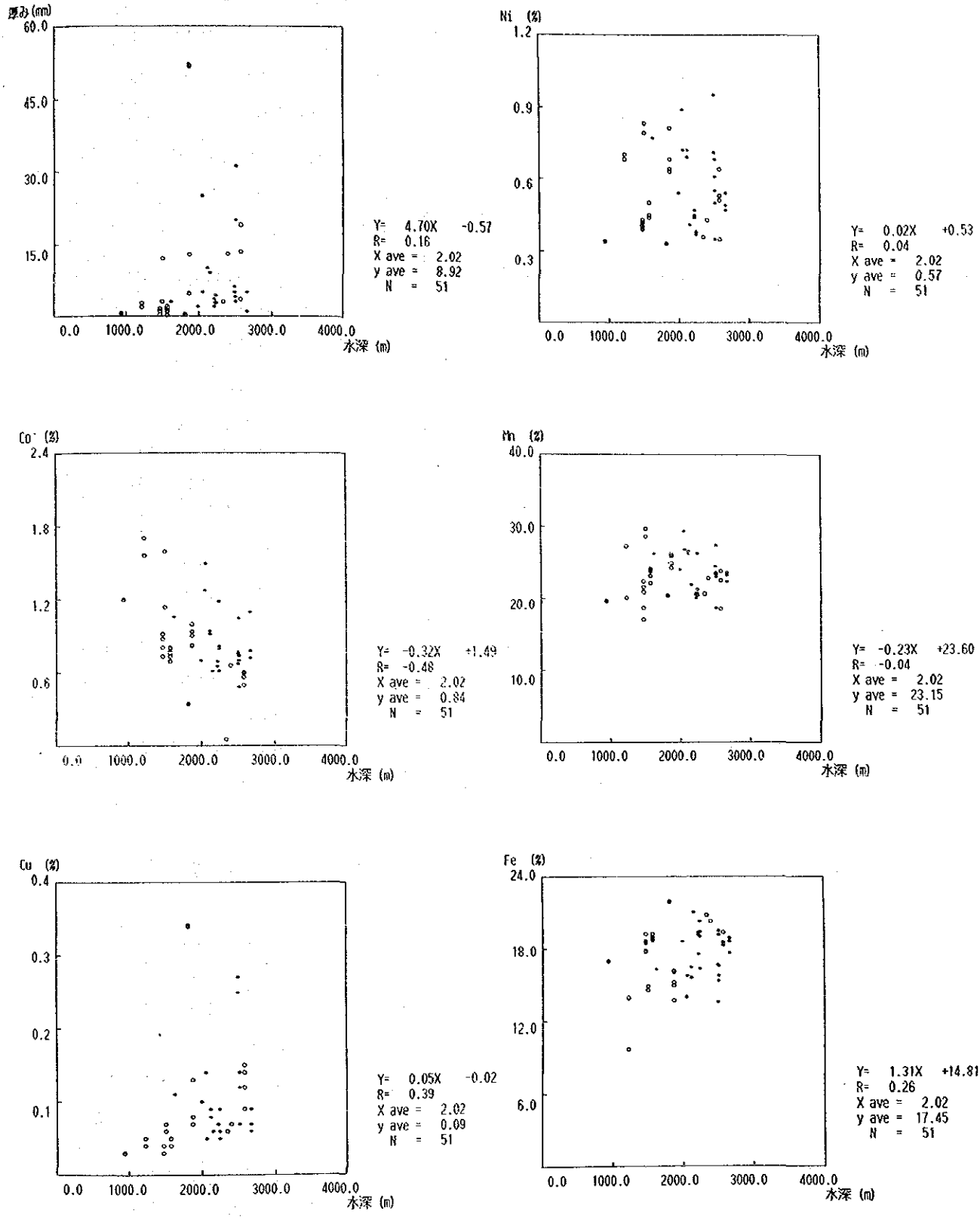

Legend: • Top, ı Top margine, ◦ Upper slope, • Middle slope • Lower slope, ı Foot, topographic position

Figure 4-3-7 Correlative Diagram among Major Chemical Components (1)

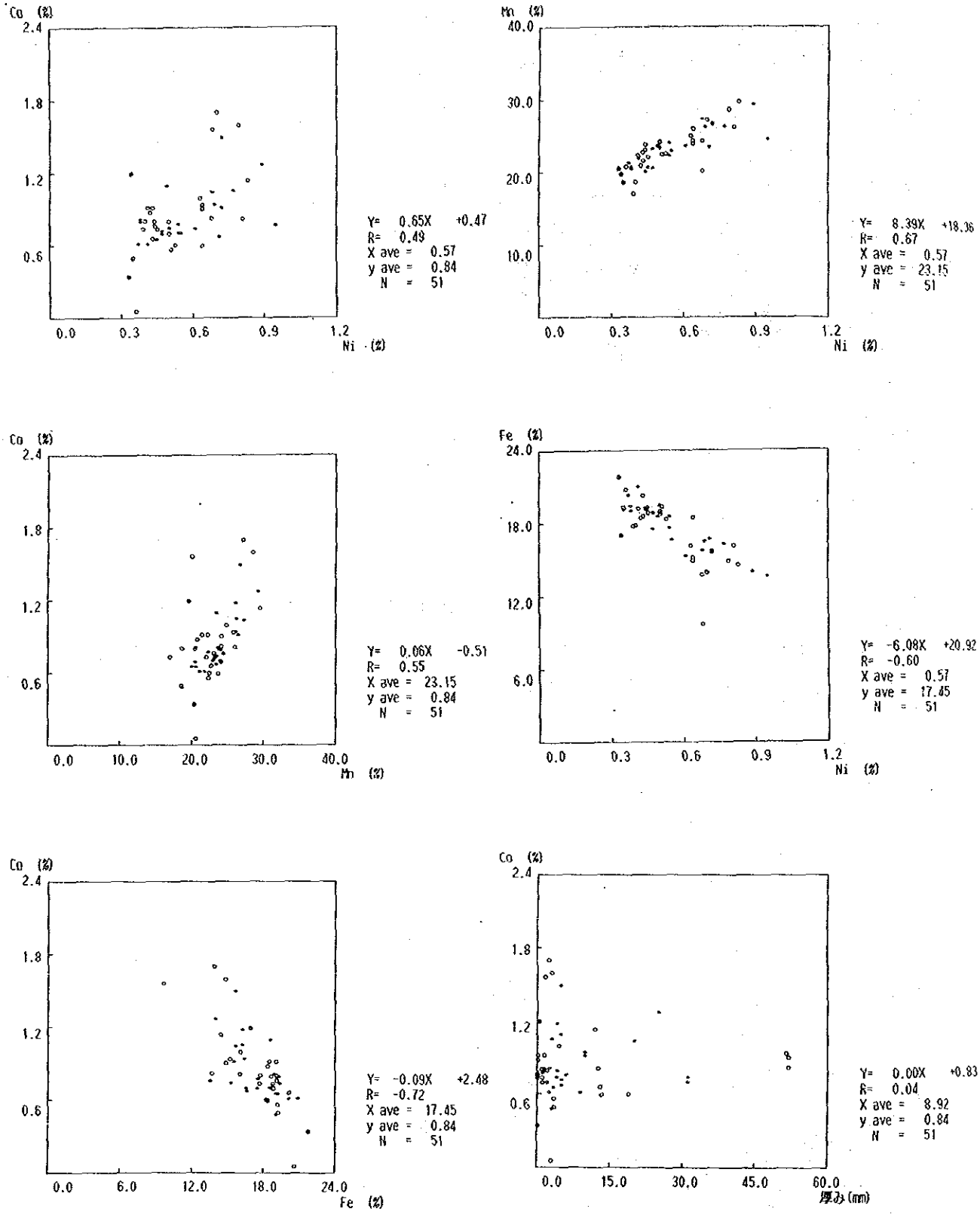

Legend: • Top, ı Top margine, ◦ Upper slope, • Middle slope • Lower slope, ı Foot, topographic position

Figure 4-3-7 Correlative Diagram among Major Chemical Components (2)

e) As for comparison by the surface conditions, no conspicuous tendency is observed except high Co, Ni and low Mn, Fe in smooth crusts.

f) As for the effect of substrates, high Co basalt and generally low Co and other metals and low Mn/Fe in limestone are noted.

g) Regarding the grade in various parts of the crust, high Co, Ni in the inner layer and the high Co, Ni, Cu, Mn and low Fe in the central part of the outer layer are noticeable.

h) Regarding the grade difference by the type of crusts, high Co, low Cu, Fe is observed in coating type. This is inferred to be related to the high Co of the cokes-like crust of the inner layer.

i) The total content of the gangue components, SiO_2, CaO, P_2O_5 and Al_2O_3 range from several percent to a maximum of about 15%.

j) Some of the features of minor element contents are; Pb>Zn, Sr 1,500 ppm±, V 500 ppm±, Pt 0.2~0.5 ppm and T. R. E. 1,500~2,900 ppm.

k) The minor element content variation by the parts of the crusts show that Pt and T. R. E. are both clearly higher in the inner layer than in the outer layer.

l) Regarding correlation, negative correlation is observed between water depth and Co content, but significant correlation is not observed between water depth and other elements. Among elements, positive correlation between Co and Ni, Co and Mn, Ni and Mn is observed and negative relation exists between Ni and Fe.

m) The comparison of the average grade of the cobalt crust in the present area with those of other marine areas are shown in Table 4-3-17. In general, the data of the survey area are similar to those of the Pacific seamounts, but Mn/Fe ratio is somewhat lower, Cu, Mn contents are lower and Fe, Co and Ni are higher than the crusts in the average seamounts of the Pacific.

4) Mineralogy

The mineralogical characteristics of cobalt crusts were studied by X-ray diffraction (Fig. 4-3-8), reflection microscope and EPMA. Nine samples (Table 4-3-18) were X-rayed, three (Fig. 4-3-9) were studied micro-scopically and two (Fig. 4-3-10) were analysed by EPMA. The results are reported below.

Table 4-3-18 Mineral Assemblage of Cobalt Crust, by X-ray Diffraction Analysis

No.	Sample No.	Mn-Mineral		Silicate Mineral						Others			Crust Type
		Undetermined Mn-Mineral*		Plazioclase	Pyroxene	Olivine	Quartz	Phillipsite	Clay mineral**	Calcite	Apatite	Magnetite	
C-4	88SB05AD05B	◇								◇			Crust
C-5	88SB05AD05E	◇											Nodule
C-6	88SB05AD05G	◇						◇					Cobble
C-7	88SB08AD02A	◇											Slub (Outer)
C-8	88SB08AD02A	◇								?			Slub (Middle)
C-9	88SB08AD02A	◇								◇	◇		Slub (Lower)
C-10	88SB08AD02A	◇											Slub (Bottom)
C-11	88SB08AD08A	◇											Slub (Outer)
C-12	88SB08AD08A	◇									◇		Slub (Inner)

◎: Abundant ○: Common •: Little ◇: Little ?: Uncertain

* Almost all δMnO_2 under microscope observation.

** Probably illite/montmorillonite mixed layer mineral.

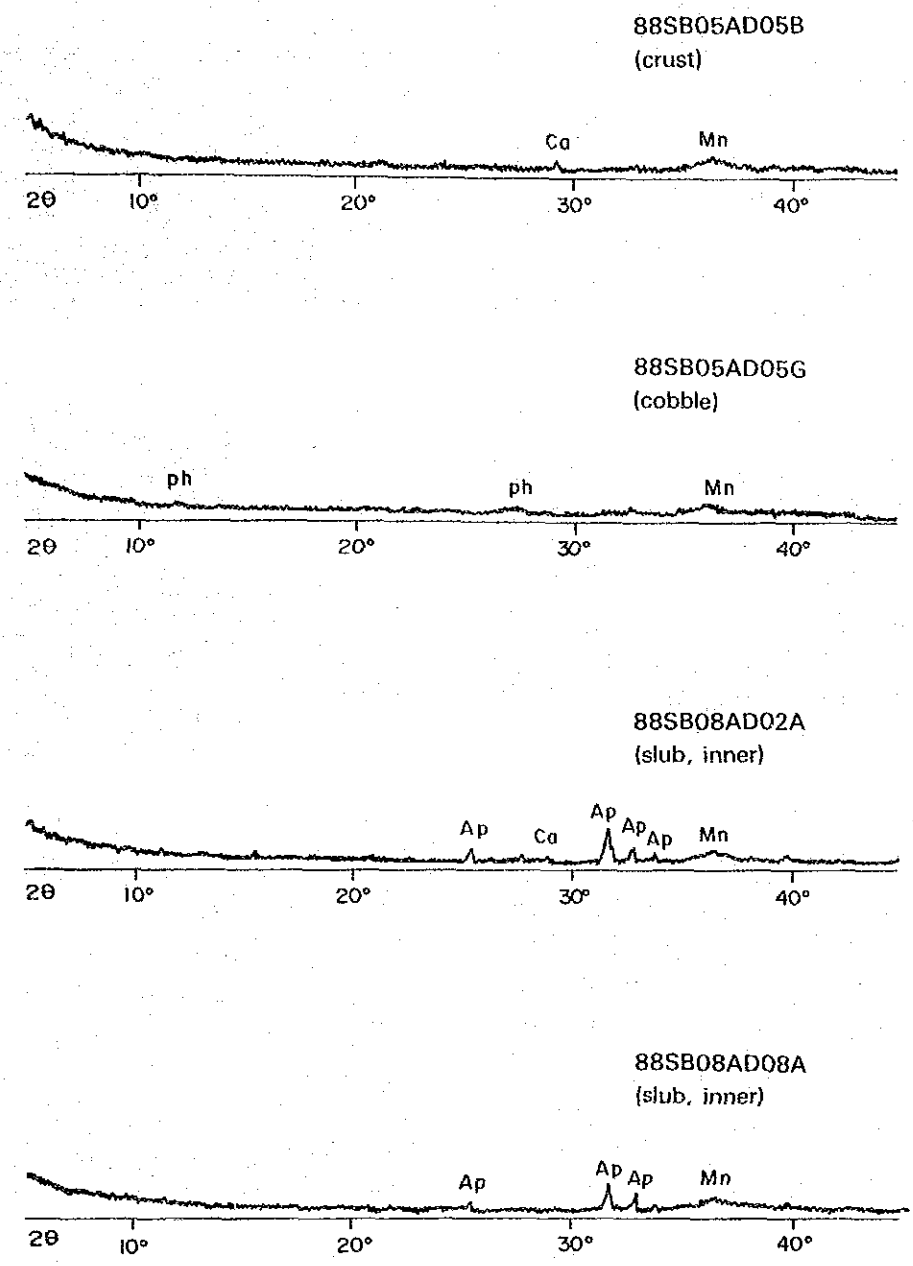

Mn : Mn-Oxide (δMnO_2), Ca : calcite
Ph : phillipsite, Ap: apatite

Figure 4-3-8 X-ray Diffraction Patterns of Cobalt Crusts

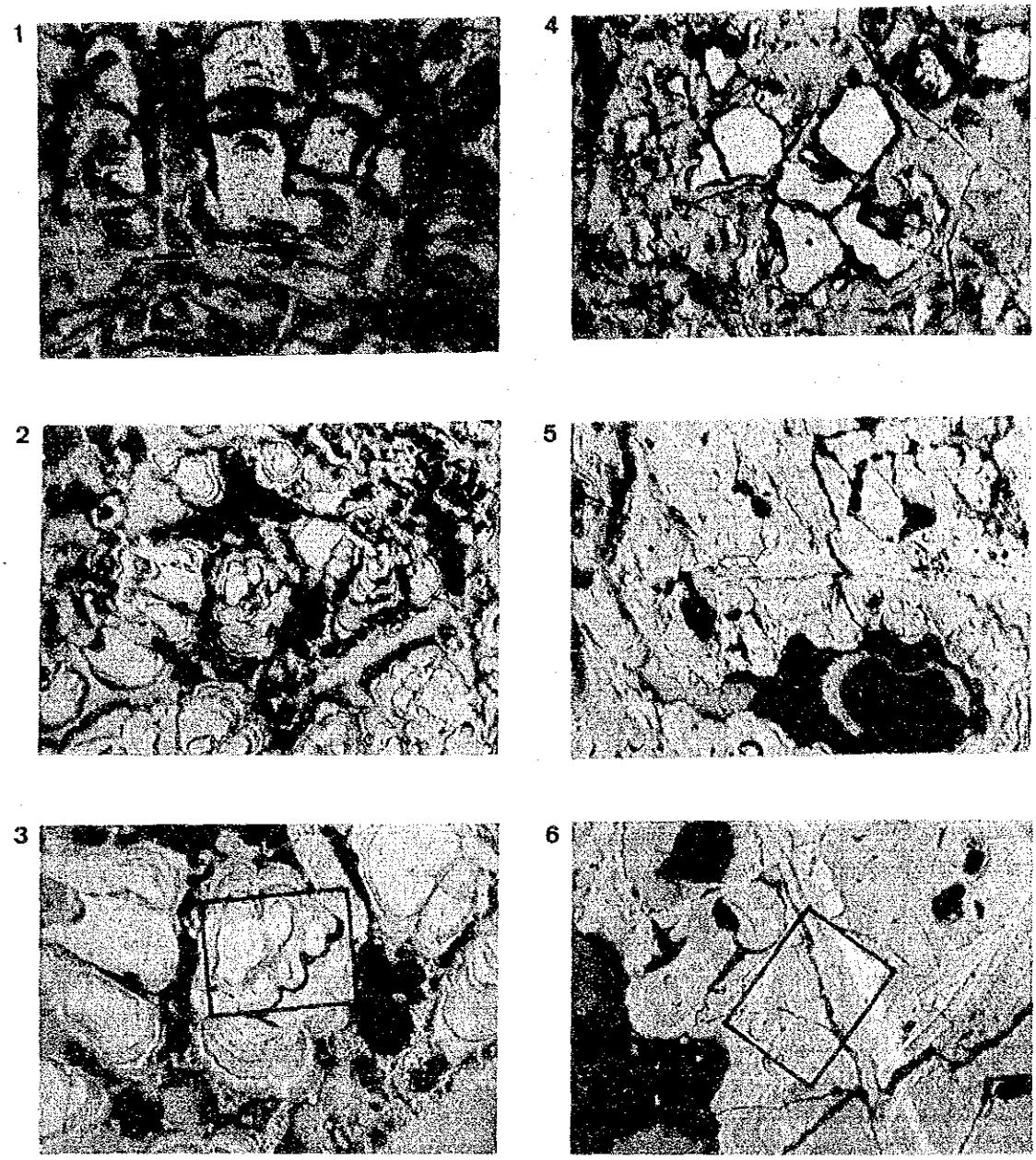

Sample No.: 1, 2, 3, (88SB08AD02A). 4, 5, 6, (88SB08AD06A).

1) x 7 (real size), stromatolite type growth structure.

2) x 7 (real size), nodule type growth structure.

3) x 19 (real size), partially enlarged of 2). Refer to Fig. 4-3-10 as for square area.

4) x 7 (real size), polypore type growth structure.

5) x 19 (real size), partially enlarged of 4).

Figure 4-3-9 Reflective Microscopic Photos of Cobalt Crusts

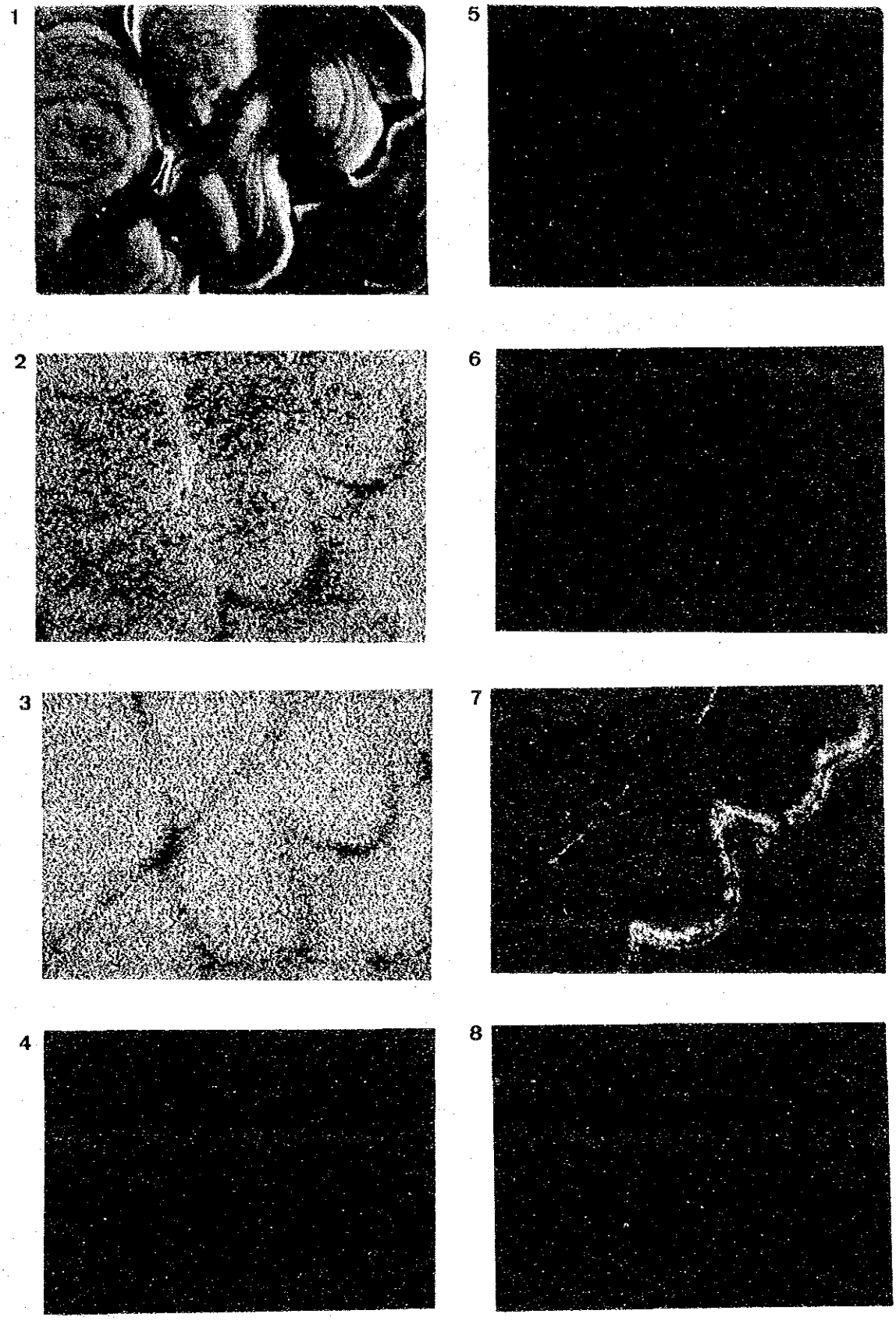

Sample No.: 88SB08AD02A. Area of the picture is shown in Fig. 4-3-9 (3).

1) SEM image of EPMA, 2) Fe, 3) Mn, 4) Co, 5) Ni, 6) Cu, 7) Al, 8) P.

Figure 4-3-10 EPMA Figures of Cobalt Crusts

a) Manganese oxide, the major component of the cobalt crusts, is δ-MnO_2 and 10Å manganite was not observed.

b) δ-MnO_2 appears isotropic microscopically. There are manganese oxides with high, low and intermediate reflectance in the samples, but they all lack the anisotropism which is characteristic to 10Å manganite and thus were identified as δ-MnO_2. The ratio of the high and low reflectance material is around 3:7.

c) The above ratio for triple-layed cobalt crusts (SB08AD02A) is 2:8, 4:6, 4:6 for the outer, middle and inner layers respectively.

d) The manganese mineral can be grouped by the form into stromatolite, polypore and nodule types, but they are all δ-MnO_2.

e) It is difficult to clearly identify δ-MnO_2 by X-ray diffraction alone. The characteristic feature is a broad peak near 37° (2θ).

f) Phillipsite, calcite, apatite and clay minerals were also identified aside from manganese minerals by X-ray diffraction.

g) The clay minerals are inferred to be illite/montmorillonite mixed-layer minerals.

h) Phillipsite is considered to have been a product of diagenesis at the sea floor. The occurrence of the mineral in the ore is indicative of the growth rate of the crust and the genetical environment.

i) The X-ray images of EPMA show a trend of Mn, Fe, Ca enrichment in the high reflectivity parts relative to the low reflectivity parts.